FUNCTIONAL DESIGN AND SCALING OF THE JUMPING MECHANISM OF THE AFRICAN DESERT LOCUST (*Schistocerca gregaria*).

by

Stephen Lawrence Katz

B.A. Occidental College, 1986.

A THESIS SUBMITTED IN PARTIAL FULFILMENT OF THE REQUIREMENTS FOR THE DEGREE OF DOCTOR OF PHILOSOPHY

in

THE FACULTY OF GRADUATE STUDIES

Department of Zoology

We accept this thesis as conforming to the required standard

The University of British Columbia

September 1992.

In presenting this thesis in partial fulfilment of the requirements for an advanced degree at the University of British Columbia, I agree that the Library shall make it freely available for reference and study. I further agree that permission for extensive copying of this thesis for scholarly purposes may be granted by the head of my department or by his or her representatives. It is understood that copying or publication of this thesis for financial gain shall not be allowed without my written permission.

(Signature)

Department of Zoology

The University of British Columbia
Vancouver, Canada

Date Nov. 26, 1992

DE-6 (2/88)

ABSTRACT

Current models for scaling of skeletal morphology were examined to test their applicability to the ontogenetic growth of an exoskeletal animal, the African Desert Locust (*Schistocerca gregaria*). It was found that the tibial leg segments of both the mesothoracic (ie. non-jumping) and the metathoracic (jumping) legs scaled in a manner that produced relatively longer, more slender skeletal elements as the animal grew. Metathoracic tibial length scaled to tibial diameter raised to the power 1.21. This result deviates both from isometric (ie. geometric similarity) and distortive (constant stress, elastic similarity) allometric models.

The mechanical properties of the metathoracic tibiae were measured using a dynamic, 3-point bending technique. The flexural stiffness of metathoracic tibiae scaled to body mass raised to the power of 1.53. This was intermediate to the predictions made by constant stress and elastic similarity models. Thus, the mechanical properties scaled in a manner similar to predictions of mechanical scaling expectations in spite of the morphological, developmental programme.

The uncoupling between morphological scaling and structural, mechanical properties is accomplished by scaling the tensile modulus of the cuticle. This strategy of altering the properties of the building material is distinct from strategies employed by vertebrate animals.

Calculations indicate that the energy stored in the substantial deflection of the adult, metathoracic tibiae during the jump may be as high as 10% of the total kinetic energy of the jump.

Using the models that generated relationships between morphology and

body size proposed by McMahon (1973, 1984) and the relationships between morphology and performance described by Hill (1950), predictions of how jumping performance measures may change as a function of body mass were tested. Performance was quantified using a high sensitivity, three dimensional forceplate. Performance parameters quantified included the force, acceleration, take-off velocity, kinetic energy and power output. With the exception of power output, each measure of performance scaled to body mass in a manner consistent with the predictions of the elastic similarity model. Power output scaled to body mass in a manner consistent with the predictions of the constant stress similarity model. The elastic similarity model is approximated by the performance of the locust in spite of the morphological design that deviates from that model's predictions.

These results indicate that the jump has separate functions in the flightless, juvenile instars and in the flying adult stage of the life history. Juvenile locusts produce take-off velocities of between .9 and 1.2 m/s that are relatively size independent. The take-off velocity in juveniles produces a distance of ballistic travel that averages between 20 and 30 cm. In adults, the take-off velocity is also relatively size independent at a level approximately twice as high as in juveniles (ie 2.5 m/s). The data suggest that in juveniles, the jump is designed to achieve a characteristic distance travelled, and in adults the jump is designed to achieve a minimum velocity necessary to fly.

Three rationales for the observed morphological programme are offered. The design may be a manifestation of a developmental constraint, it may be a response to scaling to force rather than explicitly to body mass, or it may be a design that takes advantage of the inherent deformability of long, slender beams. Thus, it may be that the tibiae, which have been treated as rigid levers, are in fact flexible springs.

TABLE OF CONTENTS

LIST OF FIGURES

LIST OF TABLES

ACKNOWLEDGEMENTS

Six years in one place and I'm supposed to be able to appropriately express my thanks to all of the people that contributed to my work here in a couple of pages....yah right.

Of the hominids that have contributed to my work the single most important individual is my supervisor John Gosline, who helped pull my graduate career off the rocks when it had floundered in rough weather. John has given me the freedom to do whatever I wanted, and I now appreciate that for the two-edged weopon that it is. John deserves a lot of credit for helping me organize much of the material in this thesis, and for first asking me "How do exoskeletal animals scale?" (or words to that effect)

I would also like to thank my committee members who have at various times been Robert Blake, Bill Milsom, Peter Hochachka, Don McPhail, Dave Jones, and Dave Randall. I would especially like to thank Bill Milsom for his editorial conscience that was put through its paces on most of the pages of this thesis.

I would also particularly like to acknowledge the contribution of Robert Blake. Of all the people in the "Big House", Bob always took me and my ideas seriously and always read my writing with care and speed. Anyone familiar with Bob will also recognize his important contribution to the discussion of actuator disks in chapter four.

There are several of my lab mates and friends that deserve credit for lightening the load in many ways. Among them I would like to thank Paul Guerette, Margo Lillie, Dottie Pabst, Calvin Rosskelly, Ignacio Valenzuela, Claudia Kasserra and her Chris's, Phil Davies, Troy Day, Laura Nagel and Joel Sawada. Of these Margo Lillie and Paul Guerette deserve special mention. It is Margo that makes the Gosline lab go when John is on his extended trips to the department of zoology at UBC, and it is Margo who I ask to critique my work whenever I feel the need to be dressed down by someone with a truly large cortex. Junior needs to be thanked simply for being so damned def, but also for reminding me not to lose my humanity in the process of doing my work (and for pointing out what a windbag D'Arcy Thompson was).

I would like to thank the people in the huts for reminding me that one can do science and still be a human being. I had been in the Big House so long I had forgotten. Sam Gopaul also deserves a big thank you for always having locusts for me in large numbers.

I would also like to thank Gillian and Izzie Muir (Izzie is the most important

non-Hominid in my stay at UBC) for listening to my ramblings and being my friends. Working with Gillian has been rejuvinating intelectual experience; collaborating with a person of Gillian's formidable intelect was stimulating and fun. I would like to thank Izzie for the conversations we've had, and for always agreeing with me.

The two people who have played far and away the largest roles in my life in the recent past, academic and otherwise, have been Mike Hedrick and Patricia Kruk.

Mike sucked me into the laugh-a-minute world of fish breathing and it resulted in what I think was a very productive collaboration. Our collaboration provided me with a much needed vacation from locust legs and an opportunity to work with my best friend. Many people have expressed surprise at the baud rate of Mike's and my communications, and they have commented on the parallel lives we have led. They don't know the half of it.

Although she may not appreciate it now, Patricia Kruk was my best friend and confidant for the five years we were together. She showed by example how hard a graduate student could work, how a high standard could be produced, and how to be serious about science. Far more significant was her continuous and unfaultering support for me and my brain. I am sure that I would never be able to thank her appropriately, even if things had worked out differently.

The two people who have contributed over my entire life to what I am now are my parents Dr.'s David and Carol Katz, and for this there could never be an appropriate thank you. I feel that whatever element of perfectionism, curiosity, confidence, dedication to logic, honesty and unwillingness to settle for other people's expectations that are a part of me are expressions of their influence. I will also never be able to thank them enough for always being supportive of me (financially and in all other ways) whenever I got in a jam.

PREFACE

Large parts of chapter two of this thesis has been published in the Journal of Experimental Biology. The full reference data are:

Katz S. L. & Gosline, J. M., (1992) Ontogenetic scaling and mechanical behaviour of the tibiae of the african desert locust (*Schistocerca gregaria*). J. Exp. Biol. **168**:125-150.

The contribution to this work made by S. L. Katz consisted of the design and construction of the testing apparatus, design and execution of the testing protocol, analyzing the data, and writing the text of the first draft of the manuscript.

To establish concurrence on this statement both authors have signed below.

The following is a release of copyright from the assignee to the author allowing the inclusion of the published material in this thesis.

CHAPTER 1.

GENERAL INTRODUCTION

> ".. But the physicist proclaims aloud that the physical phenomena which meet us by the way have their forms not less beautiful and scarce less varied than those which move us to admiration among living things. The waves of the sea, the little ripples on the shore, the sweeping curve of the sandy bay between the headlands, the outline of the hills, the shape of the clouds, all these are so many riddles of form, so many problems of morphology, and all of them the physicist can more or less easily read and adequately solve: solving them by reference to their antecedent phenomena, in the material system of mechanical forces to which they belong, and to which we interprit them as being due. ... Nor is it otherwise with the material forms of living things. "
>
> D'Arcy Thompson, On Growth and Form (1961)

This thesis is a study of mechanical design in animals. The word "design" is so important an idea to this thesis, and yet its use is fraught with teleological peril. Design means different things in different contexts. While it can mean the process of planning and constructing a device, it also may simply refer to the device itself. Evolution is a process of generating (ie. designing) biological structures, but each of these structures represents a design that we can evaluate with respect to the relationship between its structure and its function. Structures or mechanisms can be "good" mechanical designs, which function with ease and efficiency, or they can be "bad" designs, which are ill equipped to meet the demands placed upon them. Engineering provides tools that we can use to evaluate the quality of a given design. "Mechanical design" for my purposes is the relationship between the structure and the function of a specific biological mechanism whose mechanical behaviour can be evaluated with engineering mechanics.

Does the use of "design" imply the desire to find optimality? Not

necessarily. Were we to *design* a structure for use by people we might sit down and determine with high precision the loads that the device would have to endure and then build a device that meets some criteria for safety and efficiency, such as minimum weight for unit strength. While natural selection is fairly adept at weeding out "bad" designs, it probably does not *design* "good" ones by planning it out as might a human engineer. Selection works on the material that it has at hand. As such, optimality will exist only within the constraints of the available design options for a particular biological mechanism, and may not represent any globally recognised optimum. For a given biological device, departures from our pre-notion of optimality often highlights important compromises in the manufacture and use of biological structures. Thus, any particular structure (ie. design) may not be the optimal solution to any narrowly defined objective.

This thesis is an analysis of the functional morphology of the legs of the African desert locust and how leg design responds to changes in body size. In a study of the functional design of a biological mechanism it is fundamental to analyze the relationship between the mechanism and the physical environment with which it interacts. There must also be recognition that the physical environment is not independent of scale.

Why is Size Important? Why is it important to study the effect of body size on design? The reason is that physical laws, and the way in which those principles interact, are scale dependant. A familiar illustration of this assertion is the way in which the physics of the fluid environment that a sperm whale encounters (ie. the sea) is so profoundly different than that experienced by a single sperm (ie. semen). The whale's swimming is influenced to a certain extent by the viscous

character of the water, but the fluid's properties are so significant for the sperm that it is forced to swim as the whale might through asphalt on a hot day (Purcell, 1977). This difference is a manifestation of the changing relationship between viscosity and inertia that result simply because of the difference in scale between sperm and whale sized objects. As a result, the design of structures, both man-made and otherwise, must accommodate the changing influence of physical laws with changing size. It would be fruitless to test the performance of a ten centimetre model boat hull intending to extrapolate those observations to a 300 metre ocean liner without first considering the way hydrodynamic forces change over that range of scale. The scale dependant nature of the physical environment is no less significant in influencing biological designs as those man-made.

Implicit in this assertion is the idea that physical law influences design. This seems self evident in the case of man-made structures. When the influence of physical principles on man made structures are ignored or misunderstood planes crash, and boats and floating bridges sink. As Thompson noted ninety years ago, this is no less true in biological structures. Each analysis of functional morphology is an evaluation of the quality of a given design in the context of the properties of the structural and material elements of the design and the demands placed on a given structure by the physical environment.

Studying the scaling of mechanisms, biological and otherwise, can serve two functions. First, it can provide a check on our understanding of a given design. If we truly understand how a biological mechanism works, then we would be able to predict accurately how that design is altered to accommodate changes in body size. If our predictions are validated then we probably do understand how the design works. If not, the study of scaling may

serve its second purpose and reveal the heretofore unrecognized relative significance of competing design pressures, or even entirely new design principles.

In this study I have examined the ontogenetic scaling of the jumping mechanism of the African Desert Locust (*Schistocerca gregaria*), an animal with six discrete life history stages, or instars, and which varies in body mass by two and a half orders of magnitude. This scaling analysis provides some interesting contrasts to the scaling relationships observed in vertebrate skeletal designs in several respects; the locust has a protein exoskeleton rather than a mineralized endoskeleton, changes of external dimensions occur in discrete steps rather than continuously, and comparisons are made across the ontogeny of hopping animals rather than between closely related, adult walkers and runners. With these contrasts in mind, I have examined scaling in both the morphology and mechanical behaviour of the jumping mechanism in *Schistocerca* to see if there are distinctive design principles employed in the jumping legs of the locust.

Scaling models in animal design. The desire to understand the scaling of skeletal design has resulted in several models that attempt to predict how animal skeletons are modified to respond to the changing demands of increasing body size. The models are distinguished by the specific design issues that are thought to act as pressures in generating and refining a specific design. Each model predicts how the skeleton should scale if a given mechanical parameter, such as stress or deformation, is similar across the range of body sizes. Thus the predictions of each model exist within a specific context, and it is the assumptions and the context of the model that are being tested in a scaling analysis. This point is non-trivial, as I will continually make comparisons

between the data on locusts and the various models; each time testing to see if the design of the locusts' legs are responding to specific design issues implicit in each model. For this reason I will take the time to more fully detail the three most prominent models in skeletal design: Geometric Similarity, Constant Stress Similarity and Elastic Similarity.

This approach is not without controversy. Both the statistics and the scientific approach have been questioned in the study of allometry. Smith (1980), in a paper that attempted to catalogue the dangers of the indescriminant use of allometry, has suggested that the familiar methods of estimating parameters of power law functions are inappropriate because of the assumptions made in Huxley's (1932) use of allometric models. He suggests that often linear regression applied to non-transformed data make just as good a description of the data, indicating that a power law may not be an appropriate model for the biological phenomena being described. Zar (1968) has pointed out that variances are resolved in log-log transformations in a manner that makes use of the "least squares" regression a dubious technique in estimating slopes of regression of power functions. He states that an alternative model to least squares, that accommodates the variance in both the independent and the dependant variables, is a better choice for allometric models.

A more significant issue than statistical description is perhaps the identification of an alternative hypothesis in the analysis of the scaling models. Gould (1975) has pointed out that geometric similarity (the specifics of which will be detailed shortly) is treated as an alternative hypothesis in testing allometric models. He states that allometric regression is a "criterion of subtraction", meaning that the regression line provides information on the influence of body mass independent of any specific adaptation of animals at any specific point

in the range of body masses. Thus, an observed allometry may hide fundamental differences between large animals and small ones that are not strictly structural design consequences of body size. Smith (1980) echoes this as well as other criticisms, and adds that even in the case where the statistical technique reveals a characteristic power function relationship, this by itself does not indicate a specific functional relationship.

I believe that in this study the use of allometric models is appropriately performed for several reasons. In the case of each model that follows we can *a priori* establish a mechanical basis for the power law relationship. Further, we will discover that the variances are positively correlated with the means (ie. the variances are independent of the means after log transformation). For these reasons, a log-log estimation of the power function model is justified (Sokal and Rholf, 1981). In chapter four we will see that there are important deviations in adult locusts' jump performance that are not strictly a function of body size. These data are excluded from the scaling analysis. We can establish, however, that the remaining data do represent *functionally equivalent* individuals, and are reasonably analyzed with Gould's criterion of subtraction. The criterion of *functional equivalence* will be used throughout this thesis as a basis for the appropriateness of allometric analysis, and data that do not meet this criterion will be excluded from analysis.

Geometric Similarity. The Geometric Similarity Model (GSM) is a mathematical formalization of the idea of Euclidean similarity or isometry. Euclidean similarity means that geometry is maintained independent of the size of the object being considered (Thompson, 1947). Therefore, the relationships between all of the dimensions of the object are the same independent of scale,

and differences in size result from scalar multiplication of all of the object's dimensions by a single multiplier. A familiar example is a comparison between similar triangles of different size. The angles at the vertices are the same (the definition of similarity in trigonometry), and thus if the base of one of the triangles is twice the length of the other, then all of the linear dimensions are twice as large. When applied to biological systems the outcome is the same. Simply, large animals look like geometrically similar small ones.

Geometric similarity has consequences that can place real limitations on biological design. A familiar example will illustrate these as well as show how the scaling predictions are generated. Given two cubes with one having edges that are twice the length of the other, it is probably familiar that the surface area of the larger cube will be four times that of the smaller and the volume of the larger will be eight times the volume of the smaller. Thus

$$\text{Area} \propto \text{Characteristic length } (\ell)^2$$

and

$$\text{Volume} \propto \ell^3.$$

Therefore, if animals are geometrically similar their linear dimensions will scale with body mass raised to the 0.333 power, while their surface areas will scale to body mass raised to the 0.667 power.

One of the significant consequences of geometrically similar increases in the size of skeletal support structures is that the demands of mechanical loading increase faster than the ability of the skeleton to accommodate those loads. More specifically, inertial loading is a function of mass (that is volume), a third power function of characteristic dimension, while the cross-sectional area of material that carries that load is only a second power of characteristic length. In this way geometric similarity is distinct from the other scaling models in that

it is not a predictive model based on the control or similarity of any mechanical parameter, but is rather the formalization of the consequences of conserving geometry independent of size.

A solution to the increasing mechanical demands placed on geometrically similar structures is to produce distortions in the dimensions of the skeletal design to increase the amount of load-bearing material, and in so doing accommodate the increasing inertial loads. This was recognised as a design strategy by Galileo as early as 1638 (Thompson, 1917; Schmidt-Nielsen, 1984). Indeed, it was over one hundred years ago that an explicit description was made of how the diameters of trees must increase with the 3/2 power of their length in order to produce similar mechanical behaviour (Greenhill, 1881). More recently two models have been proposed that predict how characteristic dimensions of biological structures should deviate from geometric similarity to produce structures that maintain either similar normalized load (ie. Stress) (McMahon, 1984), or similar normalized deformations (ie. Strain) (McMahon, 1973) independent of scale. Because of the significance of these models to the material that will follow I will briefly detail each. In presenting a detailed description of these models in his own words, McMahon (1984) demonstrates how the predictions of the models can be arrived at with a number of different approaches. I will only develop each model in a single way that seems most appropriate for the context of locust leg design.

Constant Stress Similarity. As stated above, the loads associated with body mass increase with increasing size, but stress (σ), or the force normalized by the area over which that force is distributed, increases even more quickly. Given the scale independence of specific gravity, forces that are associated

with gravity or inertia, which is to say associated with mass, in geometrically similar skeletons scales to the third power of a characteristic length, while area scale to the second power of length. Thus stress must scale to the 3/2 power of a characteristic length dimension. McMahon (1984) suggested that by appropriately scaling diameter of a cylindrically shaped skeletal member separately from the scaling of length, a given design could achieve a constant stress in structures independent of size. In achieving constant stress, large departures from geometrically similar morphologies are produced.

The specific morphological predictions of the constant stress similarity model (CSSM) for the scaling of dimensions of bending beams can be generated starting with the following relationship from engineering:

$$\sigma = \frac{(F\ell y)}{I} \qquad \text{Eq. 1.1.}$$

where σ is the peak stress developed in a beam of length, ℓ and diameter, 2y loaded with a force, F. I is the second moment of area - a parameter that describes both the amount of load-bearing material and how that material is distributed (Wainwright et al., 1976). The notion of I is central to the subject of this thesis and will be developed in more detail in chapters two and three. Suffice to say at this point that the computational formula for I for a cylindrical beam of radius, r, is:

$$I = \frac{\pi r^4}{4} \text{ or } \frac{\pi d^4}{64} \qquad \text{Eq. 1.2.}$$

Meaning that $I \propto d^4$, which has a number of consequences. One of which is we now have a relationship between all of the parameters that determine the stress in a beam and morphological dimensions. If force is proportional to mass, and therefore volume, then we can insert these morphological relationships into

equation 1.1 and produce

$$\sigma \propto \frac{(d^2)(\ell)(d)}{d^4} = \frac{d^3\ell^2}{d^4} = \frac{\ell^2}{d} \qquad \text{Eq. 1.3.}$$

and if σ is a constant (ie. constant stress) then

$$d \propto \ell^2 \quad . \qquad \text{Eq. 1.4.}$$

So in the CSSM diameter scales to the second power of length. By substituting the relationship mass (M) $\propto d^2\ell$ we can relate the scaling of both dimensions to body mass thusly:

$$\sigma \propto \frac{(\ell^2)^2}{d^2} = \frac{(\ell^2)^2}{\left(\frac{M}{\ell}\right)} = \frac{\ell^5}{M} \quad . \qquad \text{Eq.1.5.}$$

Since σ is a constant

$$\ell \propto M^{0.20} \qquad \text{Eq. 1.6.}$$

and likewise

$$d \propto M^{0.40} \quad . \qquad \text{Eq. 1.7.}$$

This means that to build different sized skeletons of the same building material that will experience the same stresses in bending demands that the external dimension of diameter will have to scale to mass raised to the 0.40 power while length will have to scale to mass raised to the 0.20 power. Therefore, the CSSM is distinct from GSM in predicting that as structures become increasingly large they will become increasingly stout.

Elastic Similarity. In 1973 McMahon formalized another alternative to geometric similarity which has been referred to as the elastic similarity model (ESM) (McMahon, 1973; Schmidt-Nielsen, 1984). Elastic similarity predicts

morphological scaling relationships based on keeping the deformation per unit length in a bending beam scale independent, rather than peak stress as was the case for CSSM. By trying to establish a similarity based on a different index of mechanical behaviour, ESM makes a different set of predictions than GSM or CSSM. The deflection per unit length of a cantilever loaded at its end can be calculated with the following formula:

$$\frac{D}{\ell} = \frac{F\ell^2}{3\mathbf{E}\mathbf{I}} \qquad \text{Eq. 1.8.}$$

where D is the deflection of a beam of length, ℓ, loaded at its end with a force, F. **E** is the elastic modulus of the material out of which the beam is made. **E** is a property of the building material, and if we assume that little skeletons and large skeletons are made from the same material with the same properties, then the term 3**E** is scale independent and falls out of a proportionality based on morphological dimensions. Elastic similarity is based on D/ℓ being a constant independent of size and thus we can generate the proportionality:

$$\frac{F\ell^2}{\mathbf{I}} \propto \text{Constant } (C_1) \qquad \text{Eq. 1.9.}$$

which we can relate to morphological dimensions as we did for CSSM

$$C_1 \propto \frac{F\ell^2}{\mathbf{I}} \propto \frac{(d^2\ell)(\ell^2)}{d^4}$$

so

$$\frac{\ell^3}{d^2} \quad \text{or} \quad d^2 \propto \ell^3$$

Which is precisely the result produced by Greenhill (1881) for the design of trees. By once again substituting the proportionality Mass $\propto d^2\ell$, we can make specific scaling relationships for each dimension in terms of mass.

$$M \propto d^2\ell \text{ so } \frac{(M)^3}{d^2} \propto C_2 \text{ so } \frac{M^3}{d^6} \propto d^2$$

or

$$M^3 \propto d^8 \text{ so } d \propto M^{3/8} \text{ or } M^{0.375}.$$

And likewise:

$$\ell^3 \propto \left(\frac{M}{\ell^3}\right)^2 \text{ or } \ell \propto M^{1/4} \text{ or } M^{0.250}.$$

Therefore, if we were to engineer different sized skeletal designs to respond to mass-dependant, bending loads with a constant deflection per unit length of beam we would scale the diameter to the 0.375 power of body mass while scaling lengths to the 0.25 power of body mass. Similarly, if we observed biological structures scaling in this manner we might infer that selection was responding to a design pressure that placed a value on similar normalized deflections in beams loaded in bending.

It is important to remember that the predictions of elastic similarity are constructed around the assumption that the beam is acting like a cantilever loaded at its end. For a beam loaded all along its length, the deflection is proportional to the fourth power of length rather than the third (Denny, 1988). Thus the deflection per unit length in this beam is proportional to the third power of the beam's length rather than the second. For such a beam the predictions of elastic similarity are identical to those of constant stress. It may turn out that vertebrate long bones which have muscle origins and insertions along a large part of their lengths are more appropriately modelled as beams loaded over their lengths rather than just at their ends. As we shall see below, locusts' limb beams are appropriately thought of as loaded at their ends (Heitler, 1974; Bennet-Clark, 1975), and as a result, the predictions of ESM and CSSM may be

distinguished.

Limb segments that follow the elastic similarity model, and even more so those that follow constant stress similarity, become relatively more stout as the animal increases in size. These types of distortions away from geometric similarity are characteristic of what McMahon (1984) calls distorting allometries. Indeed Huxley (1932) used the general term "allometry" to distinguish distortions away from geometric similarity, or "isometry". Gould (1966) invokes the etymology of the word allometry, which means "by a different measure" to separate all those scaling programmes that deviate from isometry, which he points out means "by the same measure". In each case, however, the existing scaling strategies predict allometries that produce relatively thicker beams, rather than relatively more slender beams. In chapter two we will discover that locust leg growth does not follow any existing allometric model's predictions, but produces increasingly spindly legs.

There are also important assumptions integral to all of these models that must be acknowledged. The models have assumed a cylindrical geometry, but are used to predict the scaling of distinctly non-cylindrical anatomical structures (McMahon, 1975a, 1975b). In anatomical features with non-circular cross-sections the value of I will still be proportional to the product of four linear dimensions. In elliptical cross-sections for example, I is proportional to one axis cubed times the orthogonal axis. Therefore, as long as relative dimensions of the cross-section of a skeletal element are scale independent, that is the shape of the cross-section is the same independent of size, the predictions of the models that are based on cylindrical geometry should still be valid. The functional role of violations of this assumption are very important, and will be discussed in detail in chapter three.

Another important assumption in both of these models is that small and large skeletal structures are constructed of the same building material. Therefore, the elastic modulus will be the same independent of size. This is probably an acceptable assumption in the case of vertebrate bones where the material properties of the building material are determined largely by the mineralized components of the bones (Curry, 1984). In the case of insect cuticle, however, where the mechanical properties are determined by a protein material whose properties are alterable either by changes in cross-link density (Anderson, 1976), or by hydration state (Vincent, 1980), violations of the assumption of constant **E** can be significant. It is the exciting possibility that **E** is a scaled commodity in structural design that is the subject of chapter three.

An additional assumption in making these predictions is that the forces that the skeleton is required to support are associated with the body mass, such as gravitational or inertial loads. In cases where the predominant forces that the skeleton must bear are produced by muscular contraction, which are themselves subject to scale effects, the predictions of the models must be adjusted. The consequences of scaling the skeleton to accommodate muscular forces rather than body mass are discussed in chapter five.

These assumptions, that the building material's mechanical properties and the strategy of distributing that material will be scale independent, are precisely the assumptions that lead us to try to make inferences about the mechanical behaviour of biological devices from morphological dimensions. We will see in chapter two that in the locust mechanical properties are "uncoupled" from morphology, preventing us from making inferences about mechanics based on morphology, and in chapter three we will learn that this uncoupling results from violations of the above assumptions.

Do animals follow scaling models? Before embarking on a detailed analysis of scaling in locust legs, it is worth asking if any of the models are supported by observation? In this regard there are' little data outside of studies of vertebrate designs. Bertram and Biewener (1990) have suggested that GSM may be an appropriate scaling scheme for small animals, where breakage of the skeleton due to loading is unlikely. For small animals, having a skeleton that is sufficiently stiff to function in support and locomotion is probably the primary utility of the skeleton. They also argue that it is in large animals, where loads are likely to exceed the breaking strength of geometrically similar skeletons, where the morphology must change, or distort, to accommodate those loads. ESM scaling, such a distorting allometry, seems to be observed in the skeletal design of ungulate limb bones (McMahon, 1975), although Bertram and Biewener (1990) suggest that CSSM may more adequately describe the scaling in the larger members of that data set. It has also been suggested that McMahon's choice of Bovids was fortuitous in that the order is somewhat singular in expressing ESM (Alexander et al., 1979, Curry, 1984). In a wide range of vertebrates with a wide repetoire of locomotor styles Alexander et al. (1979, 1981) found a general tendency to following geometric similarity.

None of the models has predicted skeletal elements becoming relatively more slender with increasing size. However, this type of scaling has been observed for the scaling of femora and humeri of a wide range of bird species (Prange et al., 1979). It is not clear if this scaling of bird bones represents a strategy *per se*. Because bird bones may be air filled and thin walled (Curry, 1984) they may be able to modulate the mechanical behaviour of their long bones in ways that are different from terrestrial vertebrates and in so doing produce an unexpected allometry. The functional role of this different skeletal

design is discussed in more detail in chapter three. Remembering Gould's (1975) caution however, it is not clear if it is fair to compare hummingbirds, whose humeri are loaded dynamically, at high frequency during hovering with swans, whose humeri are loaded relatively statically in soaring.

These relationships have been tested with a variety of interspecific comparisons between adults of closely related taxa (ie. phylogenetic scaling). One could also analyze the effect of scale in the development of an individual and apply similar relationships (ie. ontogenetic scaling). In his review, Gould (1966) does not distinguish ontogenetic from phylogenetic scaling in the quality of information that each type of study provides. It is not clear, however, if the developmental programme in a single species produces a series of *functionally equivalent* skeletal designs constructed from mechanically equivalent materials (Carrier, 1983, Curry and Pond, 1989). Ontogenetic changes in material properties of bone do occur (Curry and Butler, 1975, Carrier, 1983), uncoupling to some extent our ability to infer mechanical behaviour of the skeleton from its morphology. For example, Carrier's (1983) observations of jack-rabbits suggest that in ontogeny the rabbit's bone may vary in its material stiffness (ie. modulus) by as much as an order of magnitude. The same data also indicate that neonates, juveniles and adults may not be functionally equivalent in their ability to locomote. However, if functional equivalence is maintained across ontogeny, then it should be fair to ask whether the existing models of scaling apply to that ontogenetic sequence.

These observations have been made largely on endoskeletal animals, while very little has been said on the scaling of exoskeletal animals. Prange (1977) has shown that leg segments of the cockroach, *Periplaneta americana*, and the wolf spider, *Lycosa lenta*, scale very closely to GSM over an

ontogenetic sequence. This suggests that being exoskeletal does not by itself limit the applicability of the models.

While Bertram and Biewener (1990) have made a case for body size class determining the appropriate scaling programme to follow, Bou et al. (1987) have suggested that lifestyle is more important than either body size class or phyletic affinity in determining skeletal scaling. If so, an alternative scaling of the skeleton may be demonstrated by an animal that has a locomotor mechanism that is distinctly different from that of pedestrians like cockroaches and giraffes. The jump of *Schistocerca* is a well documented mechanical behaviour (Heitler, 1974, Bennet-Clark, 1975, Alexander, 1983) and therefore provides a good contextual framework into which an analysis of scaling may be placed.

Locust jumping The jump of the locust has been the subject of intense scrutiny. Bennet-Clark (1975) has shown that the peak power outputs of the locust jumping muscle is on the order of 450 W/Kg. He has shown for adults, and Gabriel (1985a) has shown for hoppers (ie. juvenile, flightless locusts) that the average power outputs of the locust's jump, estimated from jump distance, are all higher than the maximum value for the jumping muscle. Therefore, they concluded that a spring mechanism must store the energy for the jump relatively slowly (ie. at low power outputs) during the inter-jump interval, and release the energy quickly during the jump (ie. at high power outputs). Indeed, it has also been demonstrated that the inter-jump interval length is determined by the time it takes to store a specific amount of energy in the apodeme springs (Steeves & Pearson, 1982). In support of the suggestion that the jump is the release of stored energy rather than direct muscular action, the jump

distance is not temperature dependant while the length of the inter-jump interval is in a related grasshopper, *Melanoplus bivittatus* (Harrison et al., 1991). The implication is that the increased inter-jump interval is the manifestation of lowered muscle power output at low temperatures, while the release of spring energy is unaffected because the material properties of the cuticular springs are not temperature dependant. Heitler (1974) has described the femero-tibial articulation in great detail. He has shown that the morphology of the joint is designed to provide a mechanical catch mechanism that allows the jumping muscle to store a large amount of energy without fighting to hold the leg from extending. The tibial flexor muscle contracts to deform cuticular elements in the joint, moving the line of action of the extensor muscle tendon system behind the axis of the joint, producing a "catch". Thus the muscular contraction that stores energy in the tendon also helps keep the knee bent.

When the locust decides to jump, the tibial flexor muscle relaxes to release the catch allowing the line of action of the extensor muscle-tendon system to apply a torque that extends the knee. The stored energy in the apodeme spring is released, rotating the tibial segment, and extension of the leg pushes on the ground generating a ground reaction force that propels the locust into the jump.

The films of Brown (1963), analyzed by Alexander (1983), indicate that during the jump impulse of the adult locust the primary loading regime in the metathoracic tibiae is bending. It seems appropriate, therefore, to investigate the bending behaviour of limb segments to determine the mechanical scaling of this system. Chapter two will explicitly examine the relationship between the dimensions of the locusts' legs and the mechanical properties of the limb in bending. In chapter two we will see that about 11% of the energy from the

spring goes into bending the tibiae, of which about 90% is returned in generating ground reaction force. Given the role of bending in the normal loading of the tibiae and the large scale deformation that it undergoes, we might hypothesize that elastic similarity, as a design strategy, will provide an appropriate model for the legs of locusts. The results of the analysis in chapter two suggest that while the tibiae are elastically similar in their mechanical behaviour, their external dimensions scale in a manner that is fundamentally different from any of the existing models. This indicates that the relationships between morphology and mechanical properties that form the basis of the various models' predictions are uncoupled in locust tibiae. Thus, to evaluate the total mechanical design of a complex, living machine in the context of any one scaling model may be extremely naive.

In chapter three this uncoupling is explicitly examined. The mechanical behaviour of the locusts' tibiae, or any beam loaded in bending, is a product of the amount, distribution and material properties of the load-bearing material. In chapter three the relative contributions to the leg's bending behaviour that arise from material properties are separated from those arising from the distribution of skeletal material. It turns out that material stiffness is scaled in a manner that allows the distinctive morphological scaling that is observed in chapter two.

In chapter four the scaling of jump performance of the locust is characterized. The results suggest that the jump has a separate functional role in the juveniles and the adults. In juveniles the results suggest that there is a functional distance that the hoppers are designed to achieve. The transition to winged adults has demanded a higher performance jump to generate a minimum velocity to begin flight. Within the juvenile instars, however, a

consistent expression of the predictions of elastic similarity is observed in the scaling of each of the variables that can be directly correlated with morphology.

In chapter five the significance of the morphological and mechanical design programme expressed by locusts is discussed. Three arguments are offered to explain the uncoupling that is observed between the morphological and the mechanical scaling in chapters two through four. Briefly, the first argument attempts to describe how the moulting process may form a constraint on the growth process. The second argument suggests that it may be more appropriate in some cases to scale the dimensions of the skeleton to the forces produced by muscles, which themselves scale allometrically, rather than explicitly to mass. The third argument will make the case that the relative slenderness of the legs is functionally important in taking the maximum advantage of changing mechanical advantage of the legs in the jump.

CHAPTER 2.

THE UNCOUPLING OF MORPHOLOGICAL AND MECHANICAL SCALING.

INTRODUCTION

In this chapter I have examined the ontogenetic scaling of the morphology and mechanical behaviour of the legs of the African Desert Locust (*Schistocerca gregaria*), an animal with six discrete life history stages, or instars, and which varies in body mass by two and a half orders of magnitude. This analysis of the skeleton of the locust provides some interesting contrasts to the scaling relationships observed in vertebrate designs in several respects; the locust is exoskeletal rather than endoskeletal, changes of external dimensions occur in discrete steps rather than continuously, and comparisons are made across the ontogeny of one species of hopping insects rather than between adults of closely related species of walkers and runners.

Regardless of which morphological model is considered, it is assumed that the mechanical behaviour of a skeletal member can be inferred from morphological measurements. In insects where the skeleton is also the integument and is not mineralized to nearly the same extent as bone, it is possible that the material properties of the skeleton can be modulated to meet the mechanical demands of increasing body size in ways that are fundamentally different from vertebrates. The cuticle in various parts of the locust exoskeleton shows a wide repertoire of mechanical properties (Jensen and Weis-Fogh, 1963, Vincent, 1975), which might suggest such a possibility. Hepburn and Joffe's (1974b) observation that normalized cuticular stiffness is maintained across instars would argue against the suggestion that material

properties of the cuticle are changing. However, insects are a diverse group, and it may be that some of them have developed different strategies for solving skeletal scaling problems.

The films of Brown (1963), analyzed by Alexander (1983), indicate that during the jump impulse of the adult locust the primary loading regime in the metathoracic tibiae is bending. I have, therefore, investigated the bending behaviour of tibial limb segments to determine the scaling of mechanical properties. This study will show that the external skeletal morphology predicts mechanical behaviour that is dramatically different from the observed mechanical behaviour. It will also attempt to explain how the mechanical result may be arrived at in spite of the morphological design programme.

METHODS and MATERIALS

Animal Husbandry. Animals were sampled daily from a breeding colony of African Desert Locust (*Schistocerca gregaria*) maintained at the Department of Zoology at the University of British Columbia. The animals were kept at a constant temperature of 27° C, humidity of 56%, and photoperiod of 13:11 (L:D), and fed a diet of head lettuce and bran. A sample of five individuals was collected each day beginning on the first day following emergence from the egg until approximately sexual maturity (ca. 35 days). Each animal contributed both a left and right side meta- and mesothoracic tibiae, resulting in four samples from each individual. Replicates were performed to increase precision over the first seven, and final 15 days of sampling. There was no significant heterogeneity between replicates for a given day, and so all replicates were pooled. As a result, there are different sample sizes across the time series of morphological and mechanical

measurements.

Animals were sacrificed by decapitation and weighed immediately to the nearest 0.1 mg. All of the morphological and mechanical measurements were then performed in air on tibial segments within 10 minutes of removal from the animal. Control experiments indicated that this time course did not alter the mechanical properties significantly due to exposure to air.

Morphological measurements. The length and diameter of the tibial segments of both the mesothoracic, and metathoracic tibiae were measured either with a filar micrometer eyepiece (Wild 15XSK) attached to a dissecting microscope (Wild M5), or where the tibia length exceeded the length of the micrometer's graticule (the fifth instar and adult tibia lengths), a vernier calliper. Micrometer measurements were made to the nearest 10 μm, and calliper measurements to the nearest 20 μm. Morphological landmarks were defined to provide ease of location and to indicate the dimensions of uniform limb segments. That is to say, geometrically complex morphological features associated with the joint articulations were excluded from linear measurement. In the case of the mesothoracic leg, the tibial length was defined as the length measured on the lateral surface from a point approximately level with the femero-tibial articulation to the tibio-tarsal articulation. The metathoracic tibial length was defined from the depression in the posterior surface of the tibia that occurs just distal to the knee joint articulation, at the maximal extent of sclerotized tibial cuticle, down the posterior of the tibia to a point opposite to the insertion of the first moveable spine at the tibio-tarsal joint. Diameters were determined to be the largest diameter of the semi-elliptical cross-section at the mid-shaft point. Figure 2.1 shows a graphical representation of the

Figure 2.1.

Diagram showing the anatomical landmarks used in measuring length and diameter of the tibiae. Diameters were measured at the mid length point. L, tibial length; d, tibial diameter.

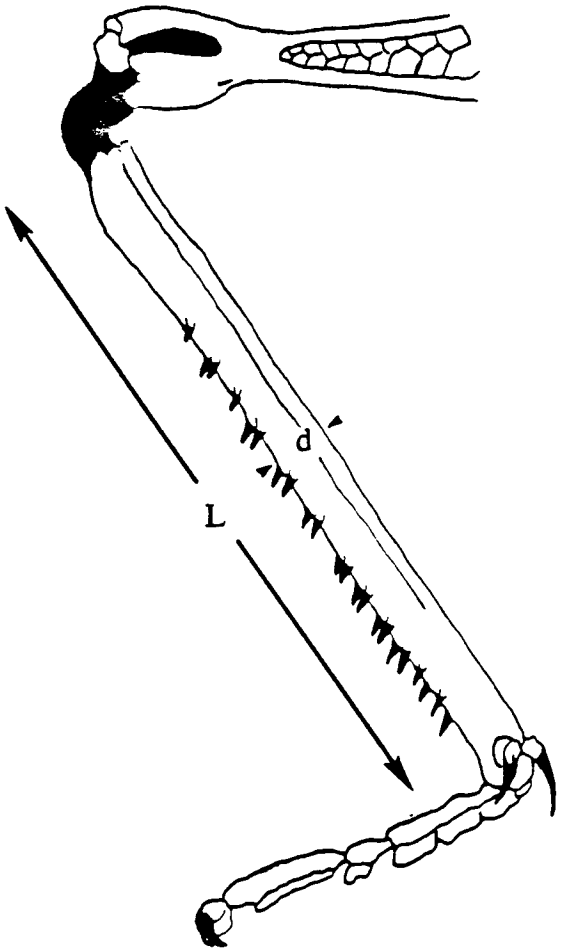
d
L

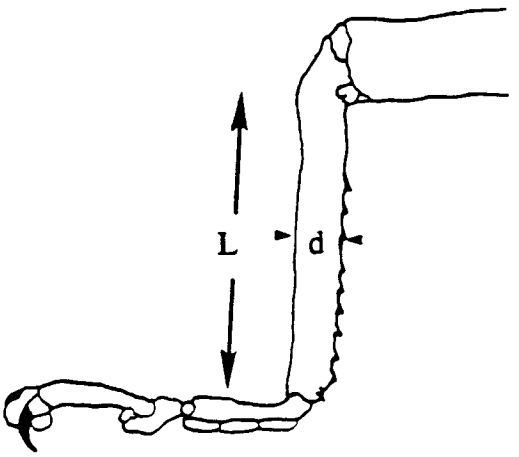
L
d

morphological landmarks.

Dynamic Mechanical measurements. After morphological measurement, each metathoracic tibia was placed in a mechanical testing frame that imposed a 3-point load with a dynamic, or time-variant, deformation. The theoretical and practical development of this dynamic testing technique have been reported previously (DeMont and Gosline, 1988, Lillie and Gosline, 1990). Therefore, only the principles and an outline of modifications made to generate 3-point bending will be described. The device itself consists of an actuator that delivers the time-variant displacement, monitored by a displacement transducer, and a force transducer that measures the resultant force developed across the test piece (ie. a metathoracic tibia) as measured at the two ends of the sample. Figure 2.2 is a diagram of the device.

The actuator consisted of a length of 0.148" (3.76×10^{-3} m) OD stainless steel hypodermic tubing attached at one end from an electromagnetic vibrator (Model V203, Ling Dynamic Systems, Royston, Hertfordshire, U.K.), and stepped down at the other end to an 18 gauge hypodermic needle. The end of the needle was cut off flush and polished smooth. Out of its end protruded a length of 8 lb nylon fishing leader. The nylon loop was adjustable and could be shortened to hold the midshaft of a test piece flush against the end of the actuator by turning a 4-40 machine screw which "spooled" up the slack nylon. The compliance of the nylon loop introduced less than a 1% overestimate of actual displacement and was ignored in subsequent calculations.

The free ends of the test piece were pulled upwards against the ends of a window cut in the side wall of a length of 0.148" (3.76×10^{-3} m) OD stainless steel tubing. The tubular holder was attached to a force transducer with a 2-56 stainless steel machine screw. The size of the window was scaled to provide a

Figure 2.2.

Diagram of the mechanical testing apparatus designed to deliver a dynamic 3-point bend. a, electromagnetic vibrator; b, inputs for driving noise signal; c, displacement transducer; d machine screw for tightening the nylon loop that held the tissue; e, stainless steel shaft connecting the vibrator to the test piece; f, force transducer and attached holder (see inset); g, tubular holder; h, test piece (ie. tibia); i, 18 gauge stainless steel tubing; j, 8 lb. nylon loop; k, cantilever beam of force transducer.

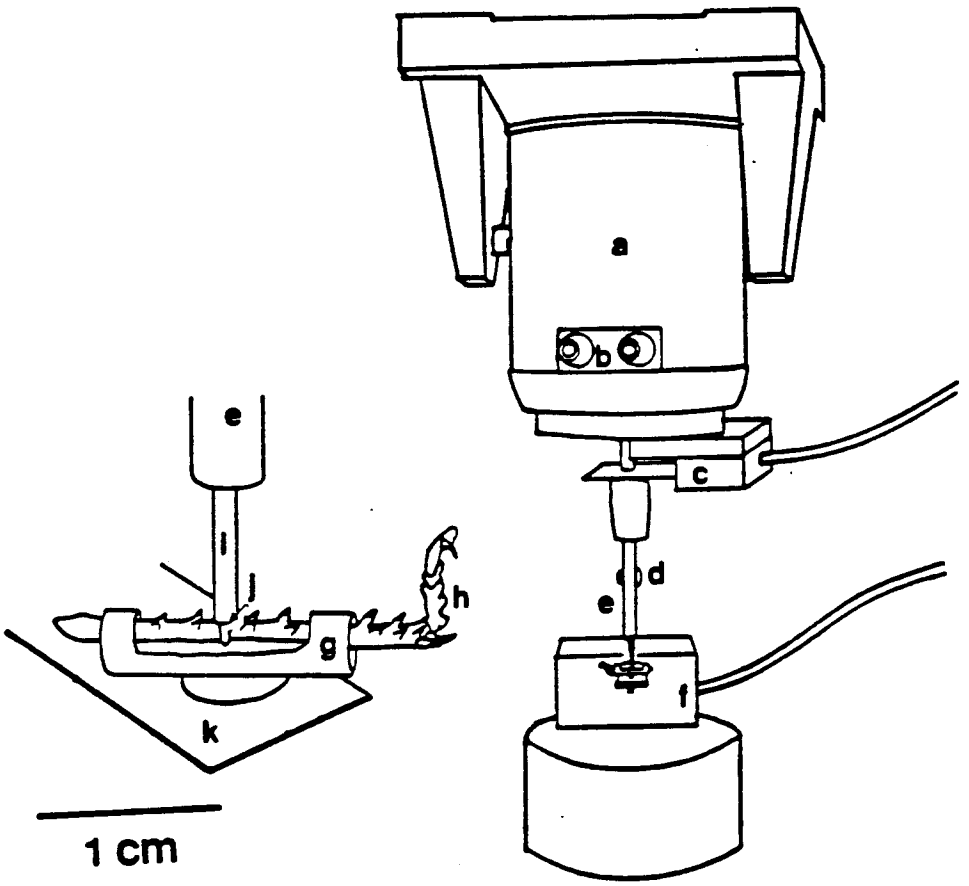
a
b
c
d
e
f
e
i
j
g
h
k
1 cm
5 cm

ratio of approximately 10:1 of test piece total working length to diameter to maintain a relatively consistent relationship of bending to shearing moments in the test pieces. In order to maintain this ratio in legs of different sizes several holders were made with appropriately sized windows. The ratio was deemed a reasonable compromise between the wish to introduce primarily a bending moment with respect to shearing moments, and the difficulties of fabricating small holders. The force developed across the test piece was measured with a cantilever-like transducer fabricated out of 0.015" (3.81×10^{-4} m) thick stainless steel shim stock. This material provided appropriately small deflections (<1% of the imposed displacements). Semiconductor strain gauges (type SR4 SBP3-20-35, BLH Electronics, Canton Mass.) were bonded on both surfaces of the cantilever. Semiconductor gauges provided appropriate sensitivity of 0.0473 Newtons/Volt. The resonant frequency of the transducer was 1.40 kHz with the smallest holder, 0.95 kHz with the largest, and .65 kHz for the ensemble apparatus.

As was described previously (DeMont and Gosline, 1988), the electromagnetic vibrator was driven by the noise generator of a spectrum analyzer (Model 5820A Cross Channel Spectrum Analyzer, Wavetek Rockland Inc., N.J.) which provided a constant power spectrum over the range of frequencies collected (0 - 200 Hz). At each frequency, the spectrum analyzer calculated both the ratio of the amplitudes of the Fourier components of the force and displacement transducer outputs, and the phase shift (δ) between the two signals. Spectra were collected from 0 to 200 Hz, and approximately 256 spectra were averaged to produce one spectrum per test piece. The flexural stiffness (**EI**) of the specimen at each frequency was calculated using the following relationship for static 3-point bending:

$$\mathbf{EI} = \frac{F \cdot x^3}{48 \cdot d} \qquad \text{Eq. 2.1.}$$

where x is the length of the test piece (ie. the length of the window in the tubular holder), F is the developed force and d is the deflection at the mid-point of the beam (rearranged from Gordon, 1978). **EI** is composed of **E** the elastic stiffness of the beam's material, and **I**, the beam's second moment of area. In these experiments the calibrated amplitudes of the Fourier components of the force and displacement transducer outputs were employed as F and d in equation 1 to produce a complex flexural stiffness ($\mathbf{E^*I}$) (adapted from Ferry, 1980).

Static tests performed as controls for the dynamic testing showed that the stress-strain curves for tibiae were linear over the range of deformation imposed on the specimen in these experiments.

E'I, the storage flexural stiffness--a measure of the energy stored elastically per loading cycle, can be found by calculating the in phase component of the complex flexural stiffness as follows:

$$\mathbf{E'I} = \mathbf{E^*I} \cdot \text{Cos } \delta. \qquad \text{Eq. 2.2.}$$

The energy loss flexural stiffness (**E"I**) is the out of phase component of the complex flexural stiffness

$$\mathbf{E''I} = \mathbf{E^*I} \cdot \sin \delta, \qquad \text{Eq. 2.3.}$$

and is a measure of the energy dissipated per loading cycle. The tangent of the phase shift ($\tan\delta = \mathbf{E''I} / \mathbf{E'I}$) can be used calculate the resilience per ½ cycle (**R**) (in %) of the structure as follows:

$$\mathbf{R} = (e^{-\pi \tan\delta}) \cdot 100 \qquad \text{Eq. 2.4.}$$

(Wainwright et al., 1976). Explicitly, **R** is the ratio of the energy recovered elastically to the energy input to the test piece in each loading cycle. All of these calculations were performed on a Digital Equipment Corporation MINC-11/23 computer.

Statistics. Except where noted, statistical tests were chosen based on criteria presented in Sokal and Rohlf (1981). Due to the non-zero variance associated with the morphometric variables measured in this study, all regressions were Model II regressions (Sokal and Rohlf, 1981). All Statistical tests were performed with the STATGRAPHICS (STSC, Mass.) statistical software package.

RESULTS

Ontogenetic accumulations of body mass followed a characteristic sigmoid curve adequately described by the von Bertalanffy growth function (Pitcher and Hart, 1982). Figure 2.3 shows the daily means of body mass as well as the fitted curve. The values of sample size for each day, listed at the bottom of figure 2.3, are the same for figures 2.3, 2.4 and 2.7. Body mass ranged from $0.0109 \cdot 10^{-3}$ kg for first day, first instars to $3.541 \cdot 10^{-3}$ kg in adult, sexually mature females. The data show that mass accumulates in a relatively continuous manner within each instar. Adult locusts continued to accumulate mass for the first four to seven days after moulting and then levelled off at their equilibrium mass. The assumptions of the von Bertalanffy growth function, that the

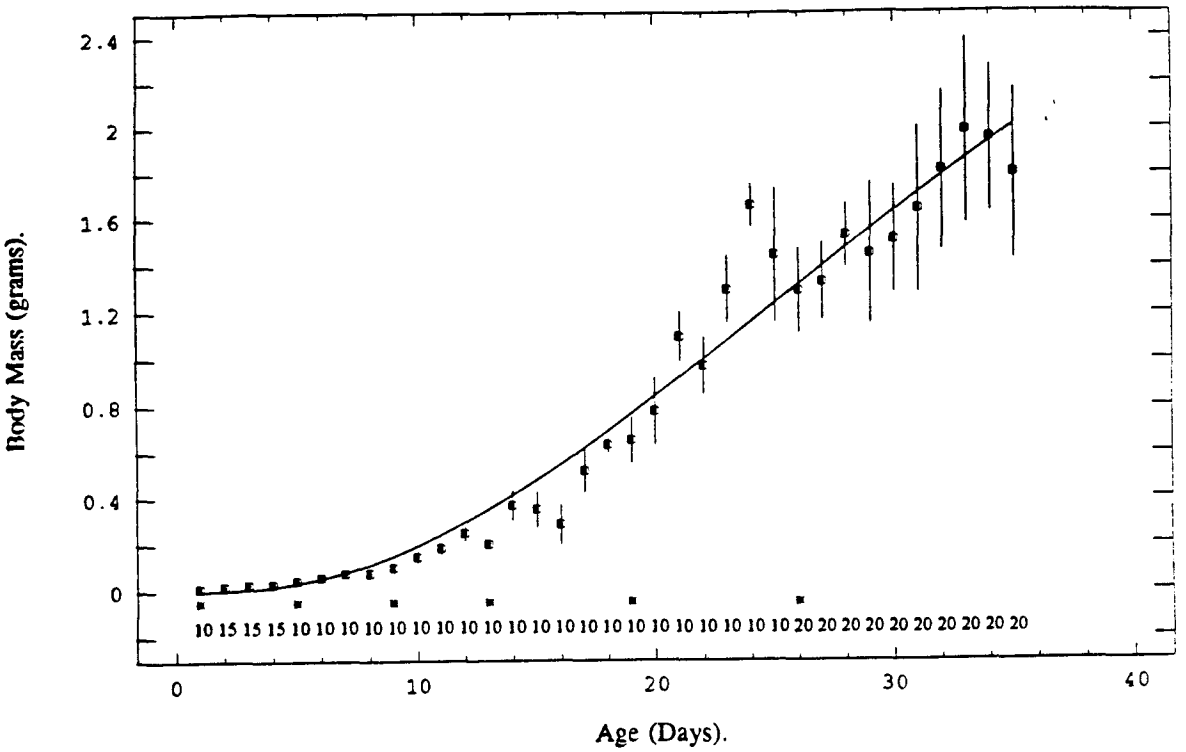

Figure 2.3.

The relationship of body mass to the age of the locust. Data are reported as means and standard errors of the mean. The regression is fitted to the Von Bertalanffy relation with the following form: Mass = $4.027(1-e^{-.045\ Age})^3$ (F_s=987.8; df=2,33; r^2=.962). Numbers listed along the abscissa indicate the sample sizes for each day, and are the same for figures 2.4a and 2.4b.

individual will grow in a logarithmic way up to a point where ingested calories are diverted from general somatic growth and to reproductive growth, seem reasonable in this case as growth levelled off at approximately sexual maturity (ca. day 30).

All allometric relationships reported here proved to be significant to the 0.05 probability level. A significant sexual dimorphism develops in adults where the females are approximately 50% more massive than males (ANOVA, F_s = 21.969, df. = 192, $p > 0.05$). Analysis of covariance indicated no significant effect of sex, beyond the effect of mass on any of the morphological or mechanical parameters measured (ANCOVA, $F_s = 2.451$ for mesothoracic tibiae diameter on body mass--the relationship most closely approaching significance, df. = 1,378). Therefore, data from both sexes were pooled in each regression.

Morphology. Figure 2.4 shows the change in tibial length (Fig. 2.4a.) and diameter (Fig. 2.4b.) with increasing age. Analysis of variance indicates significant heterogeneity between groups, and Newman-Keuls multiple range tests indicate that each instar is a homogenous, independent group. This confirms that the sample values from the population are reflecting what we believe to be occurring in individuals, that the external dimensions of leg length and diameter are not changing within instars. Analysis of variance of residuals indicated that tibial length and diameter were independent of body mass within each instar, biasing the overall allometric relationships of length and diameter against body mass (Draper & Smith, 1981). Therefore, all values for

Figure 2.4a.

Plot of tibial lengths for mesothoracic (◇) and metathoracic (□) legs with increasing age showing discontinuous growth across instars. Individual points represent means and 95% confidence intervals to show the similarities within, and differences between instars.

Figure 2.4b.

Plot of tibial diameters increasing with age. The symbols are the same as in figure 4a.

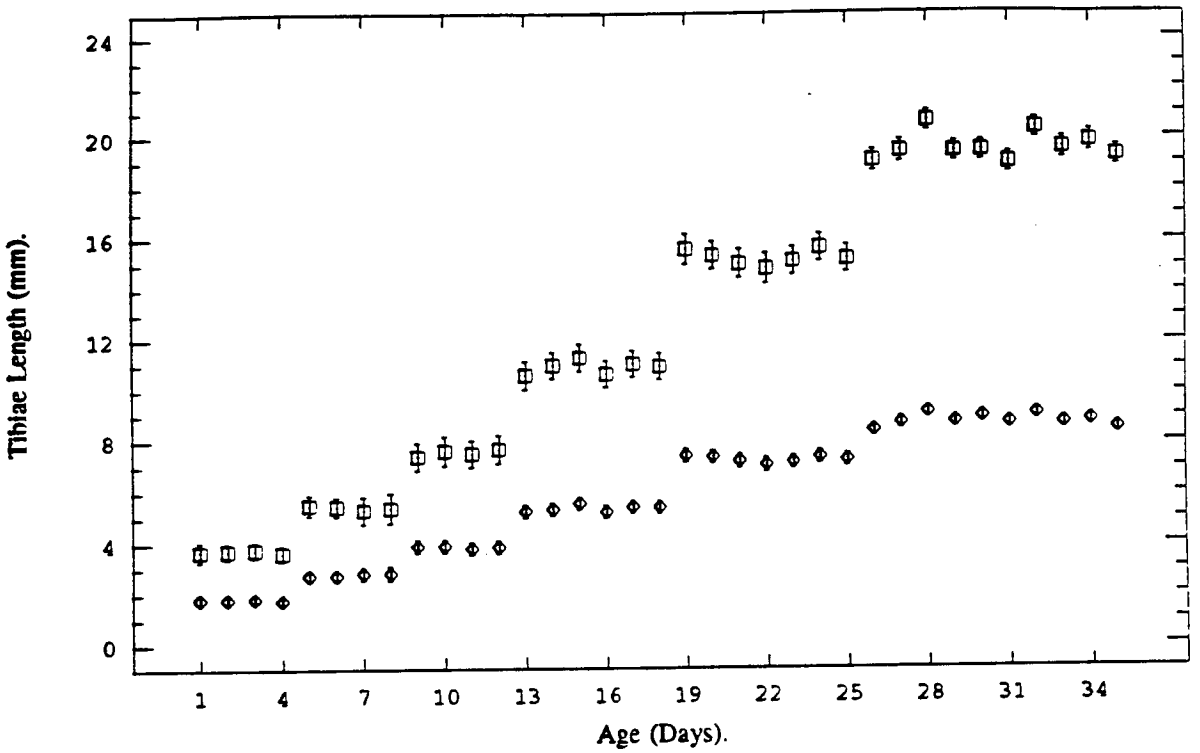
Tibiae Length (mm).
0
4
8
12
16
20
24
1
4
7
10
13
16
19
22
25
28
31
34
Age (Days).

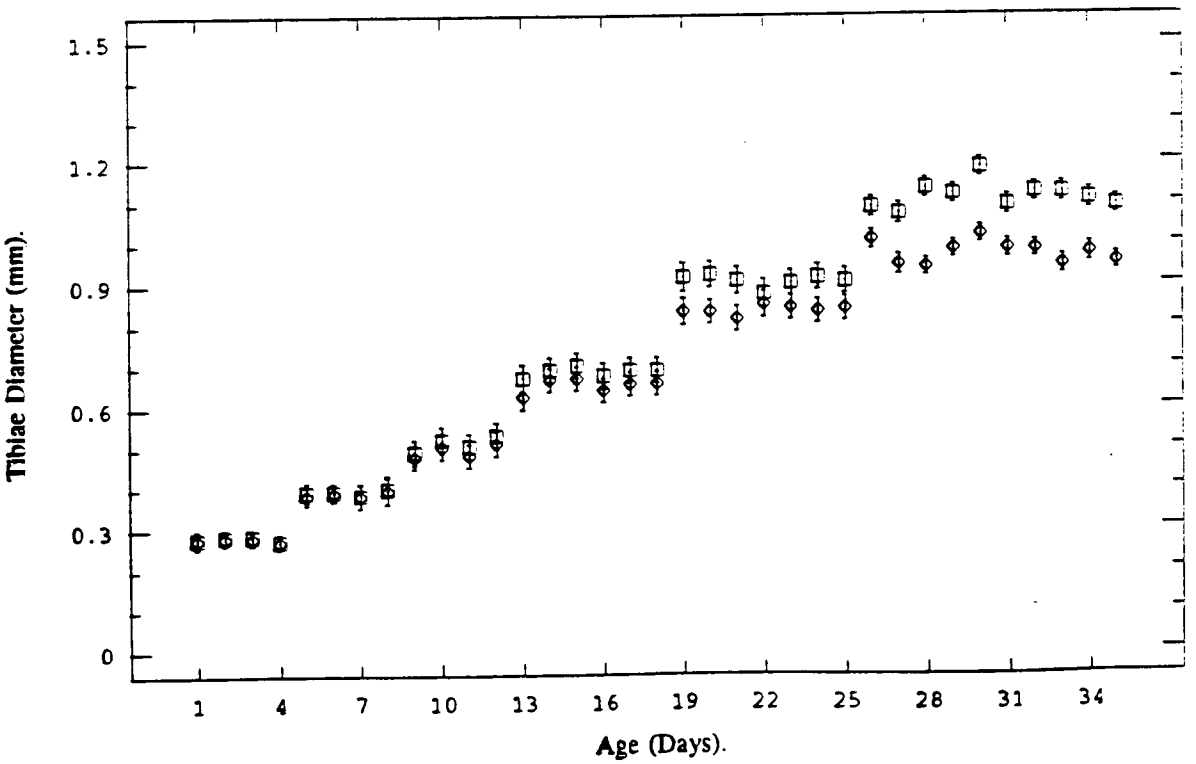
Tibiae Diameter (mm).
0
0.3
0.6
0.9
1.2
1.5
1
4
7
10
13
16
19
22
25
28
31
34
Age (Days).

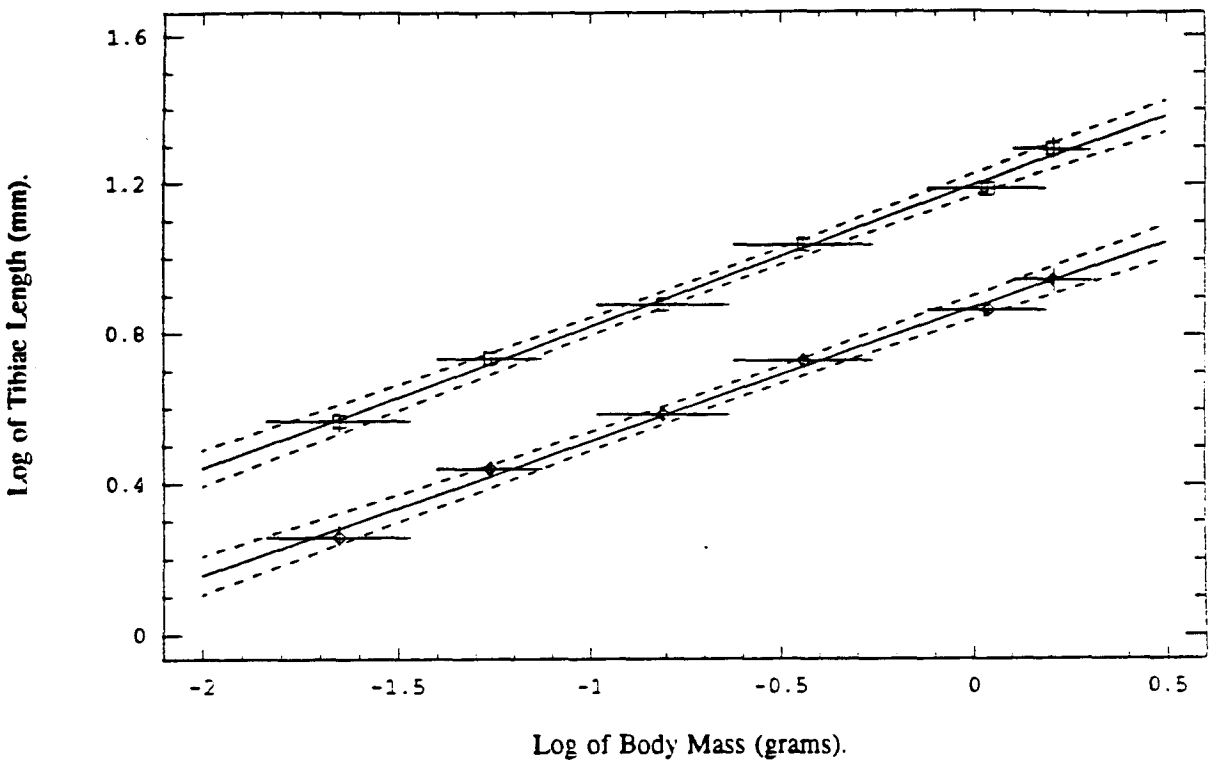

Figure 2.5.

The relationship of the log of tibial length and the log of body mass for mesothoracic (◇) and metathoracic (□) legs. Individual points represent means and standard errors for each variable for each instar. The equation of the regression for the mesothoracic legs is $y = 0.868 + 0.356 \times X$ (F_s=850.3; df=1,4; r^2=.9963). The equation of the line for the metathoracic legs is $y = 1.195 + 0.377 \times X$ (F_s=1074.1; df.=1,4; r^2=.9953). The dashed lines are the 95% confidence limit of the regression line.

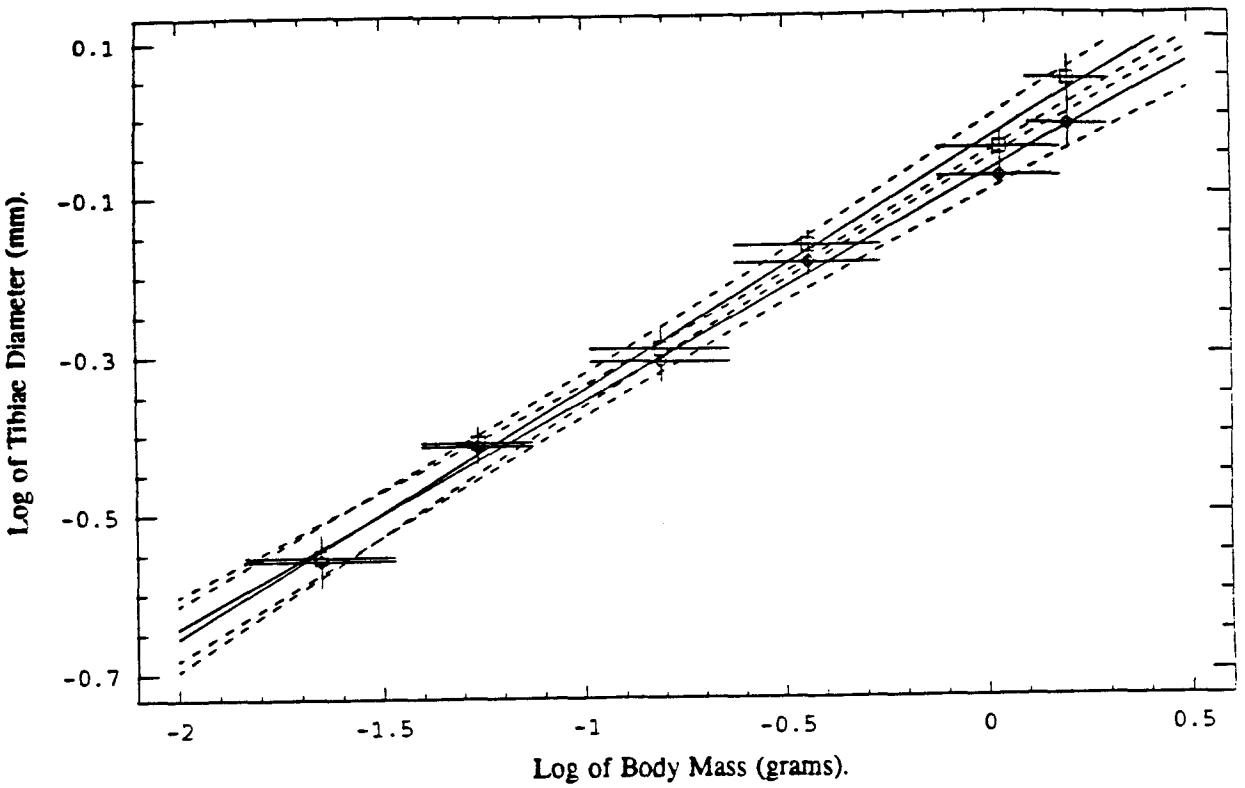

Figure 2.6.

The relationship of the log of tibial diameter and the log of body mass for mesothoracic (◇) and metathoracic (□) legs. Individual points represent means and standard errors for each variable for each instar. The equation of the regression for the mesothoracic legs is y = -0.074 + 0.284 × X (F_s=881.9; df=1,4; r^2=.9955). The equation of the line for the metathoracic legs is y = -0.033 + 0.311 × X (F_s=1004.0; df.=1,4; r^2=.9960). The dashed line is the 95% confidence limits of the regression line.

body mass, and tibial length and diameter within each instar were pooled, and a mean value for each variable for each instar was used in the allometric regressions. These data also indicate that within each instar the metathoracic legs are approximately twice as long as the mesothoracic legs, while having approximately the same diameters

Figure 2.5 and 2.6 show the log transformed plots of leg length and diameter against body mass. Metathoracic tibial lengths followed the relationship of body mass raised to the 0.38 power (SE = 0.01, r^2 = 0.996), while mesothoracic tibial lengths scaled to mass to the 0.36 power (SE = 0.01, r^2 = 0.995) (Fig 2.5.). Metathoracic tibial diameter scaled to body mass to the 0.31 power (SE = 0.01, r^2 = 0.996), and mesothoracic diameter scaled to the 0.28 power (SE = 0.01, r^2 = 0.996) (Fig. 2.6.). This indicates that as the animal grows, the limb segments are getting relatively longer and more spindly rather than maintaining a constant proportion of length to diameter, as is predicted by geometric similarity (GSM), or becoming stouter as predicted by distorting allometries (ie. ESM or CSSM). In each case, the slopes of the allometric relationships between the leg dimensions and body mass were not statistically distinguishable between the metathoracic and mesothoracic legs.

A convenient index for comparison is the allometric relationship between tibial length and diameter. The distorting allometries (ie. ESM & CSSM) predict that lengths will scale to diameters raised to a power less than one, resulting in increasing stoutness. Geometric similarity predicts an exponent of exactly 1.0 or isometry. Locust tibial lengths, however, scale to diameter raised to a power

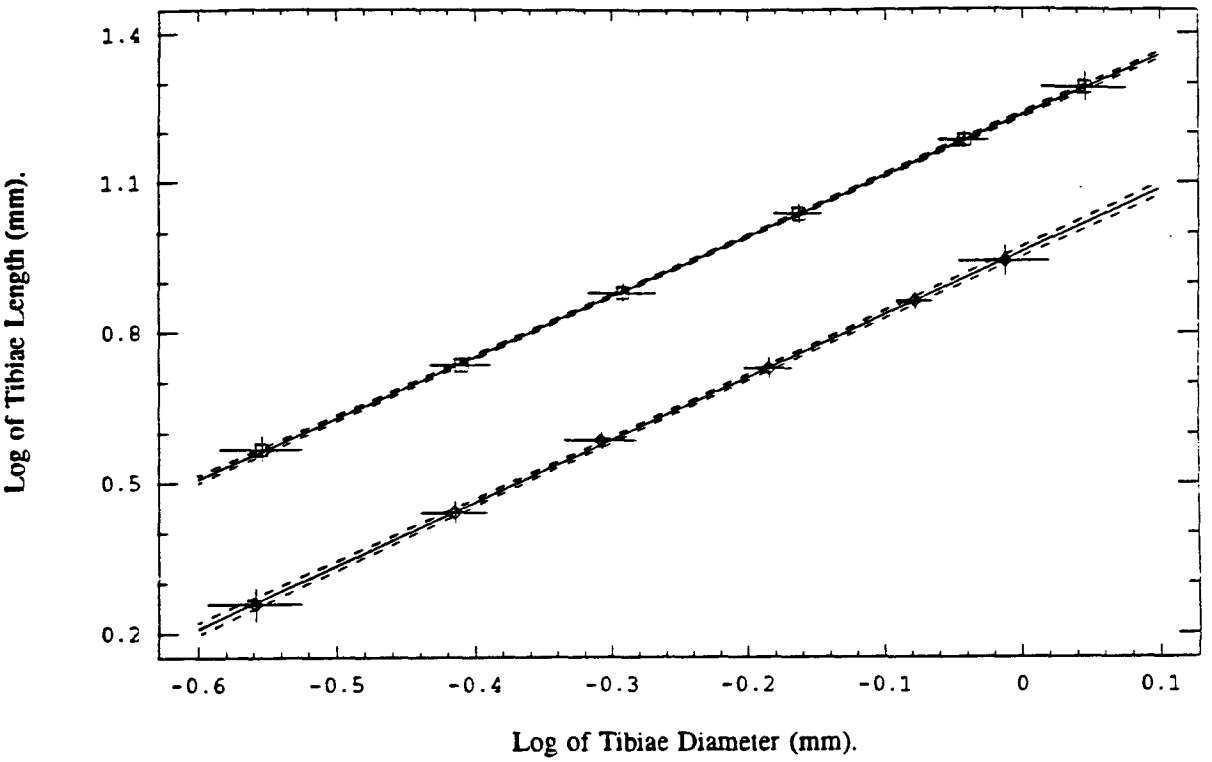

Figure 2.7.

The relationship of the log of tibial length and the log of tibial diameter for mesothoracic (◇) and metathoracic (□) legs. Individual points represent means and standard errors for each variable for each instar. The equation of the regression for the mesothoracic legs is y = 0.961 + 1.252 × X (F_s=12537.4; df=1,4; r^2=.9997). The equation of the line for the metathoracic legs is y = 1.234 + 1.212 × X (F_s=35038.2; df.=1,4; r^2=.9999). The dashed line is the 95% confidence limit of the regression line.

greater than one (1.21, SE = 0.01, $r^2 = 0.999_9$ for metathoracic legs and 1.25, SE = 0.01, $r^2 = 0.999_7$ for mesothoracic legs, Fig. 2.7.). These exponents are significantly higher ($P<0.01$ in both cases) than any existing allometric model predictions. Thus the tibiae in *Schistocerca* scale in a manner that is not only different in value from the existing models, but in direction as well. As was the case above, the slopes of the allometric relationships for leg morphology were statistically indistinguishable between the metathoracic and mesothoracic legs.

Mechanical Measurements. Figure 2.8 shows a representative spectrum of storage and loss stiffness values across the sampled frequency span. There appears to be virtually no frequency dependence to the data. The deviation of the relationship between both storage and loss stiffness and frequency from a slope of zero is significant, but only results in a 6.4% change in actual storage stiffness per decade change in frequency. Results reported by Bennet-Clark (1975) indicated that the jump impulse duration is approximately 25 to 30 ms. Although the impulse is a transient event, and therefore difficult to correlate with steady state vibration (vis a vis a biologically relevant strain rate), I decided to use the impulse duration as a measure of the half-cycle period and use 22.5 Hz (ie. a 5 point average between 20 and 25 Hz) as my reference frequency for comparison between samples. The relatively larger scatter of the energy loss data (**E"I**) is due to its dependence on what is, in this case, the sine of a small angle (Eq. 2.3), whereas the energy storage stiffness (**E'I**) depends on the cosine of a small angle and is smoother (Eq. 2.2). The approximate 30 fold

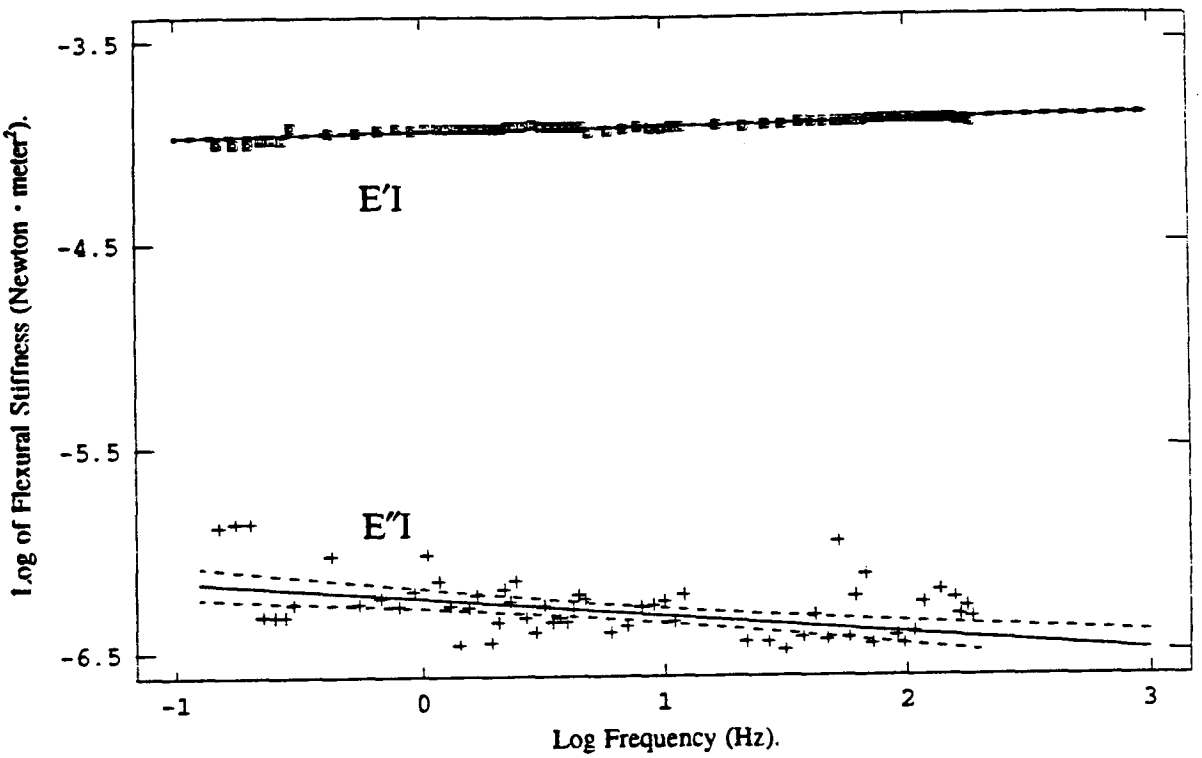

Figure 2.8.

Mechanical test data showing the log of flexural storage stiffness (**E'I**) and the loss stiffness (**E"I**) against the log of frequency of the imposed deformation for an adult locust of 34 days of age along with their regressions. The equation of the regression for the energy storage stiffness is $Y = -3.948 + 0.026 \times X$ (F_s=217.7; df=1,67; r^2=.7646). The equation of the regression for the energy loss stiffness is $Y = -6.238 - 0.085 \times X$ (F_s=19.682; df=1,67; r^2=.2271).

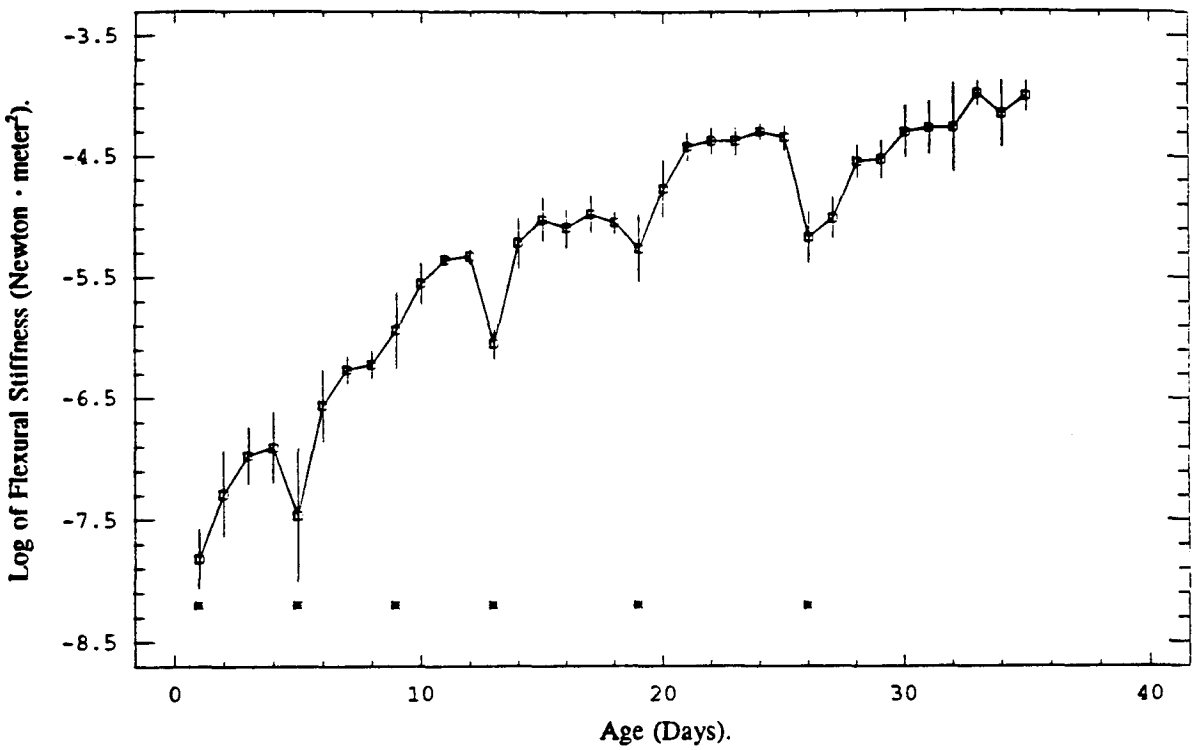

Figure 2.9.

Changes in the log of flexural storage stiffness with age. Data points are mean values with standard error of the mean. Data from individuals on the first day following a moult are denoted by *'s.

difference in energy and loss terms results in a resilience of 91% for this data set.

The time course of changes in the flexural stiffness (**E'I**) of the metathoracic tibiae describes a series of asymptotic curves, where the stiffness is relatively low immediately after a moult and increases within the next 24 - 48 hours by approximately an order of magnitude (Fig. 2.9). This seems to be a reasonable consequence of the protein cross-linking and cuticle dehydration that occurs during this period (Neville, 1975, Vincent, 1980). The lack of an appreciable decrement in stiffness on the first day of the third instar may reflect an uncertainty in aging the insects (+/- one half day) at a point where the stiffness is changing rapidly, rather than a fundamental difference in the cuticle's behaviour at that point.

The fact that the stiffness of the tibiae is relatively low immediately after moulting suggested that it might be prudent to create a separate data set for allometric analysis that excluded all stiffness values from individuals on the first day post-moult, thereby preventing the analysis of the overall scaling programme from being biased by the transient physiological events of cuticle stiffening in moulting. Flexural storage stiffness scaled to body mass raised to the 1.59 power (SE = .02, r^2 = .937) for all data, and to the 1.53 power (SE = .02, r^2 = .954) for the data without the first-day of instar individuals (Fig. 2.10). We regard the latter value as characteristic of functionally equivalent states in the population (see discussion) and appropriate for scaling comparisons.

A full series of mechanical measurements was not made on the mesothoracic tibiae, but morphological measurements indicated that within

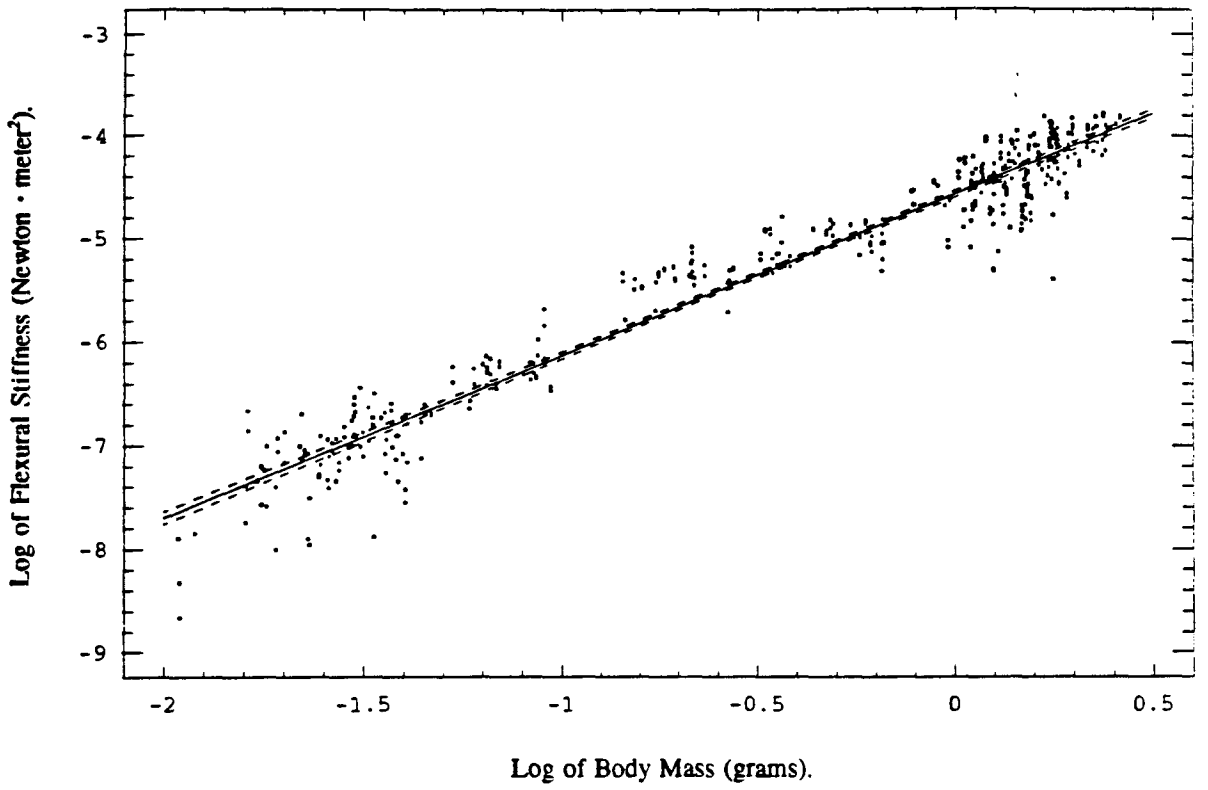

Figure 2.10.

The relationship of the log of the flexural storage stiffness and the log of body mass. Each point is the result of one mechanical test like that shown in figure 8. These data exclude points collected from individuals on the first day after each moult. The equation for the regression is $y = -4.566 + 1.532 \times X$ (F_s=7637.8; df.=1,426; r^2=.9442).

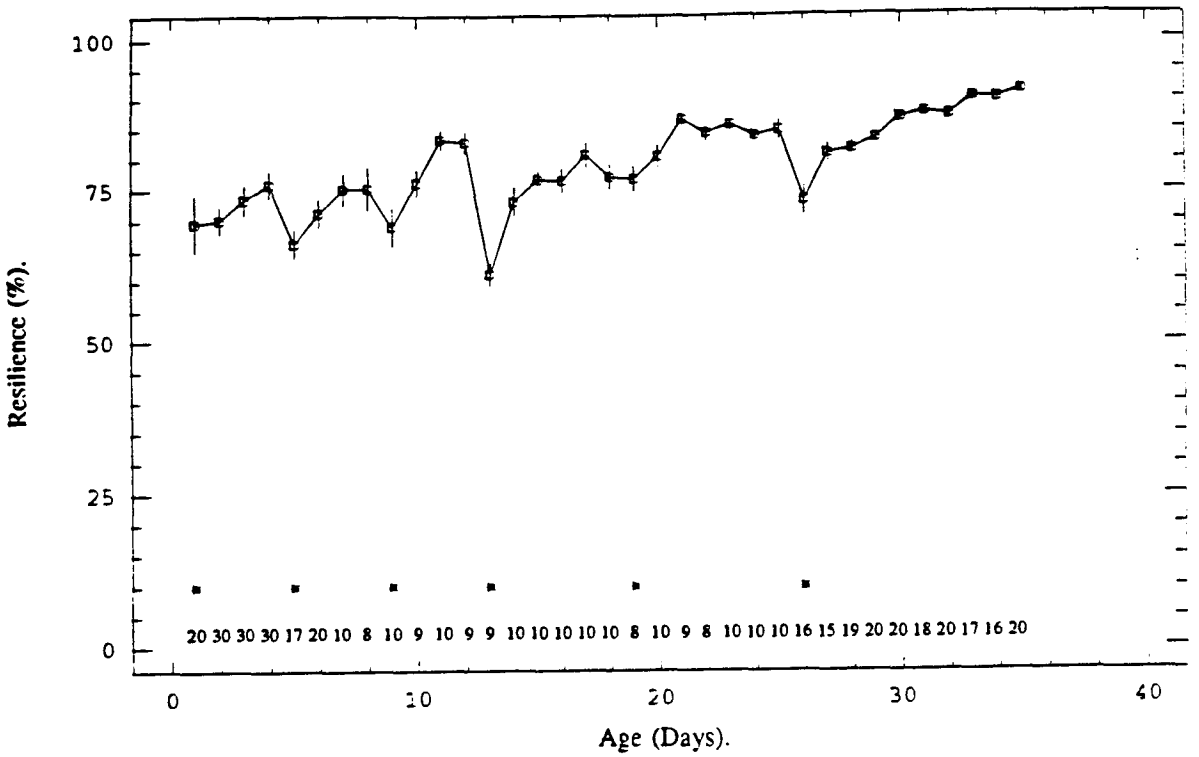

Figure 2.11.

The time course of change in resilience of the metathoracic tibia with age. Data are reported as mean values and 95% confidence limit for each day. Data from individuals on the first day following a moult are denoted by *'s. Numbers listed along the abscissa indicate the sample size for each day.

each instar they had virtually the same diameters as the metathoracic tibiae. Thus, one may expect that mesothoracic tibiae will exhibit the same flexural stiffness as metathoracic tibiae. Mechanical analysis of test pieces of equal lengths of metathoracic and mesothoracic tibia from five, 35 day old adults showed this to be the case. There was no statistical difference in the mean flexural stiffnesses ($t_s = .9918 < t_{.05(4)} = 2.776$).

The time course of resilience, shown in figure 2.11, demonstrates that resilience values also increase asymptotically from local minima on the first day of each instar and achieve higher values over time. Significant differences do exist among means across the entire life history (ANOVA of arcsine transformed resiliences, $F_s=15.928$; df.=34,460). However, it is impossible to say if this represents a real change in mechanical properties, or rather that the smaller, more difficult to handle specimens have a greater variance and therefore lower mean due to the potentially truncated distribution of resilience values (ie. resilience can not be greater than 100%). It is interesting that the mechanical resilience values for the adults approach an average value of 93%. This is very similar to the values of 93% for sheep plantaris tendon (Ker, 1981), 97% for locust resilin (Jensen and Weis-Fogh, 1954) and 91% for the most resilient synthetic rubbers (Ferry, 1980).

DISCUSSION

The scaling of *Schistocerca* tibiae results in relatively longer and spindlier skeletal elements, while existing allometric models predict at the least isometry,

if not distortions away from increasing spindliness and toward stoutness. This empirical scaling relation deviates both from theoretical predictions (McMahon, 1980, 1984, Bertram and Biewener, 1990) and from some empirical observations (McMahon, 1975, Prange, 1977, Bertram and Biewener, 1990). However, it is in very close agreement with Carrier's (1983) observations for the ontogenetic scaling of limb bones in the jack-rabbit, *Lepus*. The nature of the existing allometries that predict distortions of morphology is that when beams are longer than a critical length, with respect to their diameter and their material properties, they will either buckle and fail or will deform to a degree that is incompatible with the function of the skeletal system. In the literature it is generally assumed that design strategies must increase the mechanical stiffness of skeletal support structures, presumably by changes in morphology that increase the amount of load bearing material, to compensate for increases in the mass of the structure (eg. ESM or CSSM). Indeed, in one case where limb bones became relatively more slender in ontogeny, producing a potentially more deformable structure, there was an observed increase in material stiffness of an order of magnitude (Carrier, 1983). This makes it important, in the context of locust tibial scaling, to determine what actually happens to the mechanical properties of the leg because the observed morphology predicts the legs are becoming relatively more deformable as the animals grow.

The various scaling models can be used to predict how the flexural stiffness could scale with increasing body mass. The flexural stiffness has two components; **E**, the elastic modulus of the material from which the beam is

made, and **I**, the second moment of area--a measure of the distribution of material across the beam's cross-section. For now we may assume that small locusts and large locusts are made of the same material, so that **E** is a constant (Hepburn and Joffe, 1974b), and changes in **EI** reflect changes in **I**, which we can relate to morphology. For tubes of circular cross-section **I** is proportional to diameter raised to the fourth power. Although locust tibiae and vertebrate long bones do not have strictly circular cross-sections, we will assume cylindrical geometry, making **I** proportional to diameter to the fourth power. Given these assumptions, we can use equation 1, and allometric predictions, to anticipate how **EI** might relate to body mass. For GSM, diameter (d) scales to mass to the **⅓**, power and prediction of **EI** follows thus:

$$d \propto Mass^{.333},$$

so

$$I \propto (Mass^{.333})^4, \text{ or } Mass^{1.333}.$$

Geometric similarity, therefore, predicts that **EI** should scale to body mass raised to the 1.33 power. Via a similar process, elastic similarity predicts an exponent of 1.50, and constant stress similarity predicts an exponent of 1.60.

If one makes this same calculation using the morphological allometric relationships for the external dimensions reported here for the locust, and makes the same assumptions about **EI**, one predicts that **EI** in locusts should scale to body mass to the 1.244 power. This was not the case. The observed exponent for **E'I** as a function of body mass incorporating the complete data set was not significantly different from the prediction of constant stress similarity (slope or b

= 1.59, t_s = 0.498, df. = 507). The exponent for the data set excluding first-day of instar individuals was marginally different from the prediction made by elastic similarity (b = 1.53, t_s = 2.329, df. = 419). Both data sets were different from the prediction of 1.244 power. Therefore, in spite of a morphological programme that deviates from any expectation, the mechanical properties scale in a way that is consistent with existing models. This indicates that measurement of external dimensions alone does not provide sufficient information to determine the mechanical behaviour of the skeleton in this case. This observation poses two questions: 1) what is compensating for the morphological programme that allows the mechanics to achieve a mechanically reasonable result, and 2) what is the design "strategy" responding to in producing the observed unanticipated scaling programme?

At this point we are unable to resolve the extent to which either **E** or **I** or both are being modulated to produce the observed mechanical scaling. We are also unable to definitively discriminate the mechanical role of the endocuticle, either within or across instars. However, in chapter three we should be able to resolve the nature of the stiffness or shape changes in the tibia when we have examined the scaling of **I** in the tibiae used to collect the mechanical measurements and determined **I** for their endocuticular and exocuticular components.

Exo- vs. Endoskeletal Design. The sensitivity of **I** in thin walled exoskeletal systems to changes in wall morphology suggests a fundamental difference in

the use of exo- and endoskeletal designs. Currey (1980, 1984) has generated a model that predicts the optimal inner to outer diameter ratio (k) for a hollow bone. The model plays off the increases in **I** per unit mass that comes from using ever larger diameter, ever thinner, tubular skeletal members against the penalty of having to carry around the mass of the non-structural material inside the tube, such as marrow or fat. The analysis predicted different values for k based on the parameter that the design programme optimized, such as mass-specific strength or stiffness. For a selection of terrestrial vertebrate long bones the model seemed to effectively anticipate the relatively thick-walled tubing as an adaptation to resist failure from impact loading (Currey, 1984). A notable exception is the air-filled bones of birds, where the walls are relatively thin, in comparison to the marrow filled bones of terrestrial mammals (Currey, 1984). Figure 2.12 shows the ratio of total mass of bone and luminal contents to the mass of a solid bone with the same value of **I**, for various k ratios. An important feature of Currey's model is that the specific gravity of marrow is about half of that of bone, ie. the specific gravity ratio (Sg) is 0.50. In *Schistocerca* the Sg of the hemolymph to the cuticle material is about 0.88 (Wainwright et al., 1976). For the locust, the minimum that occurs at about k = 0.35 represents less than a 1% savings in mass over a solid rod morphology (Fig. 2.12). Measurements from the cross-section of the metathoracic tibial segment in a 10 day old adult *Schistocerca* from Jensen and Weis-Fogh (1962) show a $k \approx 0.92$, indicating that this skeletal member is not approaching the optimum associated with a minimum mass.

Figure 2.12.

Theoretical model of optimal internal to external diameter ratio (k) for hollow skeletal structures with various ratios of lumenal content to wall material specific gravity (Sg). This formulation describes beams that all have the same I. The line Sg = 0.88 is the condition that exists in *Schistocerca gregaria* which has a slight minimum at k = 0.35. Optimizing for mass specific stiffness, or impact resistance in the locust produces even shallower minima at lower k values. For a Sg equal to 0.0, which approximates the air-filled bones of birds, the model predicts thin walled tubes limited by buckling. As one moves to relatively less dense tubing material, the minima become shallower and predict thicker walls. Sg equal to 0.5 is the condition describing bone (Currey, 1980, 1984), which has a shallow optimum at $k \approx 0.7$. At Sg = 0.13 (steel tubing filled with an aqueous medium) there is a deep minimum at a k of 0.93 with a weight savings of about 51%. The boundary condition of equal specific gravities for the tubing and the inside contents (Sg = 1.00) predicts that the minimal mass solution occurs in solid rods rather than hollow tubes. The dashed vertical line originating at k=0.98 is the limit to k imposed by unstable buckling based on data for the material properties of locust cuticle (Vincent, 1980) and the analysis of buckling in Currey (1980). This represents the ultimate limit to being thin walled.

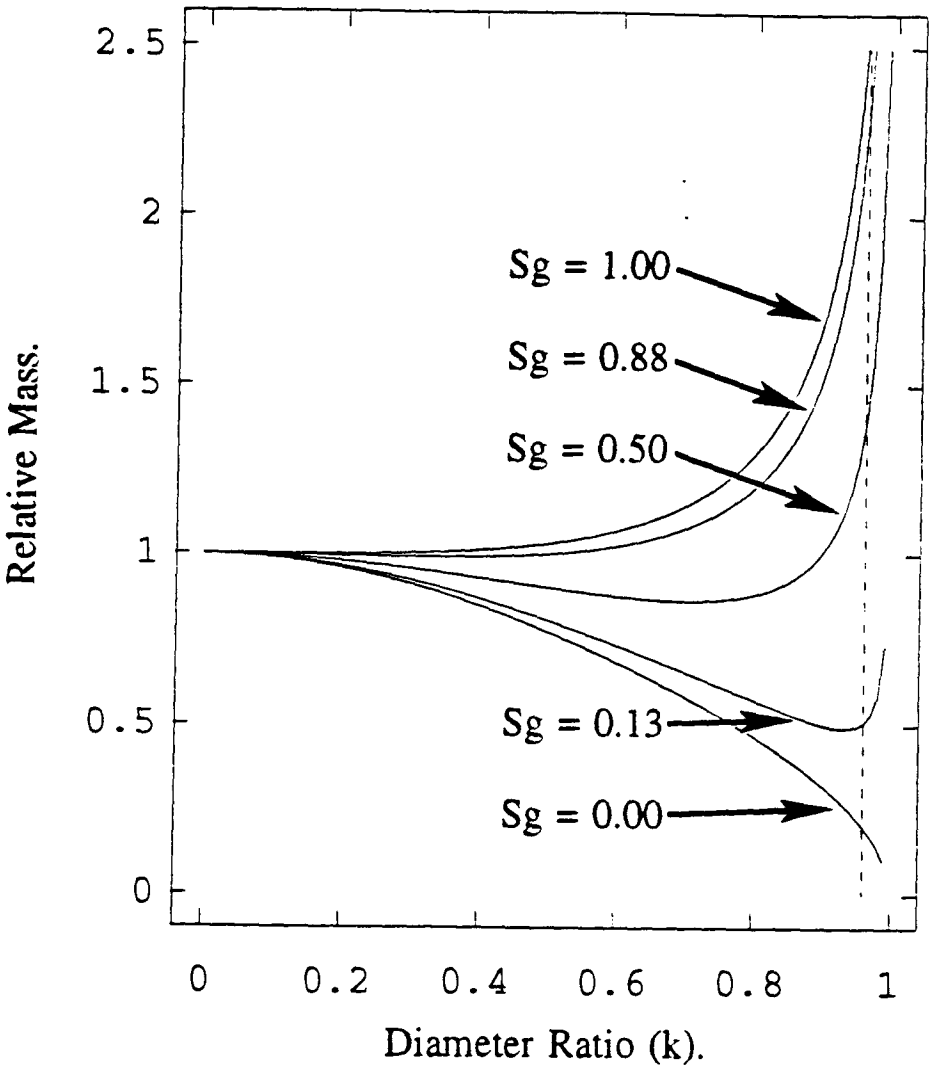
2.5
2
1.5
1
0.5
0
Relative Mass.
Sg = 1.00
Sg = 0.88
Sg = 0.50
Sg = 0.13
Sg = 0.00
0
0.2
0.4
0.6
0.8
1
Diameter Ratio (k).

The fact that insects do not have skeletons made from thick-walled tubing may indicate that minimizing the mass of non-structural material is not the over-riding design strategy. In exoskeletal animals, where the material on the inside of the tubing is the muscle and circulatory fluid, the added weight of this material may not represent the same penalty as marrow or fat does in vertebrates. If it is the locust's strategy to maximize its internal volume, then figure 2.12 predicts a thin-walled morphology that achieves large volume that is limited only by buckling (Currey, 1980). The dashed vertical line in figure 2.12 originating at k = 0.98 indicates the limit imposed by unstable buckling in a beam constructed from locust cuticle. The similarity of the observed k ratio and the buckling limit would seem to support the idea that the design in locusts maximizes internal volume.

Scaling in Cursorial & Jumping Insects. The observation that locusts' limb morphology deviates from the existing allometries while other exoskeletal animals like cockroaches and spiders do not (Prange, 1977), would seem to indicate that the exoskeletal body plan does not in itself determine the scaling of limb dimensions. That is, the exoskeletal design may have allowed this option, but evolution has not demanded that all such designs follow it. Therefore, it would seem reasonable to suggest that the developmental programme that produces the morphological scaling in *Schistocerca* represents an adaptation for some specific functional attribute. I suggest that the kinematic and energetic demands of jumping in growing animals may be met

more effectively by the allometry seen in the locust, rather than the geometrically similar growth pattern seen in cursorial animals like the cockroach.

If it is true that the morphology of the metathoracic legs is demonstrating a specialization for jumping, then we might hypothesize that the pro- and mesothoracic legs (ie. "walking legs") would scale in a manner different to the metathoracic leg ("jumping leg"), but this is not the case. It has been noted that prothoracic legs appear to follow isometry (Gabriel, 1985a); however, the data on mesothoracic legs clearly shows a similar developmental programme to the metathoracic legs. While maintaining the same scaling relationship to body mass across ontogeny, the metathoracic tibiae are twice the length of the mesothoracic tibiae. The third power dependence of deflection of a loaded beam on length (equation 2.1.) predicts, therefore, that the metathoracic tibiae are eight times more deflectable than the mesothoracic tibiae given the same flexural stiffness. Since equal lengths of mesothoracic and metathoracic tibia have the same flexural stiffness in adults, it seems reasonable to assume that the interleg similarity in stiffness per unit length would be maintained across ontogeny. Further, the peak loads during jumping are approximately 20 times the force of gravity (Bennet-Clark, 1975) and are distributed over only two jumping legs, whereas the loads of standing or walking (ca. 1 x the acceleration of gravity (**g**)) are distributed over six legs. The walking tibiae, then, may experience several hundred times less bending deflection in walking than are the metathoracic legs during jumping. Even in the case where a locust lands on a single mesothoracic leg at the end of a jump, the

kinetic energy would be absorbed by a single leg with one eighth of the compliance of each metathoracic leg. In this extreme case the mesothoracic leg would still experience four times less deflection than a metathoracic tibia. Even though the mesothoracic tibiae are probably not experiencing exclusively a bending load, this analysis indicates that they are distinctly over-built. Thus, the genetic constraint on the development of metameristic, morphological characters may limit the ability of natural selection to minimise the amount of extra material the animal carries around. It may turn out that the genetic mechanisms that control metathoracic leg development are linked functionally to the genetic control of mesothoracic legs and even perhaps to appendages on other segments of the body. Interactions across body segments, with respect to the control of expression of metameristic characters, have been seen in the bithorax gene complex in *Drosophila* (Lewis, 1978). Since jump performance, in terms of take-off velocity, is inversely dependent on body mass (Bennet-Clark, 1977), there would seem to be a benefit in keeping excess weight to a minimum. If so, then the overdesign of the mesothoracic legs may represent a penalty to be paid for the sake of having jumping legs that perform well and having a genetic control mechanism that is not specific to a single body segment. It may prove interesting to test this hypothesis by examining the scaling of antennae or mouth parts of the locust to determine the extent of this interaction.

Ontogenetic vs. Phylogenetic Scaling. In this study I have used ontogeny

as a model for the effect of body mass on the morphological and mechanical design of the limb skeleton of *Schistocerca*. I found a developmental programme that results in increasingly spindly legs, suggesting more easily deformable beams, but the mechanical properties are adjusted to produce elastically similar tibiae. I believe that this provides information about the mechanical design of jumping animals, but is ontogeny a justifiable model for the effect of body size? Is it fair to assert that the ontogenetic scaling observed in locusts demonstrates mechanical design principles? If it is, then we would expect to find similar scaling in other jumping animals.

It seems significant that the morphological scaling relationship reported here, while different from phylogenetic comparisons, is so similar to the ontogenetic morphological changes seen in the jack-rabbit (ie. tibia length $\propto$ tibia diameter$^{1.21}$ for locust, tibia length $\propto$ tibia diameter$^{1.30}$ for *Lepus*, Carrier, 1983). Also interesting is Carrier's observation that material stiffness and second moment of area of the metatarsal bones increase with the first power of body mass. This indicates that the flexural stiffness is increasing with the second power of body mass, faster even than the 1.53 power observed for locusts.

It is tempting to suggest that the similarity in *Schistocerca* and *Lepus* ontogenetic scaling is demonstrating a developmental strategy that is adopted generally by jumping animals. However, there is an important difference in the development of locusts and jack-rabbits that points to a potential danger in using ontogenetic observations to examine the effect of body size. This distinction lies in comparing animals that are not functionally similar. Both adult

locusts and adult jack-rabbits hop or leap as their mode of locomotion, but whereas juvenile locusts hop (Gabriel, 1985a), juvenile jack-rabbits prefer not to (Carrier, 1983). Carrier (1983) has reported that the neonate jack-rabbits (<300 grams) are "unsteady" locomotory performers, relying on crypsis to avoid predation. Over 600 grams, however they have developed good locomotor performance, and readily resort to jumping when startled. Whatever the pressure is that has resulted in the developmental programme in jack-rabbits, it is not the need to be a functionally adequate jumper over the entire ontogenetic range of body size. A jack-rabbit achieves high locomotor performance over only the final four fold range in body mass, while the locust achieves high performance, in terms of distance covered, at points within each instar over a 200 fold range in mass (Gabriel, 1985a). Interestingly, locusts start each instar as poor jumpers (Gabriel, 1985a, Queathum, 1991) with relatively soft cuticle (Fig. 2.9). Over the following 24 to 48 hours the cuticle stiffens by approximately an order of magnitude and their locomotor performance improves. Thus, it appears that locusts go through developmental changes within each instar that are similar to those that the rabbit goes through over its entire lifetime. In a sense, the rabbit's development is composed of a single "instar", while the locust's development is composed of functionally competent individuals that come in six different sizes. Since the post-24 hour individuals of each instar represent functionally similar locusts of different sizes, I feel confident that the scaling relationships reported here are providing important insights into the design of jumping animals.

Design in Jumping Tibiae. It is appropriate, therefore, to attempt to explain the observed skeletal scaling in the context of the locust's locomotor strategy. As Bennet-Clark (1977) points out, as animals get bigger their acceleration in jumping decreases, so that dynamic, mass-specific loading in jumping is decreasing at the same time that the relatively static accelerations encountered in standing or walking are increasing. The increasing slenderness of the tibiae may be a response to falling accelerations produced in the jump of large animals compared to small ones. If larger locusts produce less acceleration than small ones, then their longer limbs may be an adaptation to increase the time that their feet are able to do work on the ground. Adult locusts of 3.5 grams body mass produce approximately 20 **g**'s of acceleration (Bennet-Clark, 1975), while adult fleas (*Spylopsyllus cuniculus*) of 0.45 milligrams produce accelerations of over 135 **g**'s (Bennet-Clark & Lucey, 1967). Locusts tibial morphology may be following a programme that is designed to accommodate declining accelerations encountered with increasing body mass, rather than body mass per se. Therefore, scaling relationships that are attempting to explain the mechanical design programme relating morphology and body mass make predictions in a direction opposite to that seen in locusts. Counter to this argument, however, Scott and Hepburn (1976) have suggested that small locusts do not produce larger accelerations than adults. They report a constant relationship of approximately 10 **g**'s of acceleration in several African grasshoppers, as well as through the ontogenetic sequence of *Locusta migratoria*. None of their observations seems to be as large as the 20 **g**'s

reported by Bennet-Clark (1977) for adult *Schistocerca gregaria*. It would, therefore, be of value to know explicitly how the accelerations developed during the jump change from small to large locusts.

An alternate explanation for the morphological programme may lie in a re-interpretation of the function of the exoskeleton. Schmidt-Nielsen (1984) suggests that skeletons are rigid structures that act as either support beams or lever arms to be acted on by muscles to provide movement. Two observations in this study indicate that perhaps the locust tibial skeleton is acting not so much like a rigid lever arm, but rather as an elastic energy storage device. From equation 2.1 (arreanged to describe a cantilever) and a peak acceleration of 20 **g**'s (see above), the ground reaction force for a 0.003 Kg adult locust will produce a deflection at the end of the tibia on the order of 3 mm, or about 13% of the tibia length. In fact Brown (1963) has stated that some of his high speed films show the tibiae bending during jumps. The energy required to deform a linear spring is equal to one half of the product of the deformation and the force applied, which in this case is 1.2 mJ of energy for both legs together. If we incorporate a cuticular resilience of 92%, then approximately 1.1 mJ of energy are returned as elastic recoil from the tibiae during the jump. Bennet-Clark (1975) has reported that an adult female *Schistocerca gregaria* requires about 11 mJ for a jump. Thus approximately 10% of the total energy of the jump is recovered from energy stored in the tibiae. The relative increase in tibial spindliness with increasing size may represent an attempt to create a more deflectable beam, and therefore, a larger capacity energy reservoir, as

the peak accelerations are falling during ontogeny. Additionally, the high resilience values of 90 - 93% for tibial cuticle (Fig. 2.10) indicate that the material's properties are well matched to an energy storage function.

These observations suggest that it is more appropriate to think of locust tibiae as bending springs rather than simple rigid levers. This use of energy storage seems significantly different from other systems previously examined in that it does not act as a momentum collector, capturing kinetic energy from a muscular contraction in a previous stride as potential spring energy to be recovered as kinetic energy in the following stride. Instead the spring energy is stored and recovered in the same stride, not unlike the model proposed for primary flight feathers in pigeons (Pennycuick and Lock, 1976). Why then store it when mechanical hysteresis will only decrease the amount of muscular energy that does any useful work in locomotion? It may turn out that the energy stored in the tibia early in the force impulse in the jump is stored at a time when the mechanical advantage of the muscle-apodeme-tibia lever system is high, but the ability for the locomotor system to do work on the ground is low, and energy can be stored in the spring. That energy could then be returned later in time within the same loading event when the mechanical advantage of the muscle-apodeme-tibia lever system is low (Bennet-Clark, 1975), but the ability to do work is high. A useful metaphor for this type of design may be an archer's compound bow where eccentric cams alter the mechanical advantage of the bow on the arrow. When a loaded compound bow is released the force continues to rise as the arrow accelerates, producing higher velocities and

longer distances than a traditional bow where the force falls as the arrow is accelerated. It may prove that the tibial-springs are utilizing changes in mechanical advantage in the same manner, maximizing take-off velocity and as a result trajectory distance. This possible basis for a design strategy will be examined in more detail in chapter five.

CHAPTER 3.

SCALING MODULUS AS A DEGREE OF FREEDOM.

INTRODUCTION

In chapter two we learned that the scaling of external dimensions of the locust's legs does not predict the scaling of the mechanical behaviour of the legs in bending. The flexural stiffness of the tibiae scale in a manner that is similar to predictions based on the elastic similarity model, but the legs' external dimensions do not. So there is an "uncoupling" between the morphology and the mechanical properties of the legs. It was speculated that this uncoupling could be the result of two events. Either the second moment of area (**I**) of the legs could be related to the external dimensions in ways that are not obvious, or the material stiffness (**E**) of the cuticle could be changing to provide an additional degree of freedom in the design of the skeleton in accommodating increasing body size.

With respect to compensation, it is possible that the modulus of the cuticle material is altered to accommodate changes in morphology of the limb segment in order to maintain an elastically similar flexural stiffness. Certainly, the modulus increases during the immediate post-moult period of scleritization due to dehydration (Hepburn and Joffe, 1974a, Vincent and Hillerton, 1979, Vincent, 1980). Indeed, it may be that the material properties of the cuticle are different at different ages. Hepburn and Joffe (1974b) have suggested, however, that the cuticle of *Locusta migratoria* maintains a similar stiffness in tanned fifth instar and adult femoral cuticle. They suggest that the ratio of stiffness to mass is a constant for tanned cuticle across instars, and that this is a response to a

constant ratio of load developed in a jump to body mass across the instars (Hepburn and Joffe, 1974b). If the tanned cuticle of *Schistocerca* has the same modulus independent of age, then the design strategy that results in increasingly spindly legs in locusts must be fundamentally different than that observed for *Lepus*.

It is also possible that the distribution of cuticle material changes across instars, resulting in a change in **I** that is not reflected in a change in the externally measured diameter. The formula for **I** is

$$I = \int_{Y\ max\ in\ compression}^{Ymax\ in\ tension} y^2\, dA \qquad (3.1)$$

where dA is the increment of cross-sectional area located a distance y away from the neutral axis, a line through the centre of mass of the cross section normal to the bending moment (Gordon, 1978) (Fig. 3.1). The importance of this relation is that material away from the neutral axis contributes greatly to the stiffness of the test piece. Because the cuticular segments of locusts are thin walled cylinders, a small adjustment in the distribution of material on the **inside** of the cross-section of a locust leg could impart large changes in mechanical properties that are not easily inferred from measurement of external dimensions. The sensitivity to changes in internal material distribution is not necessarily true for the thick-walled bones of terrestrial vertebrates. Certainly, endocuticle is added after moulting within each instar (Neville, 1975), although it is not clear if material is added in a manner that would alter the relationship between the leg diameter and **I**. It is also not clear that accumulations of endocuticle contribute to changes in the mechanical properties of the tibiae. At apolysis

Figure 3.1.

A diagram of a beam of irregular cross-section to show the calculation of the second moment of area (**I**). The dotted line shows the neutral axis for bending loads applied in the vertical direction. The neutral axis passes through the centre of gravity, or centroid, of the cross-section. **I** is calculated as the integral of the incremental amounts of cross-sectional area (**dA**) weighted by their distance from the neutral axis squared ($\mathbf{y^2}$). This calculation was performed on video images by first identifying the centroid of the section, then summing the number of super-threshold pixel elements in each raster line weighted by the distance of that line from the centroid in raster lines squared. These values for each raster line were then summed across all of the raster lines in the cross-section.

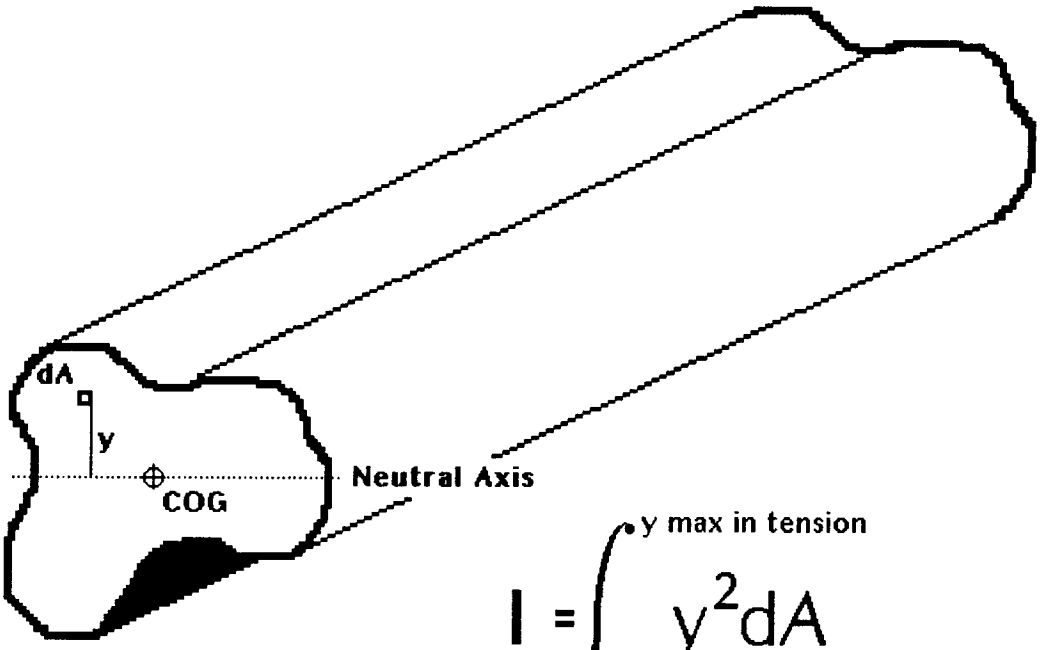

$$I = \int_{\text{y max in compression}}^{\text{y max in tension}} y^2 dA$$

(ca. 1-2 days before moulting, Queathum, 1991) there is a reorganization of the endocuticular material that involves an enzymatic digestion of the endocuticle (Zacharuk, 1976), presumably decreasing the second moment of area. However, I observed no decrement in flexural stiffness within any instar that can be correlated with the occurrence of apolysis (Fig. 2.9).

The accumulation of endocuticle also does not explain how changes might be mediated across instars. Gabriel (1985b) reported that the metathoracic tibia's cuticle thickness in the anterior direction relative to the lateral direction maintains a constant proportion across the juvenile instars, but increases by 50% in adults. This differential thickening could contribute to changes in **I** that are not reflected in external diameter. However, it is not known to what extent endocuticle accumulation is responsible for the increase wall thickness seen in adults, or why the discontinuity in wall thickness between all of the juvenile instars and the adults is not reflected in the flexural stiffness. What Gabriel's data do suggest is that if **I** is being adjusted to maintain the observed relationship between **E'I** and body mass, it is not, in juvenile instars at least, being accomplished with simple changes in wall thickness. Rather, there are probably changes in cross sectional shape that are producing changes in **I**.

In this chapter I examine this uncoupling explicitly by measuring the second moments of areas of the same legs that I tested in chapter two and tease apart the relative contributions of material stiffness (**E**) and distribution of material (**I**) to the scaling of flexural stiffness (**EI**).

METHODS AND MATERIALS.

Specimens used in this study were a sub-sample of the same specimens used in chapter two. Therefore, methods for animal husbandry, morphological measurement and mechanical testing are exactly the same. Specimens for measurement were chosen to represent the range of body masses covered in the life of the locust. Twenty-one first and second instars were chosen to represent small locusts, seven fourth instars were used to provide intermediate samples, and sixteen adults were used to provide values for the large animals. Additionally, fifty-six fifth instar samples were used to show how the changes in second moment of area occur within an instar. Individuals from the first day of each instar were eliminated from the analysis of scaling to make comparisons only between individuals that were felt to be functionally similar.

Following three-point mechanical testing described in chapter two, test pieces were placed in 37% formaldehyde solution for fixation and stored for later embedding and sectioning. Each tibia was dehydrated in an alcohol series and embedded. The technique used to produce cross-sections of the locust legs was different in the large and the small specimens. First and second instars' legs were embedded in paraffin and sectioned with a microtome at a thickness of 20 μm. Older locusts' legs were embedded in araldite. Each araldite block was sectioned at 800 μm with a bone saw. These 800 μm thick sections were epoxied to a glass slide and thinned to 0.005" (1.27×10^{-4} m) with alumina sand paper of increasing grit size. The surfaces were then polished with 600 grit polishing paper. Optical imperfections in the surfaces of the specimens

were filtered out by placing a drop of immersion oil on the section and then covering with a glass coverslip. Sections used for measurement were chosen from the approximate mid-shaft location on the tibia and had no distortions of profile associated with spurs. The cross-sections of the tibia were observed with a compound microscope fitted with a video camera. The labour intensive nature of this process resulted in the relatively small subset of the legs tested in chapter two being used in the analysis of second moment of area.

Images of the legs' cross-sections were captured from the video signal with a video frame grabbing computer interface (PIP 1024B, Matrox Electronic Systems Ltd., Dorval, Quebec, Canada) and stored in computer memory. Editing and analysis of the video images was accomplished with the V video image processing system (Digital Optics Ltd., Aukland, New Zealand) on a PC-type computer. Each 256 greyscale level video image was transformed into a binary image by manual detection of the perimeter of the entire cuticle and then the exocuticle alone and then setting a threshold greyscale level that defined the leg cross-section against the background. The perimeter of the endocuticle was produced by arithmetically subtracting the image of the exocuticle from that of the entire cuticle. The V software then integrated each of the video images to calculate the second moment of area of the cross sections that represented the entire cuticle, the exocuticular component, and the endocuticular component for each leg that was successfully sectioned.

Measurements of tibiae diameters of tibiae sections showed less than a 1% difference from values reported for the same specimens in chapter two.

Dimensional changes that resulted from the histological process were, therefore, ignored.

The image analysis software computes the second moment of area with the following summation:

$$I = \sum_y \sum_x (y-y_c)^2 \, dA$$

The image analysis software performs this integration numerically as the sum of pixel elements of a defined grey-scale level, weighted by the square of their distance from the neutral axis in raster lines for each raster line (Σ_x). The values are then summed over all the raster lines from the location of the centroid out to the margin of the section (Σ_y). Also mentioned previously, material at the margins of the cross section contribute greatly to the stiffness of the test piece. As such, orientation of the non-circular cross-sections, both in the mechanical testing and in the measurement of **I**, can have significant effects on the results. To control for the role of orientation, a sub-sample of images were printed as binary images. This sub-sample of images was recollected with the video image analysis equipment and **I** was calculated as the neutral axis was rotated through a series of orientations from +90° to -90°.

RESULTS

Within Instar Changes in **I** The time course of changes in flexural stiffness for the sub-population of locust legs used in this study are demonstrated in figure 3.2. **E'I** averaged a low value of 9.78×10^{-7} Nm^2 on the first day of the instar, and increased by about 30 fold by the second day. Thereafter, **E'I**

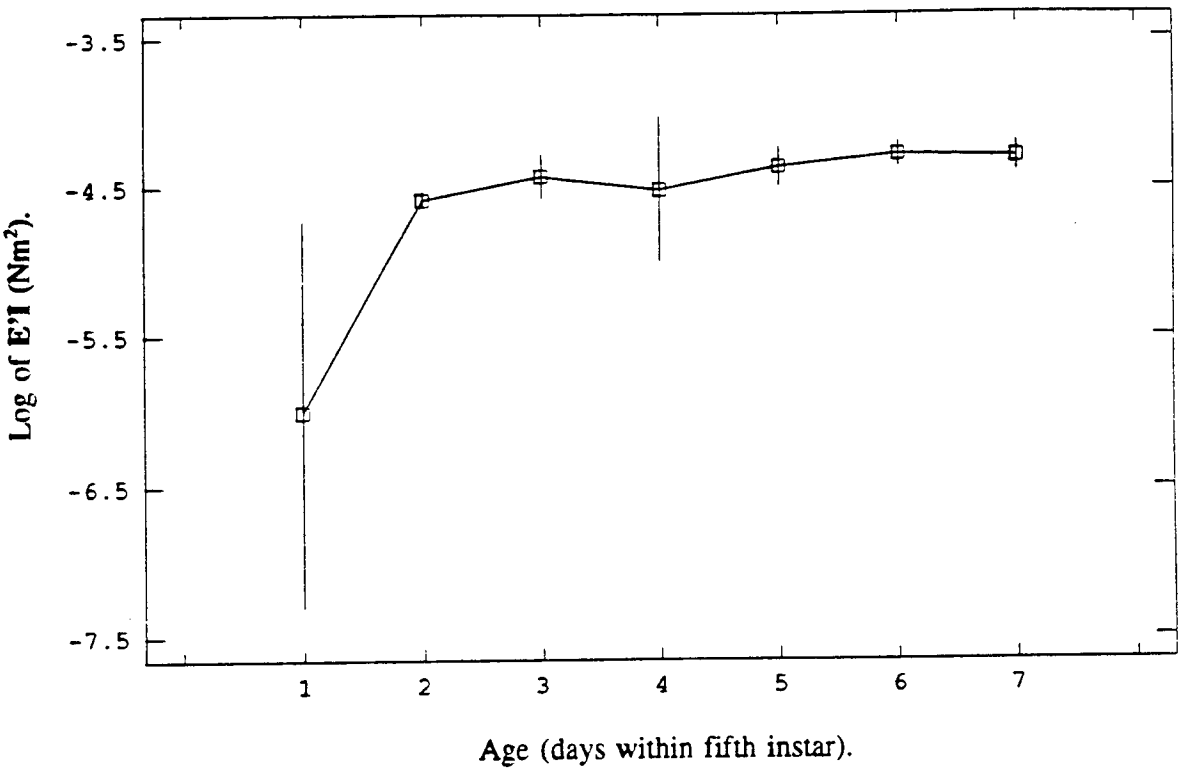

Figure 3.2.

The relationship of the log of flexural stiffness and age within the fifth instar. Data points are mean values and standard errors of the mean. Age is reported as days within the instar.

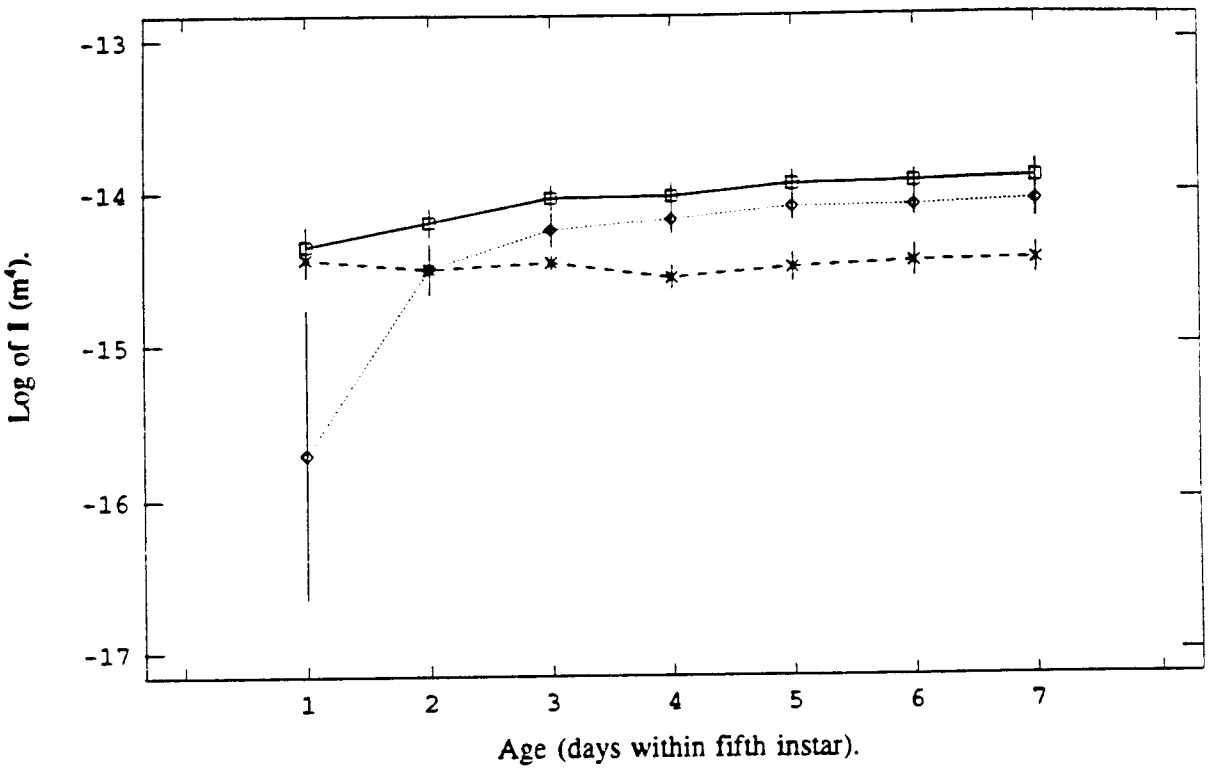

Figure 3.3.

The relationship of second moment of area (I) for the exocuticular (×), endocuticular (◇) and entire cuticle components (□) and age within the fifth instar.

remained relatively constant at a value of approximately 4.13×10^{-5} Nm^2.

The relative contributions of the cuticular components are shown in figure 3.3. Values of **I** for the exocuticle alone had a relatively high mean value of 3.60×10^{-15} m^4 on the first day of the fifth instar and remained close to this value for the remainder of the time spent in this instar. The endocuticular component started out at a low mean value of 1.95×10^{-16} m^4, but increased asymptotically until approximately day five where it attained a mean value of 8.61×10^{-15} m^4. The values of **I** for endocuticle on the first day of the fifth instar had a large variance as one of the samples had almost no measurable endocuticle. Examination of the actual cross-sections of the tibiae suggested that immediately after the moult there was no measurable endocuticle, and those samples that were taken on the first day that contributed to the non-zero estimate of endocuticular **I** reflected the uncertainty in measurement of age (+/- one half day).

Significantly, there appeared to be no detectable breakdown of the endocuticular material that could be correlated with apolysis on or about day five. However, it was observed that after day five there was a clear separation of the endocuticle from the underlying epithelial layer. Indeed, in some samples it was also possible to observe the next stage's tibia folded up within the lumen of the tibiae, indicating that the events that are associated with apolysis and the production of the next stage's exoskeleton had occurred without reducing the second moment of area of the endocuticular material.

The time course of changes in **I** for the entire cuticle is also plotted in figure 3.3. As this parameter is in fact the arithmetic sum of the **I** calculated for each of the components, it demonstrates a small increase from a mean value of 4.38×10^{-15} m^4 on day one to a mean of 1.22×10^{-14} m^4 on day three and then

remains fairly constant for the remainder of the instar.

Scaling In the sample of locust legs used in this chapter the flexural stiffness of the legs scaled to body mass raised to the 1.505 power (SE = 0.030, r^2=0.966). This slope is not significantly different from the slope of 1.532 (t_s=0.342, df. = 513, $p<0.05$) for the entire sample reported in chapter two. This indicates that the data used in this analysis represent the population as well as do those in chapter two.

Figure 3.4 shows the scaling relationships for the second moment of area for the various components of the cuticle with increases in body mass. **I** of the exocuticular component of the tibiae scaled to body mass raised to the 1.090 power (SE = 0.026, r^2=0.952). **I** of the endocuticular component scaled to body mass raised to the 1.258 power (SE = 0.031, r^2=0.949). **I**, calculated for the entire cuticle, scaled to body mass raised to the 1.195 power (SE = 0.027, r^2=0.957).

By normalizing the measured value of **E'I** from chapter two by the calculated value if **I** for both of the cuticular components we can estimate what the modulus of elasticity, **E'**, is for the tibiae. Figure 3.5 shows the scaling relationship of **E'** with increases in body mass. **E'** scales to body mass raised to the 0.311 power (SE = 0.033, r^2=0.511). This slope was significantly greater than a slope of zero (t_s=9.541, df.=89, $p>0.05$).

Values of **E'** ranged from a low value in first instars of 3.9×10^8 N/m^2 to a high value in adults of 1.6×10^{10} N/m^2. The estimated value of **E'** for adults is very similar to the value of 9.4×10^9 N/m^2 (960 kg/mm^2) reported by Jensen and Weis-Fogh (1962).

Orientation of Neutral Axis The shape of the tibia cross-sections are not

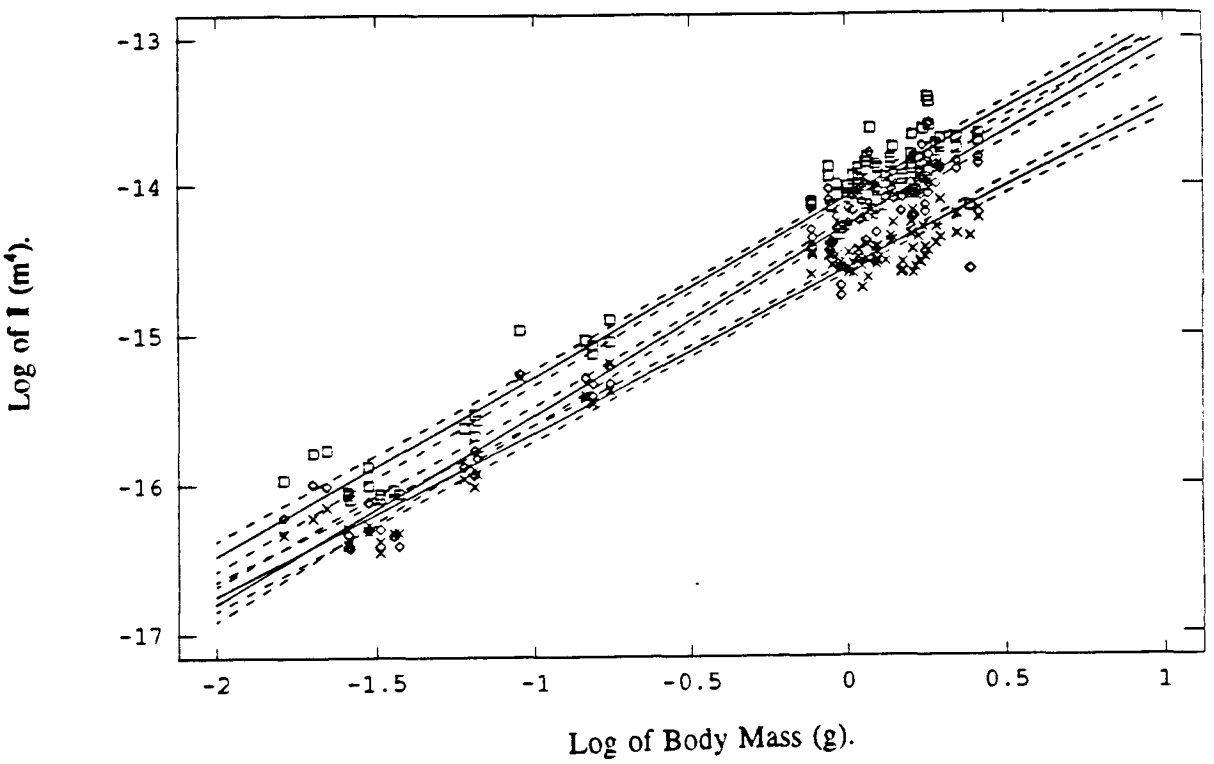

Figure 3.4.

The relationship of the log of second moment of area (I) for the exocuticular (×), endocuticular (◇) and entire cuticle components (□) and the log of body mass. The equation of the regression of exocuticular I on body mass was $y = -14.569 + 1.090 \times X$ ($F_s = 1738.74$, d. = 1, 89, $r^2 = 0.9523$). The equation of the regression of endocuticular I on body mass was $y = -14.283 + 1.258 \times X$ ($F_s = 1611.19$, df. = 1, 89, $r^2 = 0.9488$). The equation of the regression for the entire cuticle's I on body mass was $y = -14.092 + 1.195 \times X$ ($F_s = 2016.63$, df. = 1, 89, $r^2 = 0.9568$).

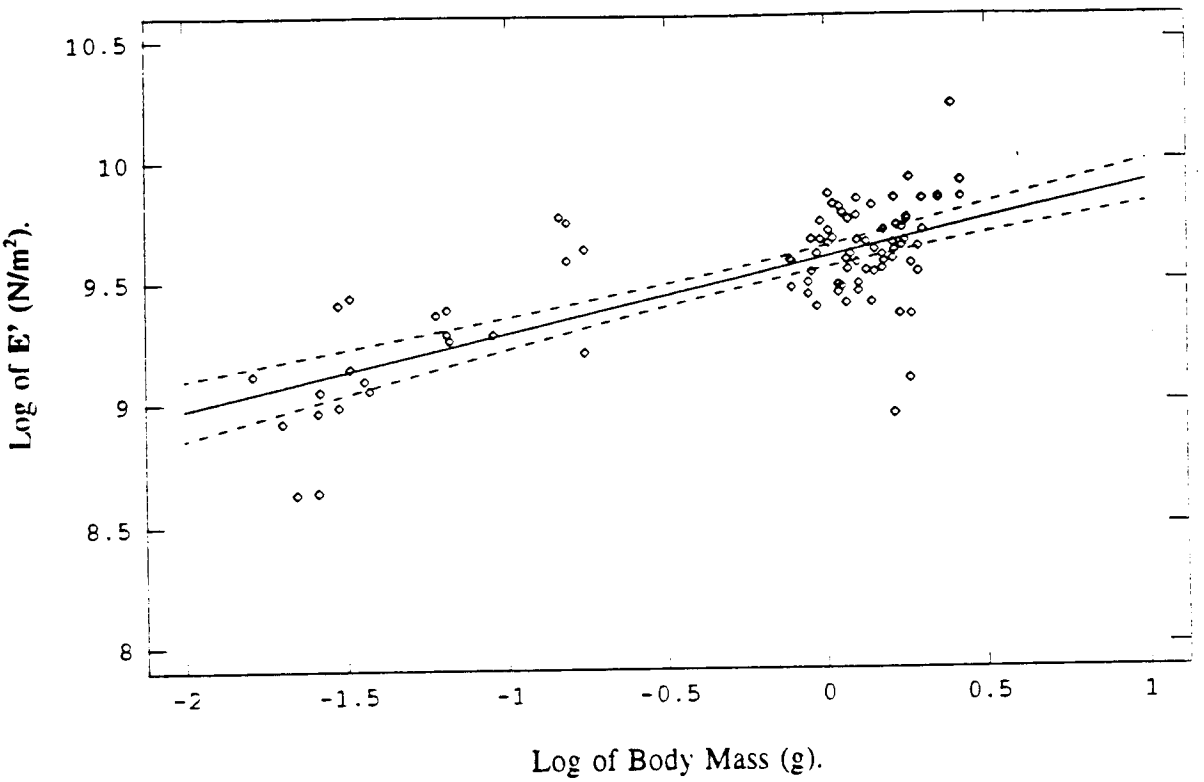

Figure 3.5.

The relationship between the log of tensile modulus (**E′**) and the log of body mass. The equation of the regression **E′** on body mass was y = 9.596 + 0.311× X (F_s = 91.040, d. = 1, 89, r^2 = 0.5113). **E′** was calculated for the entire cuticle treated as a homogeneous and continuous structure, see text for discussion.

Figure 3.6a.

Example cross-section from a fifth instar locust meta-tibia. The top of the picture is the anterior direction. For scale, the diameter of the section in the anterior-posterior direction is 2.523 mm.

Figure 3.6b.

Example of section shown in figure 3.6a processed for calculation of **I** for the entire cuticle. The inner and outer margins of the image in figure 3.6a have been defined manually, and the area of the section has been assigned a single grey-scale value. The image analysis software then performs the calculation on the image, summing over all the pixels that are of a pre-defined grey-scale level.

Figure 3.6c.

The same section as in figure 3.6a & b with the margins defined only for the exocuticle.

Figure 3.6d.

The same section as in figure 3.6a, b & c with the margins defined only for the endocuticle.

a)

b)

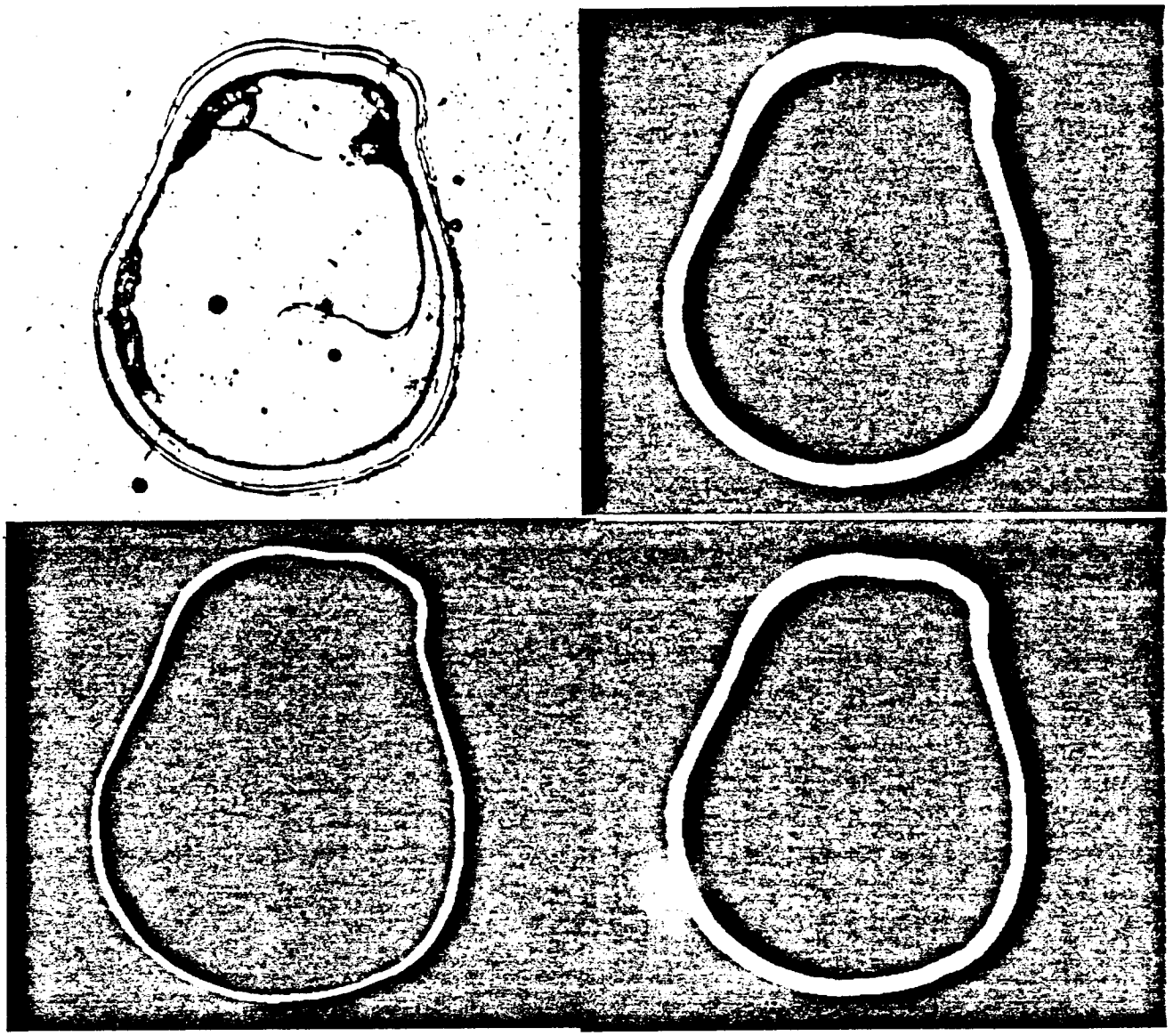

c)

d)

circular or even elliptical. They form a very characteristic shape that imparts potentially important mechanical behaviour. Figure 3.6a shows a representative cross-section from a fifth instar locust's tibia. The relatively circular, posterior margin and relatively thicker walled corners on the anterior lateral margins are very characteristic. The necking that produces the concavity at approximately the one quarter to one third point from the anterior to the posterior margin co-occurs with a membranous connection that spans the lumen of the tibia. Immediately after a moult when the cuticle is relatively soft, this membrane may provide a tensile stay that prevents the tibiae's cross-sections from becoming circular until the cuticle hardens.

Figure 3.7 shows how the value of I for the cross-section of six legs changes as the neutral axis is rotated through a range of angles from +90° to -90°. Individual legs show a local minimum of I along the anterior-posterior axis, with I increasing by as much as 3% with a rotation of 5° to either side. The average behaviour shows a more modest increase in stiffness as the neutral axis is rotated through $\pm$ 5° of 0.4%. The average values for I only drop by an average value of 4.54% when rotated through $\pm$ 20°. This is contrasted with an ellipse of similar aspect ratio where I falls by 6.40% (Fig. 3.8).

So far, I have talked about cross sections that were free of any morphological feature that was associated with spurs, but spurs do exist and their contribution to the mechanical behaviour of the tibiae must be considered. The presence of spurs produces a bilaterally asymmetrical distortion in the relatively circular perimeter of cuticle along the posterior margin of the tibiae cross-sections. The distortion takes the form of a bump that puts more material away from the neutral axis on alternating sides of the tibiae. Presumably, this distribution of material increases I and shifts the orientation of

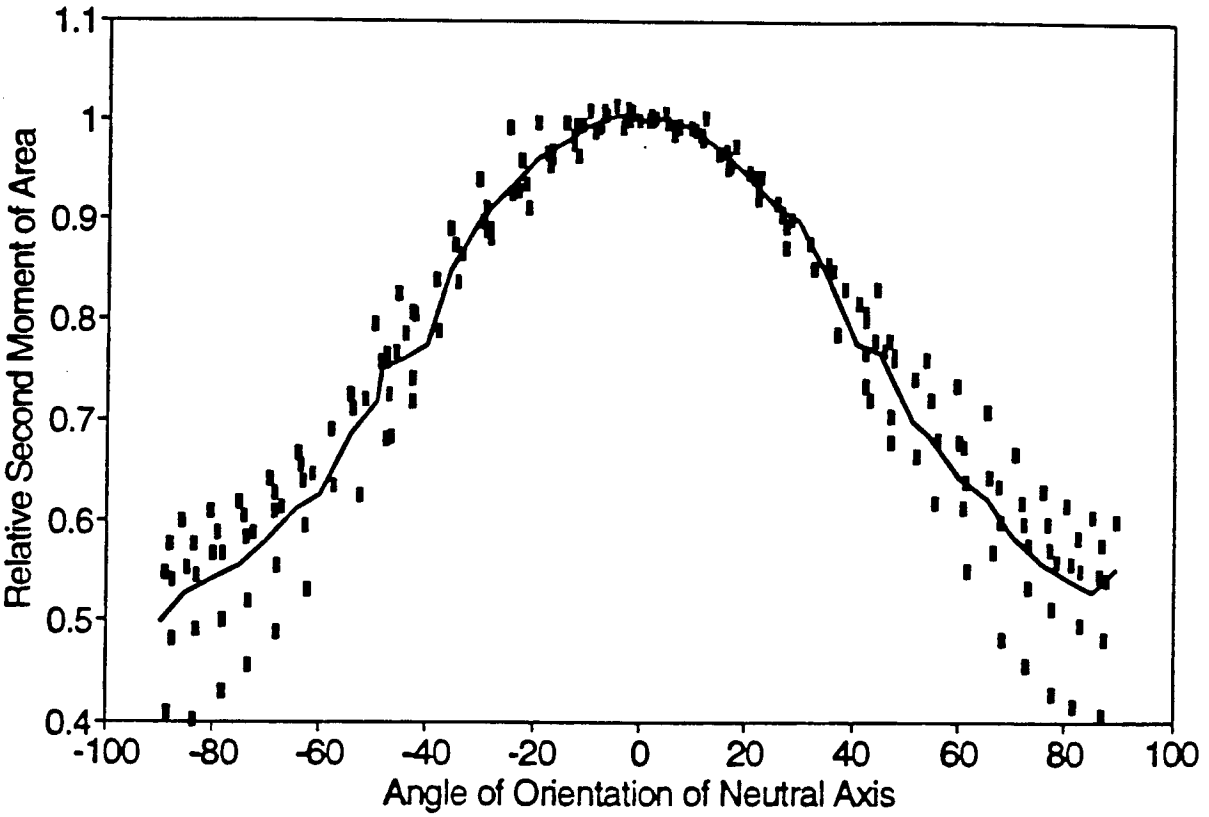

Figure 3.7.

Plot of the relationship between I and the orientation of the neutral axis for a sample of six legs (■) and their average value at each orientation.

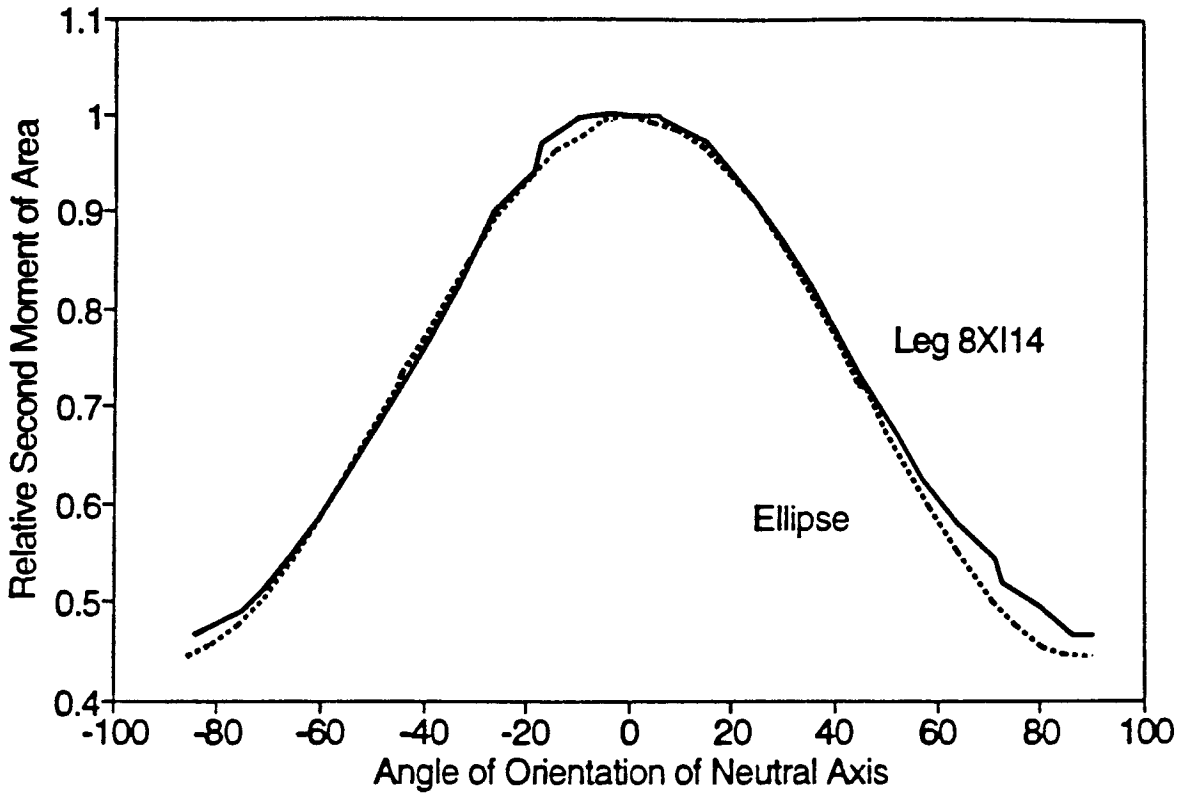

Figure 3.8.

Comparison of the effect of orientation of neutral axis on I for an example leg and an elliptical cross-section of similar aspect ratio.

Figure 3.9a.

Example cross-section from the same leg as shown in figure 3.6a with the base of a spur projecting from the posterior margin of the section.

Figure 3.9b.

Example of section shown in figure 3.9a processed for calculation of **I** for the entire cuticle in the same manner as in figure 3.6b.

Figure 3.9c.

The same image as in figure 3.9b, but flipped around its centre of gravity so that a mean influence of the spurs on **I** on both sides of the leg could be estimated.

a)

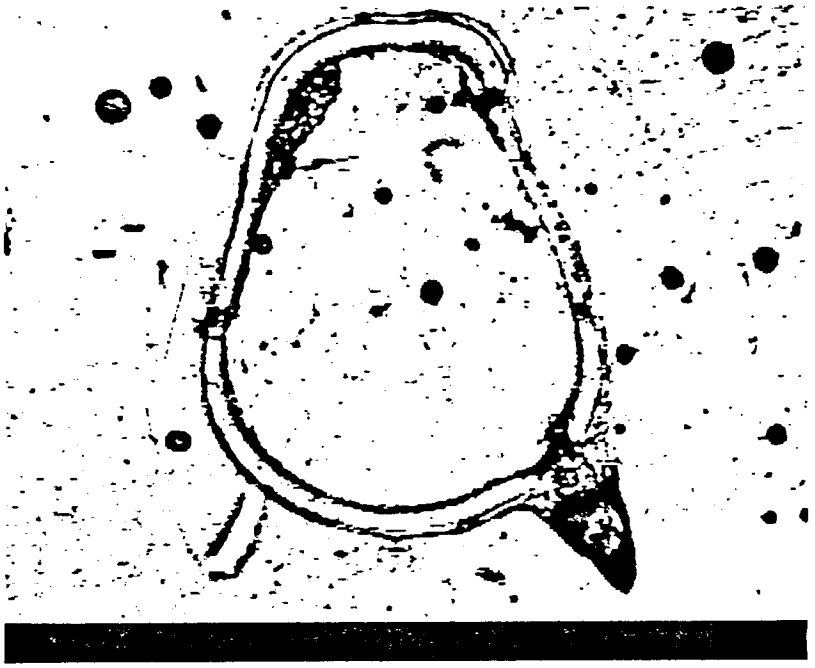

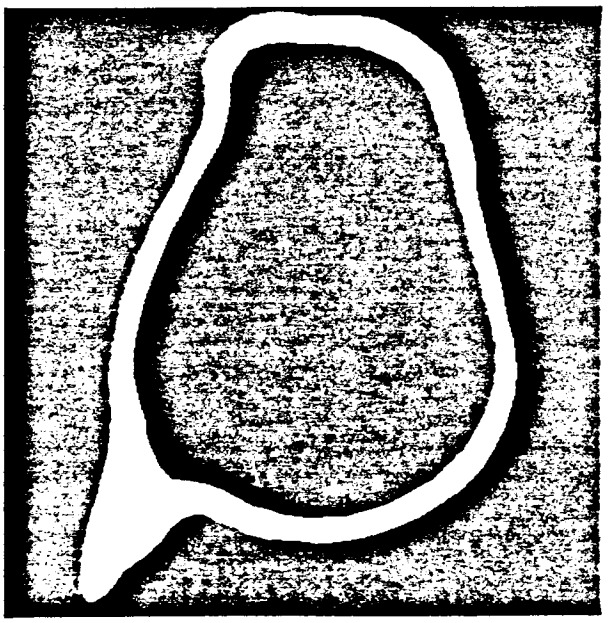

c)

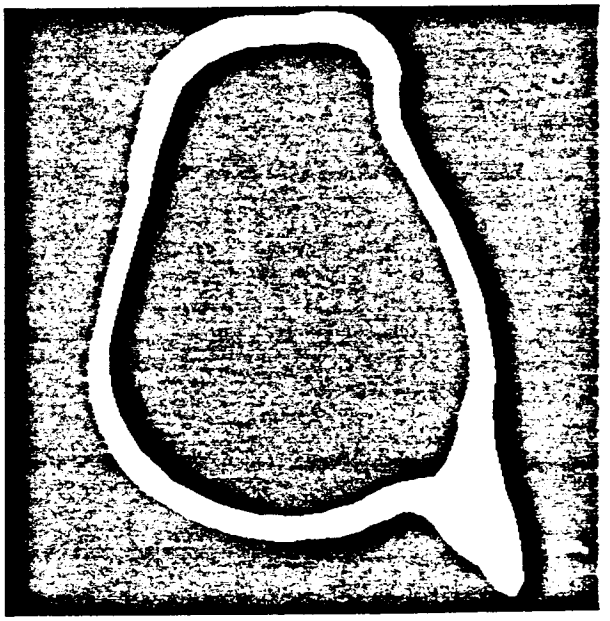

d)

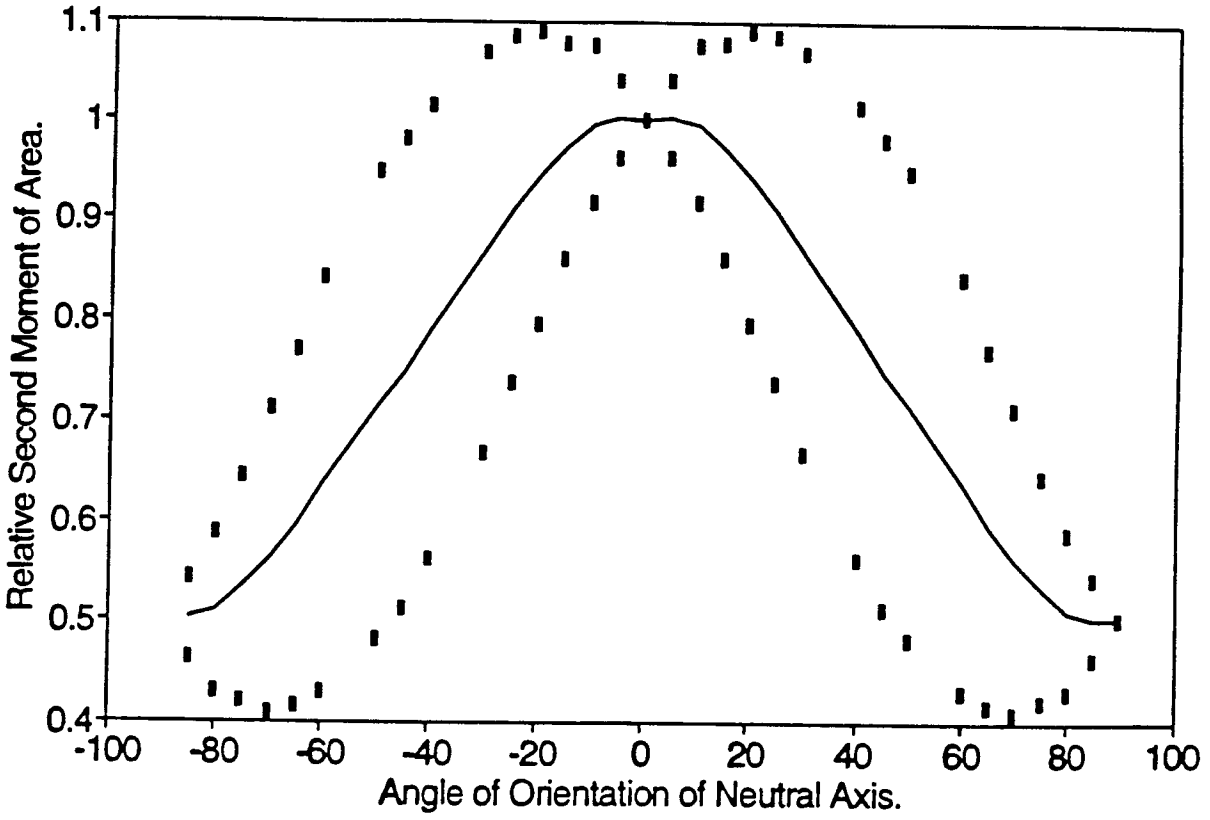

Figure 3.10.

Plot of the relationship between **I** and the orientation of the neutral axis for an average leg with spurs on both sides. Data calculated for each individual cross-section (dotted lines) are superimposed on the average behaviour (solid line) of a leg with spurs on alternating sides along its length.

maximum stiffness toward alternate sides of the tibiae. This should result in an average behaviour that has a deeper and broader local minimum of stiffness along the anterior-posterior axis. Figure 3.9a is a figure of a tibial section with a spur on one side. Figure 3.10 is the relative **I** of a composite section generated by reflecting the section in figure 3.9b through its centre of gravity along the anterior-posterior axis. The neutral axis is then rotated through the same range of orientations as figure 3.7. The composite behaviour should represent the average behaviour of the tibia along its length. This plot shows that there is a modest local minimum of stiffness at the anterior-posterior axis. This might suggest that the spurs play an important mechanical role in amplifying any built-in stability to the loading of the tibiae in bending.

DISCUSSION

Within Instar Changes in **I** The data on how the values of **I** change within the fifth instar seem somewhat equivocal on the question of the relative contributions of the two cuticular components toward whole tibia stiffness. Over the first three days the rapid increase in endocuticle matches the rapid increase in flexural stiffness. If the material stiffness is constant over that period these results would suggest that the stiffness demonstrated by the whole tibia resides largely in the endocuticular component. Over the final five days of the instar the flexural stiffness is more reflective of changes in **I** in the exocuticle, suggesting that the exocuticle is making the most significant contribution to flexural stiffness. The data of Hepburn & Joffe (1974a) indicate that during the first 24 to 36 hours the cuticle, which over that time period is almost entirely exocuticle, increases in modulus by almost an order of magnitude. If so then we can not really depend on the correlation between **I** and **EI** to provide

information on the relative contributions of the cuticular components to tibial stiffness. From information provided by Zacharuk (1976) and Queathum (1991) on the effect of apolysis on the endocuticle, it was anticipated that changes in the endocuticle would be uncorrelated with changes in **EI** (see introduction this chapter). The fact that this was not the case prevents me from being able to discriminate the contributions of the cuticular components based on my data on fifth instar locusts. For this reason, in estimating the elastic modulus I will consider the exocuticle and endocuticle as homogeneous and continuous components as did Jensen and Weis-Fogh (1963). As a result the modulus values that are estimated represent lumped parameters for entire cuticle, and the stiffness for each component may be different.

Scaling In chapter two we observed that if **I** is a function of the fourth power of the diameter of the limb segment, then **I** should scale to body mass raised to the 1.244 power. Our observation that **I** for the entire cuticle scales to body mass raised to the 1.195 power is not significantly different from that prediction (t_s= 1.862, df.= 91 ,$p < 0.05$). This provides an answer to our original question of the nature of the observed uncoupling of morphology and mechanical properties. The locusts are achieving elastically similar flexural stiffness by scaling the material stiffness of the cuticle, rather than applying an allometric scaling to **I** by changing the relative distribution of material in the cross section. This conclusion is reflected in figure 3.5 where **E** scales to mass raised to the 0.311 power.

Of all the scaling relationships reported in this thesis, the relationship between **E'** and body mass has the poorest statistical strength. This is perhaps not surprising, as the variance in these data are the product of variability in the

mechanical measurement of **E'I** and the variability in estimating **I.** Still the relationship is highly significant (F_s = 91.04, df. = 1,89) as a descriptor of the data. Therefore, I feel reasonably sure that the elastic stiffness of the cuticle material is being treated as a scaled commodity in the design of the locusts' legs.

Because the modulus is changing in functionally similar hoppers the scaling of modulus for these legs seems different from that for Jackrabbit bones (Carrier, 1983). In the locust the modulus is scaling to provide an additional degree of freedom in adjusting morphology to accommodate increasing loads with increasing size. Given a design strategy that tries to keep a constant deformation per unit length with increasing size, the non-mineralized skeleton of the locust can adopt morphology that is not predicted by the elastic similarity model. So now we know **how** the uncoupling between morphology and mechanical behaviour is accomplished, but it remains to be seen **why** it is uncoupled. Indeed, this may presuppose that the morphology demonstrated in the locust leg is an adaptation to a specific design issue. In chapter five I will offer three hypotheses for why the locust might have adopted the scaling of the morphology of its legs that it did.

I do not know the nature of the changes that I have observed in **E'**. The cuticle is a fibre-reinforced composite material (Neville, 1975) and there are a number of ways these materials can be modified (Wainwright et al., 1976). It would be interesting to investigate whether the animals are altering the protein polymer that glues the chitin crystalline fibres together, by altering hydration or cross-link density perhaps, or if the crystalline fibres are themselves altered, by geometry (ie. aspect ratio) or volume fraction for instance.

For the endocuticular and exocuticular components of the cuticle **I** is scaled to body mass differently. I have treated the cuticle as homogeneous in

material properties resulting in a preliminary conclusion that the modulus is a scaled commodity. An alternative hypothesis is that the modulus for each component is different and scale independent, and that the amount of each component is varied to produce the average behaviour that is observed for entire tibiae. If this were true, we could estimate how different in modulus the components would have to be to produce the lumped behaviour. I believe this alternative hypothesis can be rejected by considering the limits to this design strategy. The hypothetical limiting cases are where one or the other component has a stiffness of zero and the scaling of the average system is strictly a reflection of the scaling of **I** of the non-zero stiffness component. Specific to this case we need to know if we assume moduli for the cuticular components, the inner of which's **I** scales to body mass$^{1.258}$ and the outer of which's **I** scales to mass$^{1.090}$, can we get the entire structures **E'I** to scale to mass$^{1.53}$? The answer would seem to be no. Even if the modulus of the exocuticle were zero, the entire cuticle's **E'I** would only scale to body mass$^{1.258}$. Therefore, even if we accept the assumption of zero stiffness for the exocuticle, which seems unreasonable, we are forced to conclude that the modulus of the cuticular components is altered in response to changes in body size.

Orientation of Neutral Axis The observation in figure 3.7 & 3.8 that orientation has so little effect on the value of **I** near orientations around the anterior-posterior axis suggests the interesting possibility that the cross-sectional shape of the tibiae provides a built-in stability to the limbs. One can imagine that some fraction of the jumps that a locust makes in its lifetime are made off morphologically complex surfaces. As a result it is also possible that the loads encountered during the jump impulse will not be applied collinearly with the

anterior-posterior axis. If the tibiae has a more elliptical cross-section, then any off-axis loading will tend to flex the leg in the medial lateral axis--a direction in which **I**, and therefore relative stiffness, is reduced by approximately 50%. However, the marginally greater roll off with angle of rotation of **I** for the ellipse relative to the locust leg demonstrates the subtle degree of this stability.

The influence of spurs on the flexural stiffness of the tibiae may be more significant than the composite behaviour estimated in figure 3.10 might suggest. Individual sections with spurs have no local minimum of stiffness around their maximal stiffness values which themselves are oriented about 25° off of the anterior-posterior axis. At each segment of the length of the leg that has a spur the primary loading will be off the axis of greatest stiffness. As a result each little piece of leg will be subject to flexion in the direction of the anterior-posterior axis, lateral to its direction of greatest stiffness. The magnitude of the flexion in this small length of leg will itself be small because of the large dependence of deflection in a beam on length (Eq 1.8). Further, distal to each small, laterally loaded segment of leg will be a similar small segment loaded in the opposite direction because it has a spur on the other side. It may turn out that this alternating pattern of laterally flexed, short beams produces greater stability than the composite section will suggest.

I would prefer not to draw too strong a conclusion from the analysis of the shape of this length-averaged or composite cross-section for two reasons. First, it is not clear that the mechanical properties of the tibial wall are homogeneous between the inter-spur and spur cuticle; and second, it might be purely coincidental that a spur which may be developed as an anti-predator mechanism also influences mechanical behaviour in an externally evaluated, positive manner. It is possible that the presence of spurs acts to produce stress

concentrations that would compromise any improvement in stability derived from their presence. Bertram and Biewener's (1988) model for pre-bend in vertebrate long bones was constructed around such a compromise. The bones are predicted to be pre-bent only when the value of loading predictability outweighs the cost inherent in increased bending loads. Without more detailed knowledge of the consequences of spur formation on the local loading of the cuticle, I am unprepared to commit to an interpretation of the mechanical role of the spurs in stabilizing the bending deformation of the tibiae.

Indeed, the preceding discussion supposes that the spurs are serving primarily a mechanical role in stabilizing bending of the tibiae in jumping, but it is likely that their design has responded to pressures related to defence from predation rather than to jumping. Therefore, to fully analyze their design it would be necessary to balance the design constraints operating on both bending beams and sharp spines. Because I do not have sufficient quantitative information to fully evaluate these potentially competing design criteria I am unprepared to express an opinion about the mechanical role of the spurs in leg bending.

CHAPTER 4.

HOW HARD DO LOCUSTS JUMP?

INTRODUCTION

In chapter two the scaling of limb length was shown to produce relatively longer and slimmer limb segments in larger locusts, an observation that was at variance with any existing scaling model (McMahon, 1973, 1984, Bertram & Biewener, 1990). It was suggested that the observed scaling relationship between limb shape and body size might represent a design feature associated with a jumping mode of locomotion. In order to evaluate this hypothesis we need to know how the mechanical loading of the limb segments is related to size across the same ontogenetic sequence.

Previous work of other investigators has provided some of this information, but the literature contains conflicting information about the relationship between force production and body size in jumping locusts. Bennet-Clark (1977) showed that the distance travelled as the result of a jump is directly proportional to the square of the velocity produced in the jump impulse and that velocity is the result of an acceleration developed over a time interval. However, the accelerations produced in the jump are inversely proportional to the leg length of the jumping animal. The functional significance of this relationship is manifest in the relatively longer legs of jumping animals to reduce loading in the leg skeleton, and the relatively higher accelerations in smaller animals because of their absolutely shorter legs. For typically observed accelerations he cites one and a half gravities (**g**'s) for larger vertebrates, such as leopards and antelope, all the way up to 200 **g**'s for the 0.45 mg rat flea

(Bennet-Clark & Lucey, 1967), with mean accelerations of about 24 **g**'s for first instar *S. gregaria* and about 10 **g**'s for adults (Bennet-Clark, 1977). For adult locusts peak accelerations of about 18 **g**'s are reported (Bennet-Clark, 1975).

In contrast, Scott and Hepburn (1976) reported that across the ontogenetic sequence of *Locusta migratoria* there is a relatively constant peak acceleration of about 10 **g**'s produced in the jump impulse. They also report that this relationship is demonstrated in a sample of six different species of locusts and grasshoppers, indicating that this relationship is consistent and general. Further, they observed a consistent relationship between adult, femoral cuticle stiffness and the forces in jumping. They concluded that constant acceleration produced in jumping was functionally significant in matching the changes that occur in cuticular stiffness over the same developmental increase in body mass. Thus, the mechanical properties of the locomotor structures are appropriately matched to the loads they encounter in normal use.

Gabriel (1985a) has reported that over the first four instars, *Schistocerca gregaria* jump approximately the same distance, but the jump distance increases by about 300% in adults. Gabriel's data suggest, then, that across the juvenile instars take-off velocity is similar. If the analysis of Bennet-Clark (1977) is correct, then as the accelerations fall in larger animals, the duration of force production must increase to produce the same take-off velocity (ie. the integral of acceleration over time) across instars. However, if Scott and Hepburn (1976) are correct in that acceleration is a constant of 10 **g**'s, then the duration of the force development is also a constant regardless of leg length. These two predictions would not seem to be compatible, and without a resolution it is difficult to attempt any functional analysis of the morphological design program

described in the previous chapters.

It is also important to evaluate the functional significance of the jump performance to the animal. Others have suggested that how fast an animal accelerates is potentially adaptive in that prey that produce high accelerations are difficult to follow and catch (Emerson, 1978). As a result, the performance parameter that is thought to be the most functionally significant and has received the closest scrutiny is the acceleration produced in the jump. Emerson (1978) has proposed alternative models that either regulate acceleration or vary acceleration with increasing body size to discriminate strategies for predator avoidance in frogs. I will make the case that peak acceleration is not the critical design issue in the jump of the locust.

In this chapter I have attempted to quantify the loading experienced by the legs of the locust during the jump impulse. Using miniature force plate techniques I have measured the force, acceleration, velocity, displacement, kinetic energy and power output during ontogenetic development as well as the trajectory angle in the jump impulse of locusts on each day of life from the first day after emergence from the egg until full sexual maturity (day 45). The wide range of body mass covered by the locust has allowed me to determine scaling relationships for performance and to compare these relations with existing models. The data provide clear evidence that the jump plays different roles in the locomotor performance of the locust at different times its life history. The flightless, juvenile instars are jumping to achieve a functional distance and the adult locusts are jumping to achieve a velocity critical to the initiation of flight.

METHODS and MATERIALS

Animal Husbandry. Animals were sampled daily from a breeding colony of African Desert Locust (*Schistocerca gregaria*) maintained at the Department of Zoology at the University of British Columbia. The animals were kept at a constant temperature of 27° C, humidity of 56%, and photoperiod of 13:11 (L:D), and fed a diet of head lettuce and bran. A sample of five individuals was collected each day beginning on the first day following emergence from the egg until approximately two weeks after achieving sexual maturity (ca. 45 days).

Five jumps from each individual were collected, for a total 25 jumps for each day in development. Each individual was weighed to the nearest 0.1 mg after its final jump. Occasionally, the jump event produced un-interpretable force traces due to transient, large amplitude noise. Video images made during several of these jumps indicated that this was the result of slippage between the tarsus of the locust and the surface of the platform. Any jumps that showed evidence of transient forces were eliminated from the data set. As a result, there are varying sample sizes for each day. Adult locusts were allowed to jump with their wings intact and unencumbered. Control experiments where the wings of adults were held closed with cellophane tape were not significantly different in terms of peak force production from those where the wings were free to open (t_s = 0.067, df. = 14, $p<0.05$).

In this chapter the term impulse is used in the same sense as that in Bennet-Clark (1975) in that it does not refer to the exchange of momentum explicitly, but rather the interval of the jump that can be characterized by ground reaction forces above one gravity.

Figure 4.1a.

Diagram of the force plate used in this study viewed obliquely from above. This view demonstrates the relative positions of the windows cut into the hollow box tubing. The arrows show the relative orientation of the forces that each set of strain gauges perceives; v, vertical forces; h, horizontal forces; f, fore-aft forces. a. position of the force sensing strain gauges.

Figure 4.1b.

Diagram of force plate viewed obliquely from below. This view shows the relative positions of the strain gauges (a), balsa wood platform (b), the base plate to which the force plate was attached (c), the machine screw that held the platform in position (d), and the lead wires from the fore-aft gauge (e) and horizontal gauge (f). The scale bar represents 2 cm.

a)

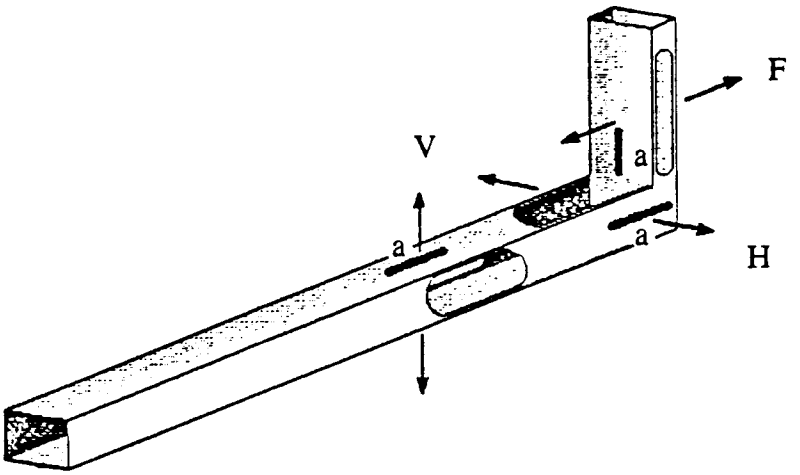

b)

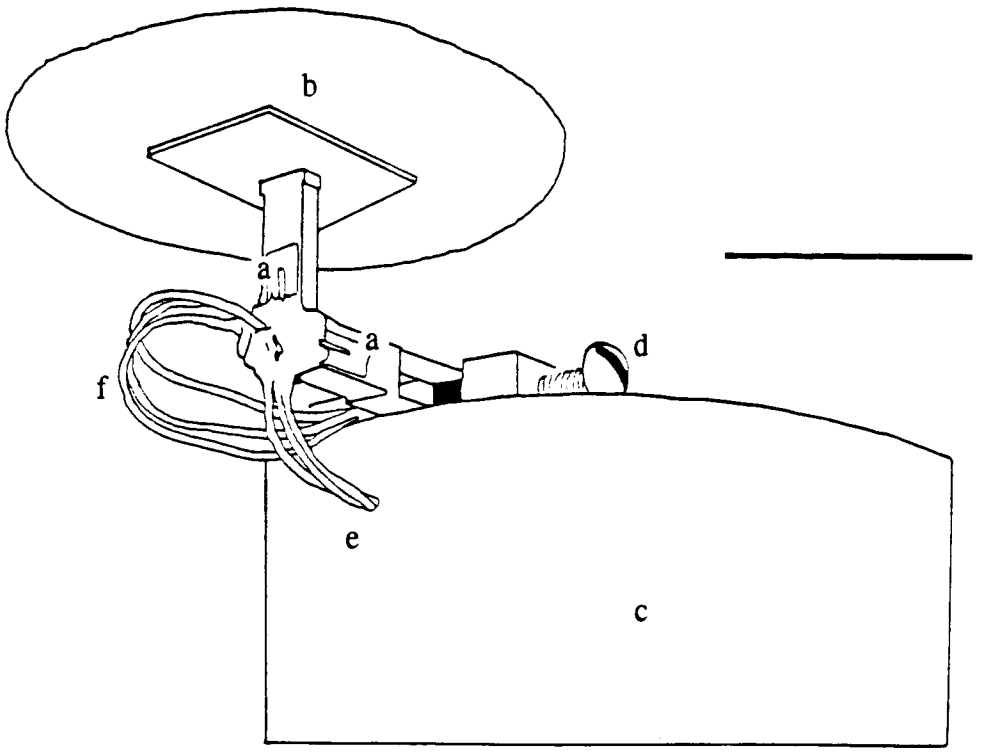

The Force Plate. Figure 4.1 is a diagram of the force plate used in this study. Vertical, horizontal and lateral forces produced in the jump of the locust were measured simultaneously with a force plate similar in design to that described by Full and Tu (1990), but modified to achieve higher sensitivity and frequency response. For instars one through four a balsa wood platform measuring 1.5 × 0.75 × 0.15 cm was bonded to the end of a series of hollow, brass box-beams. For fifth instars and adults a larger, circular balsa wood platform measuring 2.5 cm in radius and 0.25 cm thick was bonded to the pre-existing platform to provide a larger surface from which the larger locusts could jump. Within one centimeter radius of the centre of the platform the position of the locust resulted in a less than 1% change in the force output of the device. Jumps outside of this region were eliminated from the data set. The force sensing elements were similar to those described by Full & Tu (1990) in that semiconductor strain gauges (type SR4 SBP3-20-35, or SBP3-05-35, BLH Electronics, Canton, Mass.) were bonded to the outer surfaces of double cantilevers produced by machining windows in the sides of the box-beams. The mass of the platform was reduced to improve frequency response by having only one set of double cantilevers for each of the three principal components of force application. The resonant frequencies ranged from a high of 1.543 KHz for the most distal cantilever pair, to a low of 527 Hz for the most proximal pair. Force sensitivity was enhanced by machining the leaves of the double cantilever down from a thickness of 0.015" (3.81×10^{-4} m) to a thickness of 0.007" (1.17×10^{-4} m). This modification produced a sensitivity of 12.60 V/N for the most proximal gauge and a sensitivity of 28.30 V/N for the most distal gauge.

Mechanical crosstalk between these gauges was low, but to further minimize crosstalk between the vertical and lateral gauges a small piece of

telescoping box-tubing was welded into the lumen of the beam between the two sensitive elements. Serial calibrations in various orientations in three dimensions indicated that crosstalk interactions where a proximal gauge influenced a distal gauge produced less than a 1% change in the distal gauge output. These were deemed insignificant. Of the three potential interactions in the other direction only the interaction of the most distal gauge with the most proximal proved to affect the proximal gauges output by more than 3% and this was addressed in the analysis by a recursive loop in the analytical process that estimated the actual output of the proximal gauge. At no time did noise exceed 5% of the signal magnitude. Therefore, no signal filtering was employed.

The resistive elements in the strain gauges formed half of a bridge circuit whose DC output was amplified and collected at a rate of 5KHz on three channels of a digital, storage oscilloscope (Data Precision, Data 6000A Universal Waveform Analyzer, Analogic Co., Peabody, Mass., USA), and transferred to an IBM-PC type computer via serial communications for later analysis.

Jumping Arena. All jumps were performed under a clear, plexiglass dome enclosure. The dimensions of the enclosure were 0.45 m wide by 0.33 m deep by 0.58 m tall. The force plate was placed in the centre of the floor of the enclosure on a sheet of Sorbothane, vibration dampening rubber. A balsa wood surface measuring 0.25 m by 0.15 m, was constructed with a hole the same size and shape of the force platform. This surface was placed in the enclosure so that the force plate became a small portion of a larger, relatively continuous surface from which the locusts could jump. For each jump event the locust was placed on the force sensing portion of the wooden surface and allowed to jump freely. Reluctant individuals were enticed to jump with loud

noises or abrupt movements in their visual fields. No electrical stimulation was employed. The possibility that this enclosure inhibited the performance of the locusts was not investigated.

Data Analysis. The three digitized signals were resolved via vector addition into two arrays: one contained the resultant force vector magnitude, and the other an angle to the horizontal for each 200 μs sample. A baseline of zero Newtons was established by calculating the arithmetic average of the first 83 data points (ie. one period of a 60 Hz noise signal) in each force array with the locust standing on the force plate. Thus, the vertical force records are reported in excess of one body weight. The beginning (or ending) of the jump impulse was defined by the force rising above (or falling below) a threshold level that was 2.5% of the maximum force. Force values were normalized by body mass to produce an array representing the instantaneous acceleration. Each acceleration array was integrated numerically to produce the velocity developed by the centre of gravity for each moment in the jump impulse. The initial value of velocity was assumed to be zero, and the velocities were integrated to calculate the displacement of the centre of gravity at each moment in the jump impulse. Additionally, the product of the ground reaction force and velocity arrays gave the power produced in the jump. The values of end-impulse velocity and body mass were used to calculate the kinetic energy (KE) produced in the jump with the familiar formula: $KE = \frac{1}{2}\,mass \cdot velocity^2$. The horizontal distance covered by the jump was estimated using the ballistic equations reported by Bennet-Clark (1981, 1984).

Statistics. Except where noted, all statistical tests were chosen based on criteria presented in Sokal and Rohlf (1981). All relationships were judged significant at the 0.05 probability level. All statistical tests were performed using

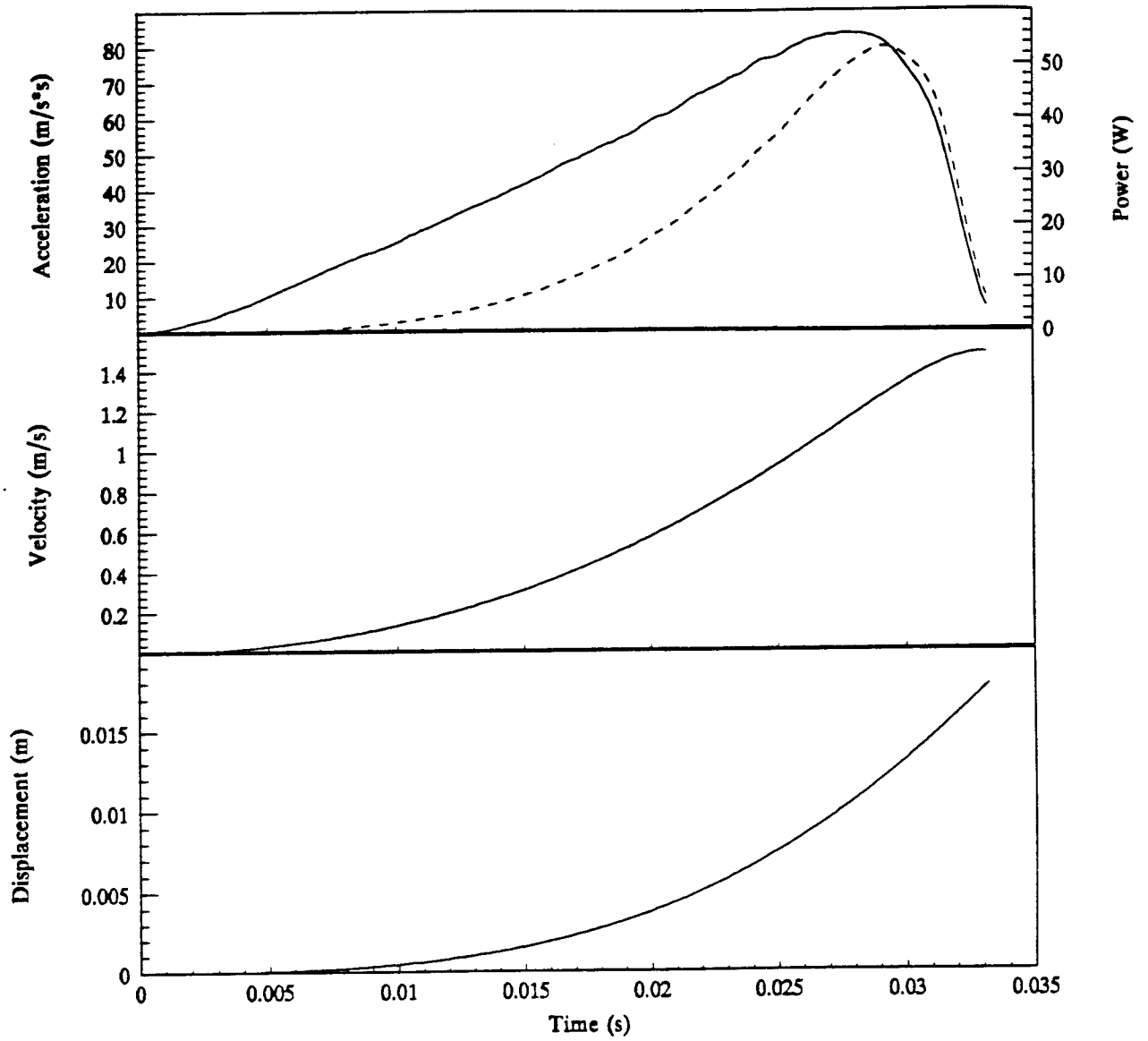

Figure 4.2.

Sample output for a 0.5007 gram fourth instar individual showing the time course of force, velocity, movement and power production. Calculations of the various measures of performance are described in more detail in the text.

the STATGRAPHICS (STSC, Mass, USA, Ver. 5) statistical software package.

RESULTS

Figure 4.2 is a representative data set from a single jump of a 0.5007 g fourth instar locust. The force envelope shows the relatively slow development of force and the rapid fall in force. The entire impulse lasted 32.8 milliseconds, and peak force was achieved at approximately 27 milliseconds, or approximately 82% of the impulse duration. In both first instars and adults the time of peak force shifted later in the impulse duration. This resulted in a relatively more rapid fall in force following the peak force output. Thus, there are subtle differences in the shape of the acceleration envelope that have consequences for the estimation of performance that will be discussed below. This force production profile is not consistent with the optimum described by Bennet-Clark (1977) for minimizing the mass of the skeleton. He suggested that force should be produced at a constant level during a jump impulse so that large magnitude forces do not produce intolerably high stresses in the skeleton. Ker (1977) has pointed out that this force envelope is the consequence of the coupling of an unloading, elastic energy storage device with rapidly decaying force, and a mechanical lever system that is increasing its mechanical advantage to take advantage of that decaying force.

Within each impulse the angle that the force vector makes with horizontal (ie. the trajectory angle) did not seem to change significantly or systematically. The standard error of the trajectories within a single jump impulse had a high value of 1.6 degrees in first instars and a low value of 0.3 degrees in adults. Inspection of the arrays of trajectory angles indicated that the data were not stationary, with the majority of the variation in the data occurring early in the

jump impulse when the forces were low and the vector addition of the relatively noisy force arrays produced relatively high variability of the calculated angles. After the approximate one quarter point in the impulse the forces are higher, making the signal to noise ratio larger, and the variance of the trajectory angles are even smaller than calculated for the entire time series. This means that it is a fair approximation to assume constant trajectory angle and integrate the acceleration and velocity arrays as scalar rather than vector variables to calculate velocity and distance moved by the centre of gravity respectively. It also suggests that there is a large degree of stability built in to the design of the jumping mechanism of these locusts. The time course of the jump impulse (ca. 15 milliseconds in first instars) makes it unlikely that a neural reflex is capable of modulating muscular control over the jumping mechanism to make fine adjustments to trajectories during the impulse.

There is a sexual dimorphism in body mass that develops in the adults, where females become 50% to 75% heavier than males. Analysis of covariance indicated that for juvenile instars there was no significant effect of sex beyond the effect of body mass on any of the variables examined (ANCOVA, $F_s = 3.133$, df. = 1, 447, for peak acceleration on body mass, the relationship most closely approaching significance.) As such, the data for both sexes were pooled for all juvenile instars for the purposes of performing regressions. In the case of the relationship between movement of the centre of gravity and body mass there was no significant effect of sex beyond the effect of body mass for the entire life history (ANCOVA, $F_s = 2.737$, df. = 1, 874). Therefore, the sexes were pooled for this entire data set. The distinction between juvenile and adult locusts in this context is not completely arbitrary, as the jump itself may have different functional significance in different stages of the life history (see below).

Figure 4.3a.

The relationship between body mass to the age of the locust. Data are reported in means and standard errors of the mean in all three parts of this figure. A regression fitted to the Von Bertalanffy relation produced the following description of the data: Mass = $3.468(1-e^{-.059\ Age})^3$ (F_s=927.8, df=2,43, r^2=.937). The data for adults represents both sexes, and as a result, the varience for the adult data is larger than for preceeding stages.

Figure 4.3b.

The relationship between measured ground reaction force to the age of the locust. A regression fitted to the Von Bertalanffy relation produced the following description of the data: Force = $2.141(1-e^{-.019\ Age})^3$ (F_s=964.0, df=2,43, r^2=.955).

Figure 4.3c.

The relationship between peak acceleration to the age of the locust. These data are reported as means and standard errors of the means for the peak acceleration achieved within individual jumps rather than simply dividing the values in figure 3b by those in figure 3a.

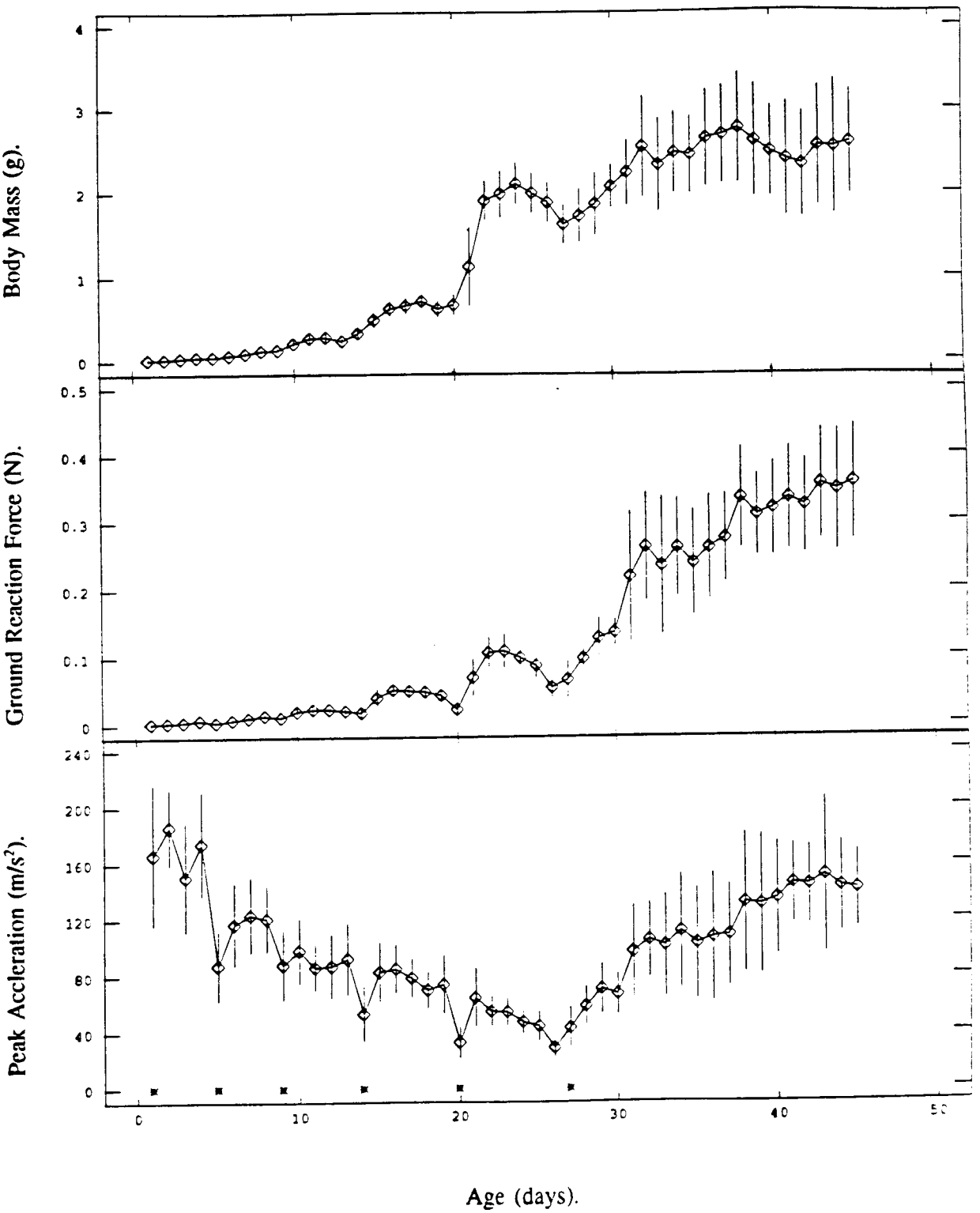
Body Mass (g).
Ground Reaction Force (N).
Peak Accleration (m/s²).
Age (days).

Both the relationships of body mass and peak ground reaction force as functions of age describe sigmoid curves. Body mass increased in a logistic way before levelling off near the end of the fifth instar (Fig. 4.3a.). Fitting a von Bertalanffy growth model to the relationship between body mass and age (Pitcher and Hart, 1982) resulted in a relationship not significantly different from that reported in chapter two for a similar series of individuals (F_s= 9.187E-5, df.=1, 76, p>0.05). Ground reaction force also increases in a logistic manner, although more slowly, and it does not begin to level off until after the moult into adulthood (Fig. 4.3b.). A similar growth model fit to the data on ground reaction force results in a period of exponential increase in force that is less than half of that for body mass ($(e^{-.057*Age})_{mass} > (e^{-.019*Age})_{force}$, F_s=14.808, df.=1, 86, p<0.05). This is manifest in a relatively rapid increase in body mass occurring around an age of 20 days, while the force increases rapidly around day 30. This seven to ten day lag between the age of rapid increase of mass and the age of rapid increase of force means that normalizing force by body mass produces a "U"-shaped relationship between acceleration and age (Fig. 4.3c.).

To analyze allometric relationships log transformations were employed to convert curvilinear, exponential relationships into linear ones. This has allowed the convenient comparisons of the scaling exponents that have been transformed into characteristic slopes. Data from individuals on the first day of each instar seemed to be systematically distinct from the rest of the data from that instar. It would seem to be the result of the physiological events involved in moulting that also result in low cuticular stiffness and resilience immediately after moulting (Hepburn and Joffe, 1974, chapters two & three). To prevent the transient events of cuticular stiffening from biasing the regressions, and to make comparisons between data collected from individuals that we believe to be

functionally similar (chapter one), data from individuals on the first day of each instar were excluded in calculating the slopes of the scaling relationships.

The relationship between log of peak ground reaction force and log of body mass (Fig. 4.4a.) shows a relatively linear region from the smallest individuals up to the fifth instars, but adults fall above this relation. The regression of the log of peak force on the log of body mass, including both juvenile and adult data, produced the relationship: Log Force = 0.914·Log Mass + 1.678 (SE = 9.89E-3, r^2 = 0.880). The slope of this relationship appears to be similar to that reported for *Locusta migratoria* (Scott & Hepburn, 1976). However, an analysis of variance of the residuals showed a significant lack of fit (F_s = 22.6775, df. = 1, 260, $p<0.05$), and the regression was deemed an inappropriate description of the data (Draper and Smith, 1981). The regression of the data consisting entirely of flightless juveniles had a slope of .732 (SE = 7.69E-3, r^2 = 0.925) and ranges from a low value of 1.99 mN on the first day of emergence from the egg to a high of 166 mN in fifth instar individuals.

The relationship in figure 4.4b. between log of peak acceleration and log of body mass demonstrates an apparent functional relationship over the first five instars, but a pronounced increase in performance in adults. The values range from approximately 25 **g**'s in first instars to about 5 to 7 **g**'s in fifth instars. The data at larger sizes, where the accelerations are once again in the 20 to 25 **g** range, are composed entirely of winged adults. As in the relationship between force and mass, a significant, non-random distribution of the residuals in the regression of log of acceleration on log of mass for the entire data set (F_s = 22.7327, df. = 1, 260, $p<0.05$) made this an inappropriate description of the data. As such, the regression of acceleration on body mass was performed only on flightless, juvenile individuals. The relationship had a slope of -0.269 (SE

Figure 4.4a.

The relationship beteen the log of peak ground reaction force and the log of body mass. Each point is the result of one recorded jump like that shown in figure 2. These data exclude points collected from individuals on the first day after each moult. The equation for the regression calculated for juvenile individuals is $Y = 0.992 + 0.732 \times X$ (F_s=9045.75, df.=1, 735, r^2=.9249). The dashed lines are the 95% confidence limits of the regression line.

Figure 4.4b.

The relationship between the log of peak acceleration produced in each jump and the log of body mass. The equation of the regression line calculated for juvenile individuals is $Y = 0.989 - 0.269 \times X$ (F_s=1213.52, df.=1, 735, r^2=.6228). The dashed lines are the 95% confidence limits of the regression.

Figure 4.4c.

The relationship between the log of jump impulse duration and the log of body mass. The equation of the regression line calculated for juvenile individuals is $Y = 2.448 + 0.277 \times X$ (F_s=4409.27, df.=1, 735, r^2=.8571). The dashed lines are the 95% confidence limits of the regression.

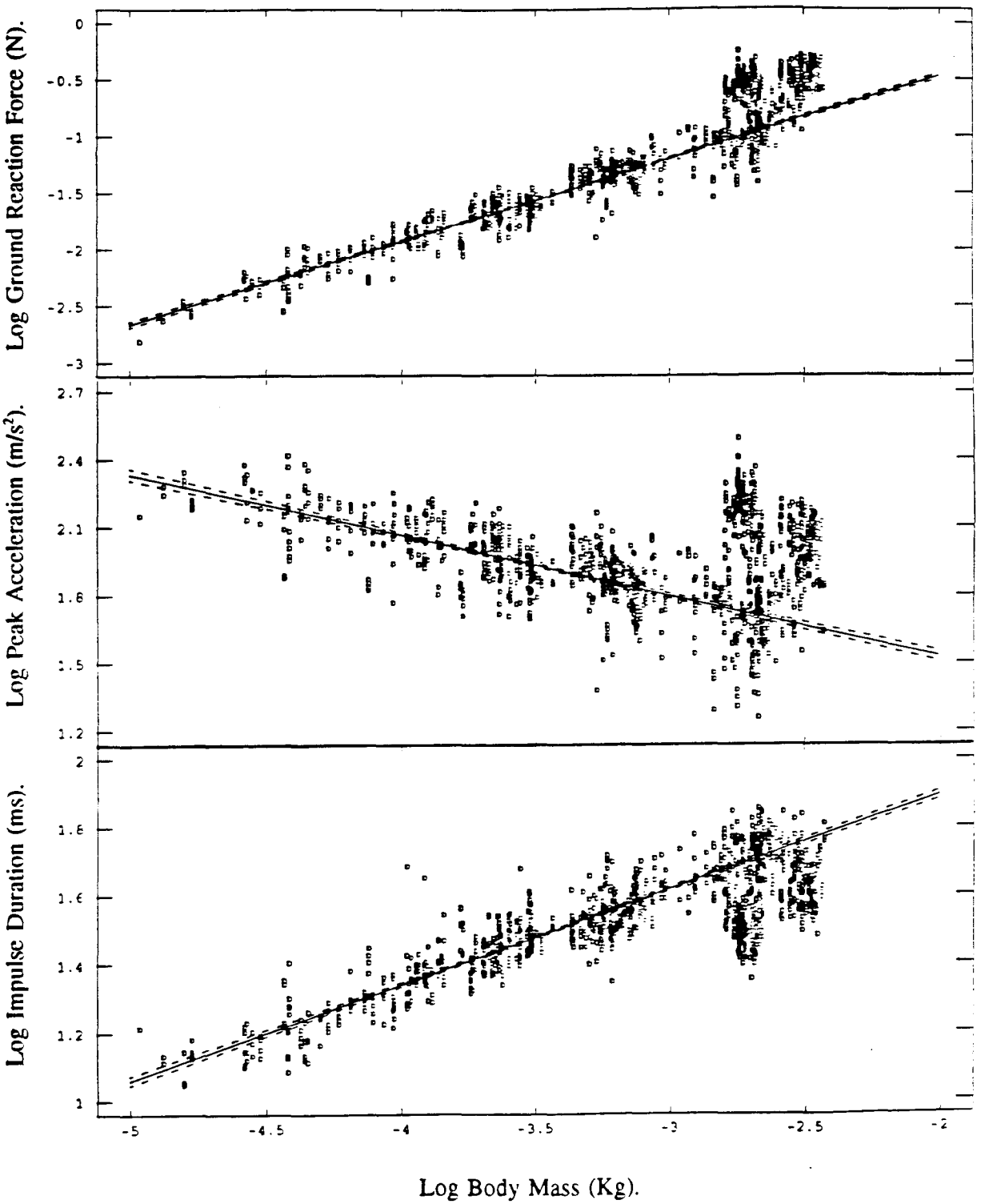
Log Ground Reaction Force (N).
0
-0.5
-1
-1.5
-2
-2.5
-3
Log Peak Acccleration (m/s²).
2.7
2.4
2.1
1.8
1.5
1.2
Log Impulse Duration (ms).
2
1.8
1.6
1.4
1.2
1
-5
-4.5
-4
-3.5
-3
-2.5
-2
Log Body Mass (Kg).

= 7.72E-3, r^2 = 0.623).

As the animals grow the duration of the force impulse increases in length from a low value of 12 milliseconds in first instars up to a high value of 65 milliseconds in fifth instars, before falling to 20 to 30 milliseconds in adult locusts (Fig. 4.4c.). These data also show a consistent relationship over the first five life history stages before an inflection at the transition to adulthood. The regression of the log of jump impulse duration on the log of body mass, over the flightless portion of the life history, had a slope of 0.277 (SE = 4.18E-3, r^2 = 0.857), which, while opposite in sign, is not significantly different in magnitude from the slope of the relationship between acceleration and body mass (t_s = 2.913E-8, df. = 1,470, p>0.05). This means that as the animals grow through the first five instars they produce lower accelerations, but they develop that acceleration over a longer time.

By compensating falling accelerations with increasing impulse durations, juvenile instars produce roughly the same take-off velocity in the jump independent of age or size (Fig. 4.5.). The flightless, juvenile instars are leaving the ground at approximately 1.2 to 1.3 meters per second, while the adults are achieving about 2.5 meters per second. The values for adults show good agreement with the value of 2.63 metres per second based on the jump distance of a 3 gram female locust estimated by Bennet-Clark (1975). For juveniles, the regression of the log of take-off velocity on the log of body mass has a slope of 0.053 (SE = 5.25E-3, r^2= 0.138) (Fig. 4.5b.). While this slope is statistically different from zero (t_s=10.832, d.f.=736, p<0.05), it only resulted in an 21% increase in take-off velocity over the one hundred and seventy fold range of body mass covered in the juveniles. In the adults the accelerations produced are as high as those produced by the first instars, but the legs are

Figure 4.5a.

The relationship of velocity produced in the jump to the age of the locust. Data are reported as means and standard errors of the mean. The first day of each instar is marked with an *. The dotted horizontal line marks the 2.5 m/s minimum flight speed observed by Weis-Fogh (1956).

Figure 4.5b

The relationship between the log of velocity produced in the jump and the log of body mass. The equation of the regression line calculated for juvenile individuals is $Y = 0.277 + 0.053 \times X$ (F_s=117.33, df.=1, 735, r^2=.1377). The dashed lines are the 95% confidence limits of the regression line.

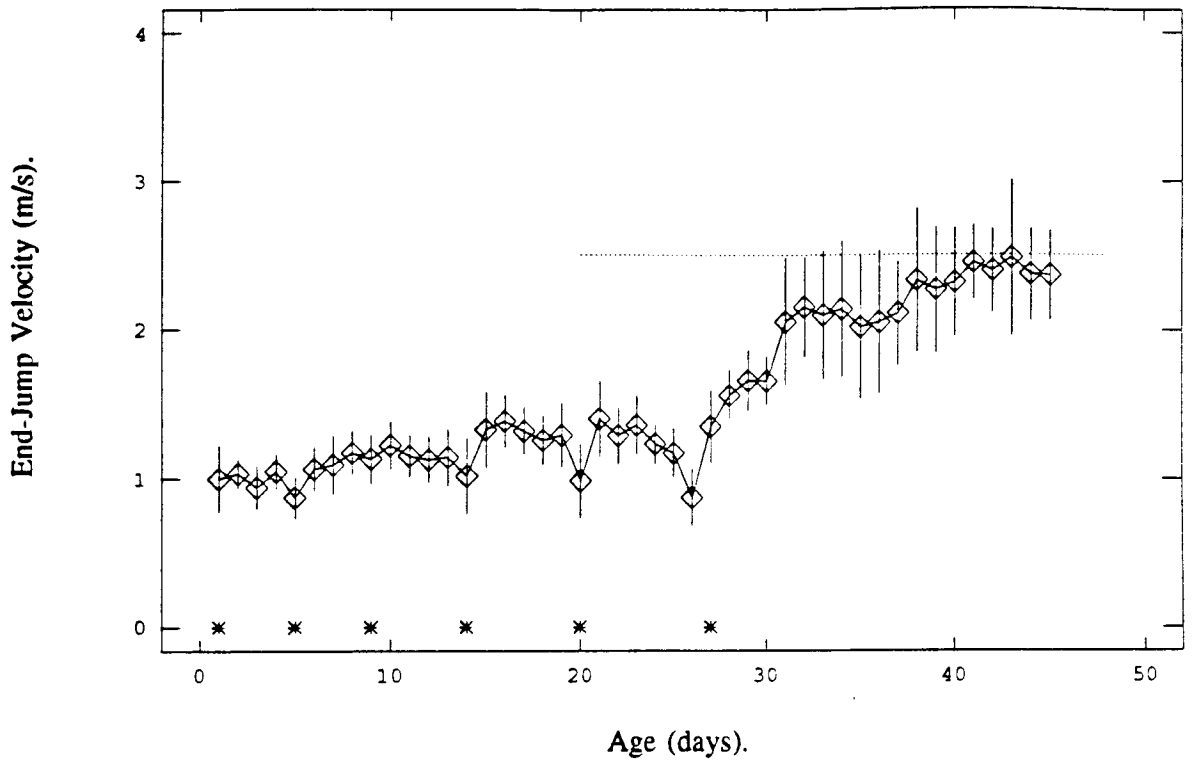
End-Jump Velocity (m/s).
4
3
2
1
0
0
10
20
30
40
50
Age (days).

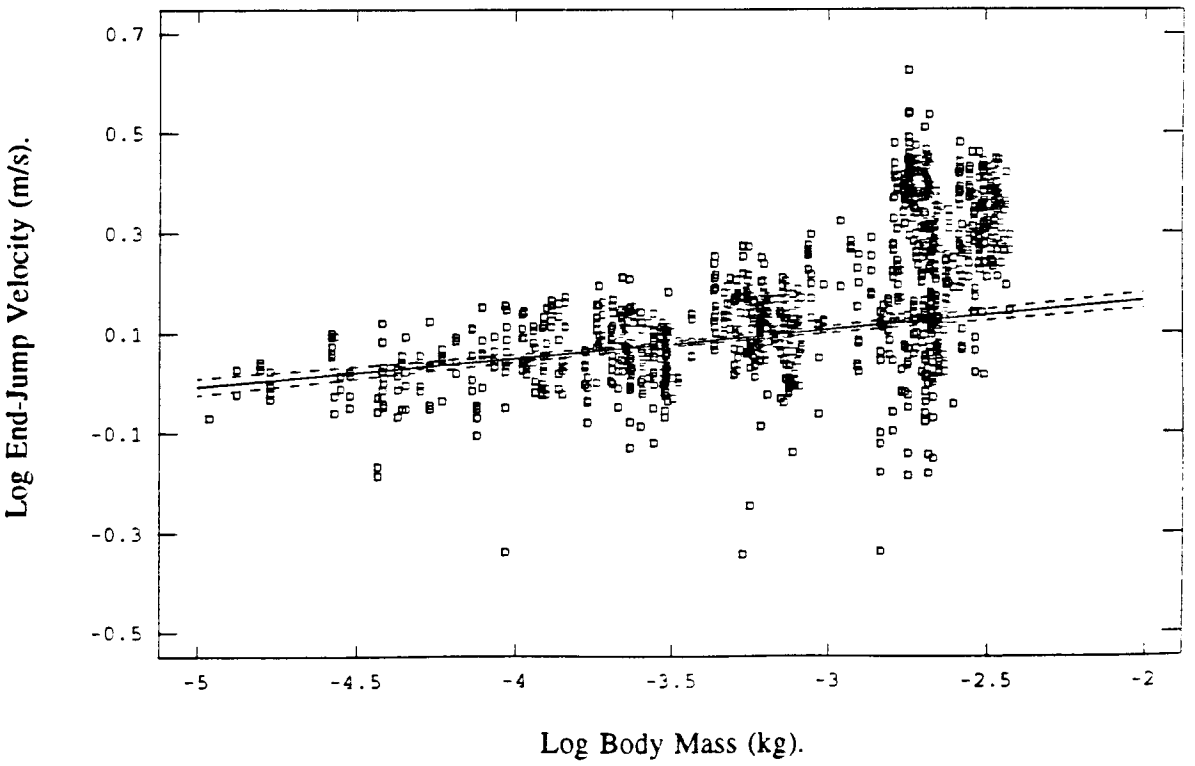
Log End-Jump Velocity (m/s).
0.7
0.5
0.3
0.1
-0.1
-0.3
-0.5
-5
-4.5
-4
-3.5
-3
-2.5
-2
Log Body Mass (kg).

approximately five times as long (Chapter two), so both the acceleration distance and impulse duration are greater than in first instars. As a result, the take-off velocities are about double those of the previous instars (Fig. 4.5a.). Observation of newly moulted adults indicated that for several days they do not fly. They spend their time hanging from vertical surfaces basking or flapping their wings without leaving the ground. It may be that their wing cuticle requires some time to dry and harden before it becomes sufficiently stiff to provide an adequate lifting surface. Alternately, the observation that they are flightless for several days into the adult stage may reflect the fact that relatively low velocities are achieved in the first six days of adulthood compared with those after day 30.

The kinetic energy of the jump, calculated at the end of the jump impulse, follows a similar time course as force production, with a large increase in energy in the adult stage (ca. day 30) compared with the juvenile stages (Fig. 4.6a.). The values ranged from a low of 0.004 millijoules in a first instar locust to a high of 15.99 millijoules in an adult. The time course of jump energy within the fifth instar follows a parabolic trajectory, where the energy production is similar on the first and last day of the instar. This is similar to that described for the sixth instar in *Schistocerca americana* (Queathem, 1991). However, none of the earlier instars show this timecourse. In the fourth instar of *S. gregaria* the energy rises on the first two days of the instar and then levels off for the remainder. It may be that the more rapid development in *S. gregaria* relative to *S. americana* (≈35 days to sexual maturity vs. ≈60 days, respectively), and the shorter time spent within each instar masks the changes in the cuticular energy transmission mechanisms to which Queathem attributes the changes in performance that she observed.

Figure 4.6a.

The relationship of kinetic energy produced in the jump to the age of the locust. Data are reported as means and standard errors of the mean. The first day of each instar is marked with an *.

Figure 4.6b

The relationship between the log of kinetic energy produced in the jump and the log of body mass. The equation of the regression line calculated for juvenile individuals is $Y = 0.253 + 1.114 \times X$ (F_s=11238.60, df.=1, 735, r^2=.9386). The dashed lines are the 95% confidence limits of the regression line.

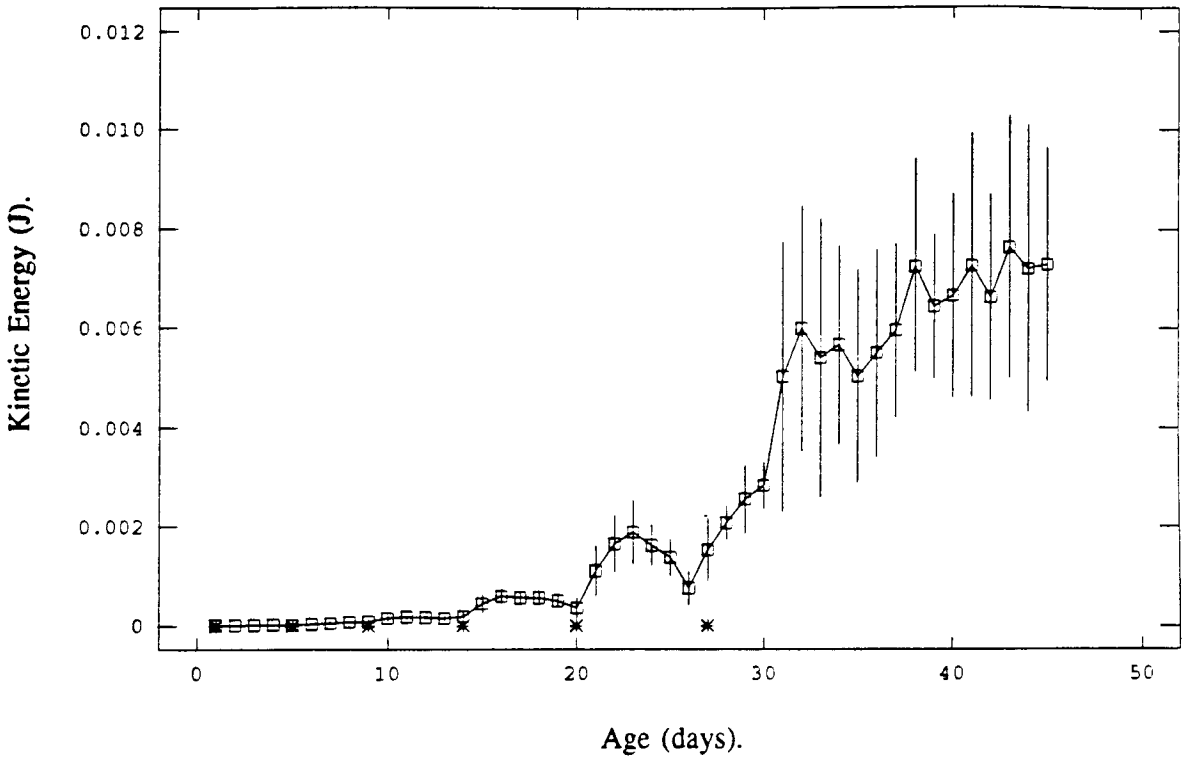
Kinetic Energy (J).
0.012
0.010
0.008
0.006
0.004
0.002
0
0
10
20
30
40
50
Age (days).

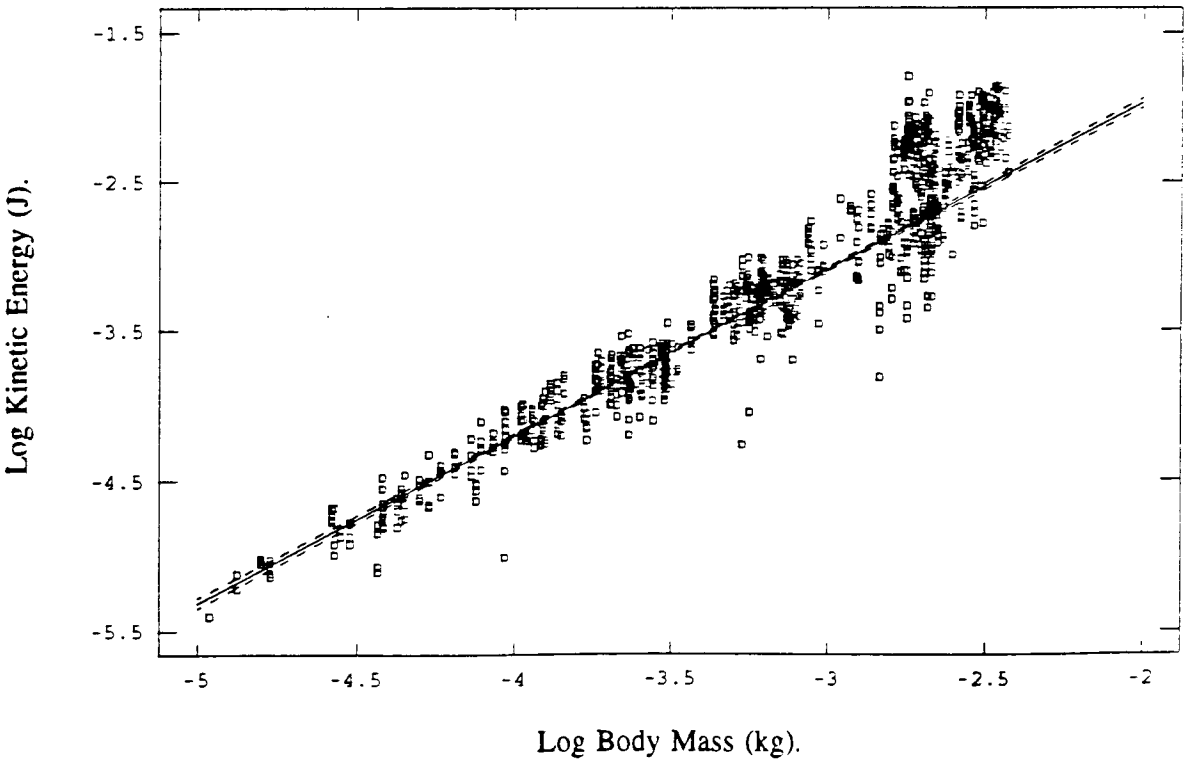
Log Kinetic Energy (J).
-1.5
-2.5
-3.5
-4.5
-5.5
-5
-4.5
-4
-3.5
-3
-2.5
-2
Log Body Mass (kg).

The scaling relationship between log kinetic energy and log body mass (Fig.4.6b) had a form similar to that for force and mass (Fig. 4.4a.). The regression of the relationship for juvenile instars had a slope of 1.114 (SE = 0.011, r^2 = 0.939), which is significantly different from a slope of 1.0 (t_s = 10.831, d.f. = 735, $p < 0.05$). The adult locusts produced approximately four times as much kinetic energy as the regression for juveniles would have predicted for animals of adult body mass.

Power developed during the jump follows a time course similar to that for force production (Fig. 4.7a.). This is not surprising as power is the product of force, which follows a sigmoid time course, and velocity which is relatively constant at the separate juvenile and adult levels. The values for peak power output range from 1.105 mW in first instars to 1.379 W in adults. The values for average power output in the jump impulse are about one third of the peak values. For the juvenile instars, peak power output scaled to body mass raised to the 0.772 power (SE = 0.014, r^2 = 0.836) (Fig. 4.7b). Values for average power output scaled to body mass raised to the 0.830 power (SE = 0.014, r^2 = 0.862). The difference in these slopes is significant (F_s = 8.578, d.f. = 1, 1136, $p < 0.05$), and represents a subtle change in the shape of the force production envelope with increasing peak acceleration, as mentioned previously.

By normalizing the power output of the jump by the amount of jumping muscle, we can calculate the specific power output of the jumping muscles and estimate the degree to which elastic energy storage must be employed to amplify the maximal muscular power output of approximately 450 W/Kg of muscle (Bennet-Clark, 1975). Gabriel (1985a) has published values for the proportion of body mass that is femoral, jumping muscle in the locust. She highlighted a 50% increase in relative muscle mass between the fourth instar

Figure 4.7a.

The relationship of peak power (◇) and average power (□) produced in the jump to the age of the locust. Data are reported as means and standard errors of the mean. The first day of each instar is marked with an *.

Figure 4.7b

The relationship between the log of peak power (◇) and average power (□) produced in the jump and the log of body mass. The equation of the regression line calculated for peak power for juvenile individuals is $Y = 1.126 + 0.772 \times X$ (F_s=2900.77, df.=1, 569, r^2=.8360). The equation of the regression line calculated for average power for juvenile individuals is $Y = 0.789 + 0.830 \times X$ (F_s=3546.39, df.=1, 569, r^2=.8617). The dashed lines are the 95% confidence limits of the regression line.

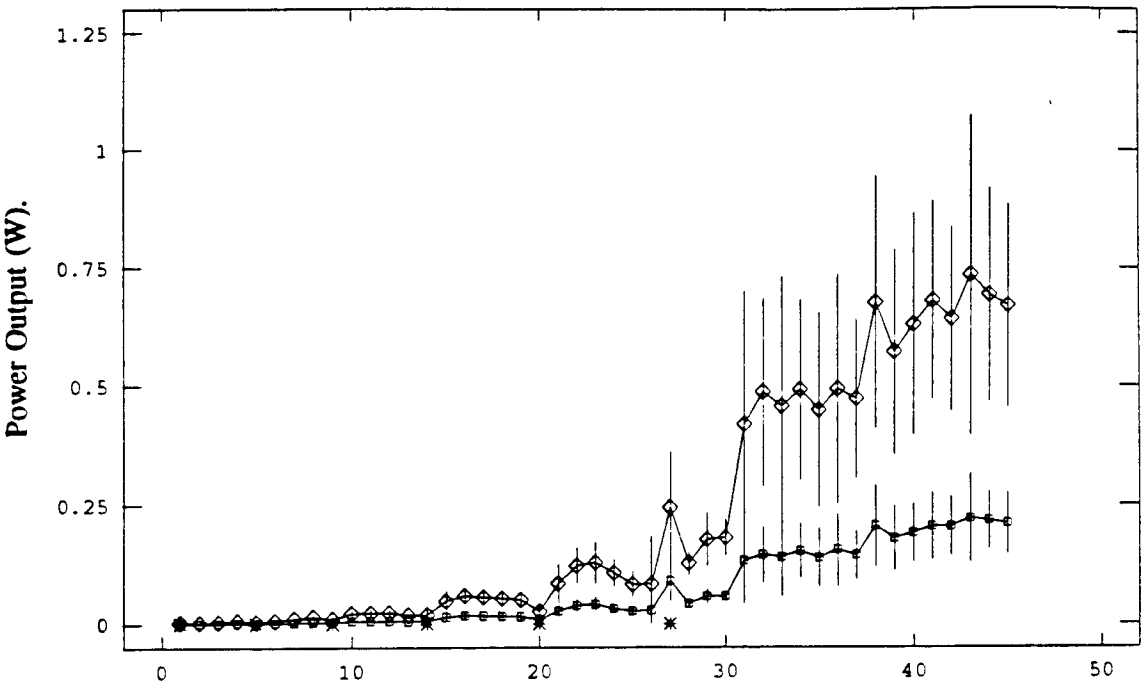
Power Output (W).
1.25
1
0.75
0.5
0.25
0
0
10
20
30
40
50
Age (days).

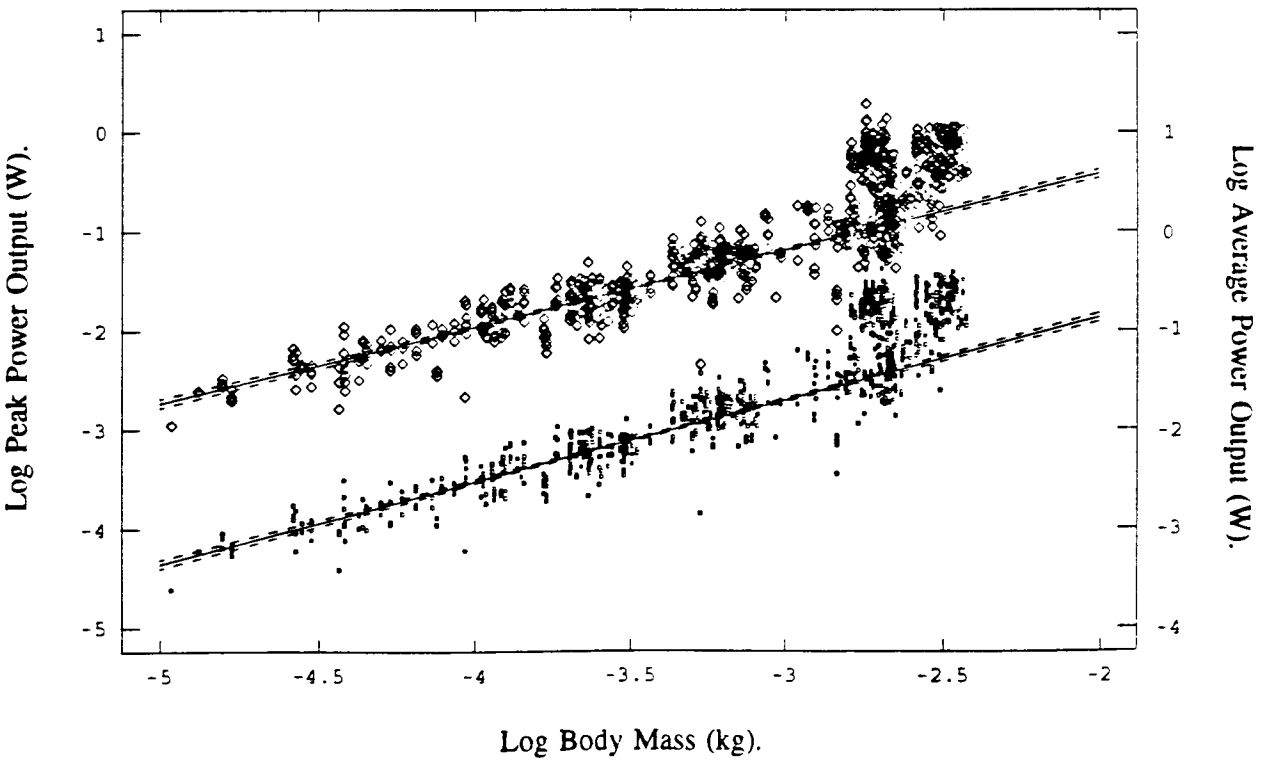
Log Peak Power Output (W).
1
0
-1
-2
-3
-4
-5
-5
-4.5
-4
-3.5
-3
-2.5
-2
Log Body Mass (kg).
Log Average Power Output (W).
1
0
-1
-2
-3
-4

and adult stages. However, she did not specify the age within the instar that these values represent. Additionally, there is quite a lot of variation in the values for relative muscle mass in the juvenile instars, from a high value of 6.1% in first instars to a low of 4.3% in the fourth instars, with no clear temporal trend. For these reasons I have chosen to average her values for all of the juvenile instars to produce a value of 5.56% of whole body mass that is jumping muscle for all five juvenile instars, and use her value of 6.3% for adults.

The daily averages for peak, specific power output range from a low of 850 W/Kg of muscle in fifth instars to a high value of 5,200 W/Kg in the adult stage (Fig. 4.8a.). However, individual jumps had values as high 11,600 and as low as 250 Watts per Kilogram. These data agree well with those estimated by Gabriel (1985a) based on distance travelled in jumping. It also suggests that on occasion the power outputs of the jump (250 W/Kg) are well within the range for maximal muscle power output (450 W/Kg, Bennet-Clark, 1975). Average mass specific power output mirrors the data for peak power output at values approximately one third less. If a trend exists, it seems that the specific power output declines from a relatively high value in the first instars down to the fifth instars before rising to the highest levels in the adults. For the juvenile instars, peak, mass-specific power output scaled to body mass raised to the -0.228 power (SE = 0.014, $r^2 = 0.308$) (Fig. 4.8b.). Average mass specific power output scaled to body mass raised to the -0.170 power (SE = 0.014, $r^2 = 0.207$). These slopes were significantly different ($F_s = 8.578$, d.f. = 1, 1136, $p < 0.05$), but similar to the analysis above, I feel this difference is a consequence of the shape of the force production envelope.

Biewener (1989) has suggested that larger animals may reduce the bending moments applied to their long bones relative to those in small animals

Figure 4.8a.

The relationship of peak mass specific power (◇) and average mass specific power (□) produced in the jump to the age of the locust. Data are reported as means and standard errors of the mean. The first day of each instar is marked with an *.

Figure 4.8b

The relationship between the log of peak mass specific power (◇) and average mass specific power (□) produced in the jump and the log of body mass. The equation of the regression line calculated for peak mass specific power for juvenile individuals is $Y = 2.417 - 0.228 \times X$ (F_s=253.69, df.=1, 569, r^2=.3084). The equation of the regression line calculated for average mass specific power for juvenile individuals is $Y = 2.079 - 0.170 \times X$ (F_s=148.09, df.=1, 569, r^2=.2065). The dashed lines are the 95% confidence limits of the regression line.

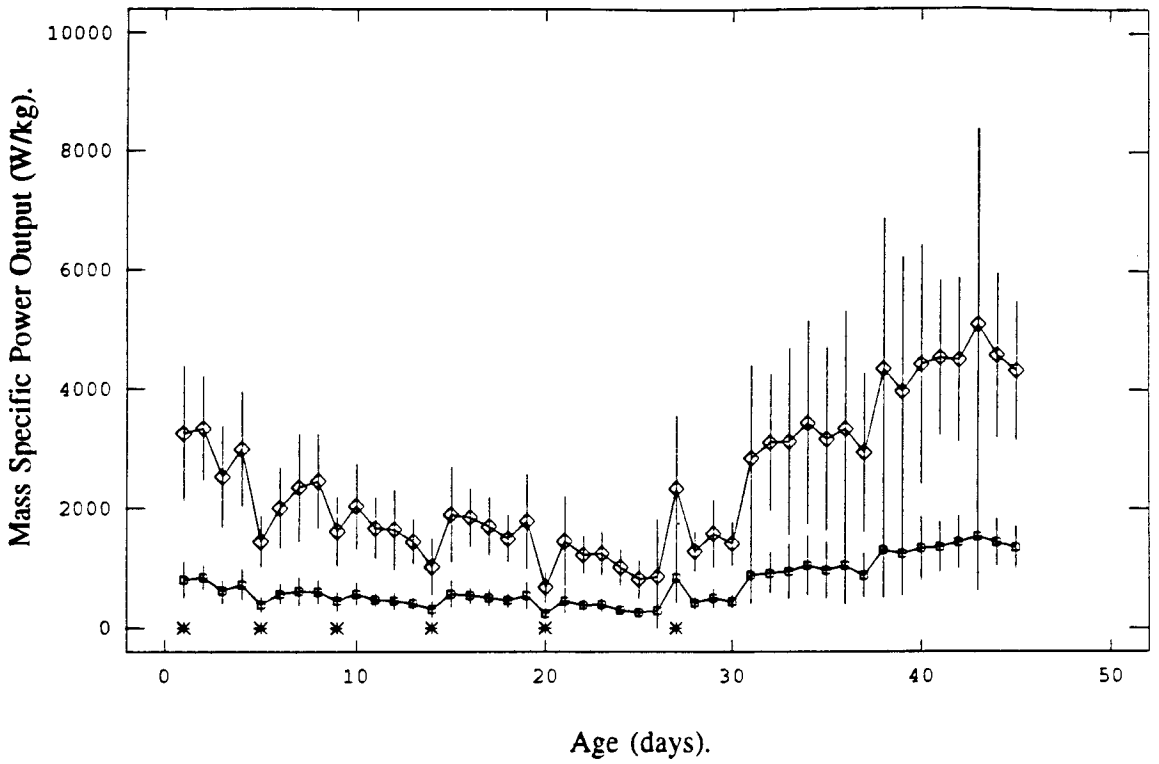
Mass Specific Power Output (W/kg).
10000
8000
6000
4000
2000
0
0
10
20
30
40
50
Age (days).

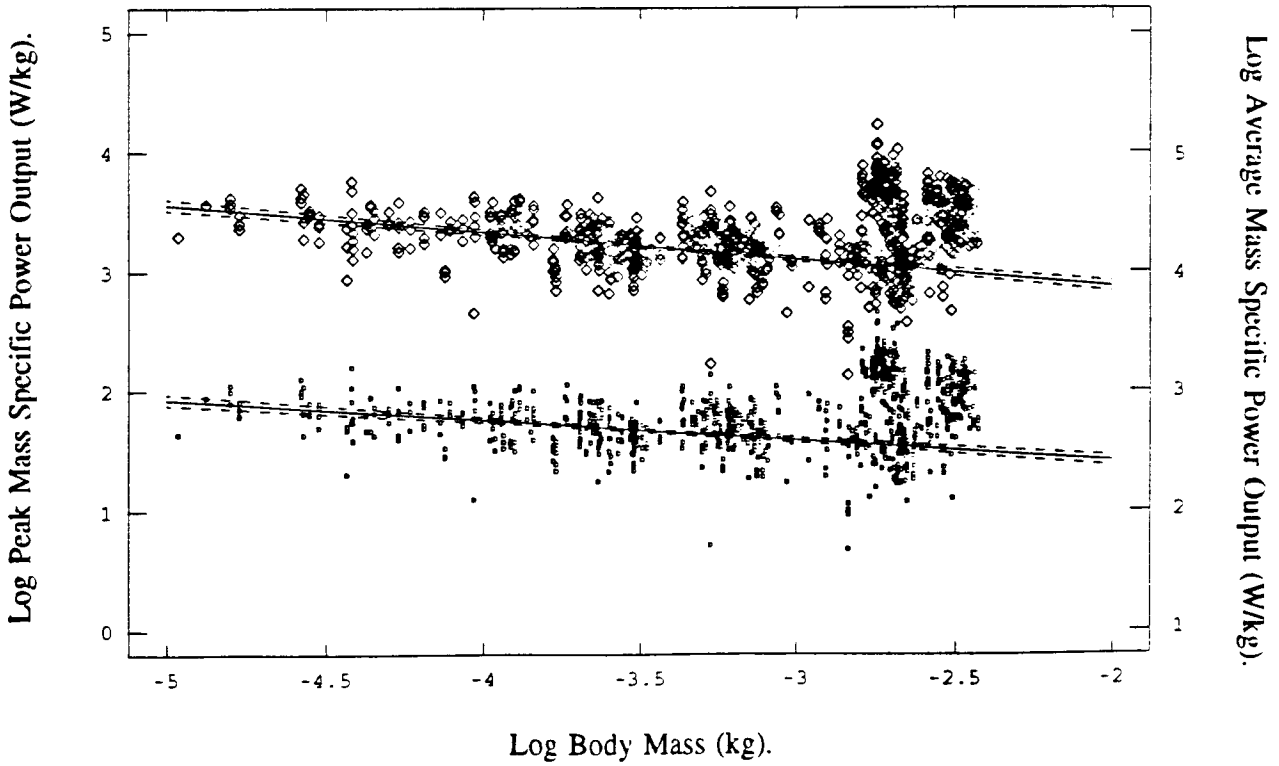
Log Peak Mass Specific Power Output (W/kg).
5
4
3
2
1
0
-5
-4.5
-4
-3.5
-3
-2.5
-2
Log Body Mass (kg).
Log Average Mass Specific Power Output (W/kg).
5
4
3
2
1

by adopting more upright postures. It is possible that large locusts use different postures immediately before a jump, and may go through different kinematic motion during a jump relative to small instars. Such kinematic differences may affect conclusions drawn from morphological and mechanical comparisons. Figure 4.9 shows the relationship between the log of centre of gravity movement during the jump impulse and log body mass. This relationship does not seem to show the discontinuity between juveniles and adults seen in the other measures of performance. The regression for the entire data set has a slope of 0.378 (SE = 3.70E-3, r^2 = 0.885), which is not significantly different from the slope of 0.375, for the relationship between the log of tibial length and log body mass for these locusts (F_s= 0.0838, df.= 1, 1363, $p < 0.05$) (chapter two). This suggests that the distance over which the acceleration is developed is a constant function of leg length regardless of size or age. It also suggests that if the jump impulse starts with the knee joint fully flexed, (and this seems reasonable based on the anatomy of the catch mechanism (Heitler, 1974)), then the jump is kinematically similar in small and large locusts, with no postural scaling. Additionally, any discontinuity in performance at the transition to adulthood, in terms of velocity or acceleration, is not the result of some kinematic or postural feature of the jump mechanism, but is rather a reflection of changes in the power generating mechanism.

From ballistics we can estimate the distance covered by locusts once they leave the ground and become projectiles. Bennet-Clark (1975) presented the following formula to predict the distance covered by a ballistic projectile:

$$d = \frac{v^2 \sin 2\phi}{\mathbf{g}} \qquad \text{eq. 4.1.}$$

where d is the distance covered, v is the take-off velocity of the projectile, ϕ is the angle from horizontal and **g** is the acceleration due to gravity. For a

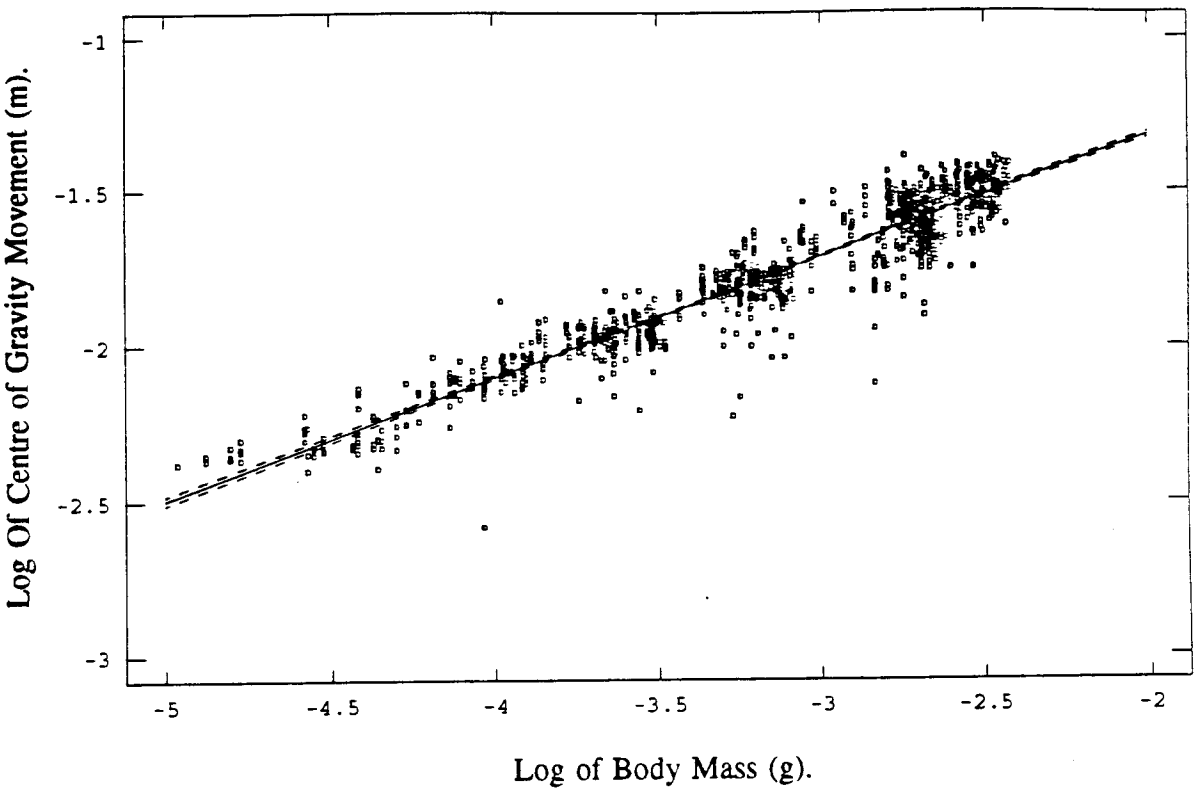

Figure 4.9.

The relationship between the log of the movement of the locusts' centres of gravity during the jump impulse and the log of body mass. The equation of the regression line calculated for juvenile individuals is $Y = -0.676 + 0.355 \times X$ (F_s=5339.12, df.=1, 735, r^2=.8790). The equation of the regression line calculated for all individuals is $Y = -0.570 + 0.378 \times X$ (F_s=10445.36, df.=1, 1360, r^2=.8849).

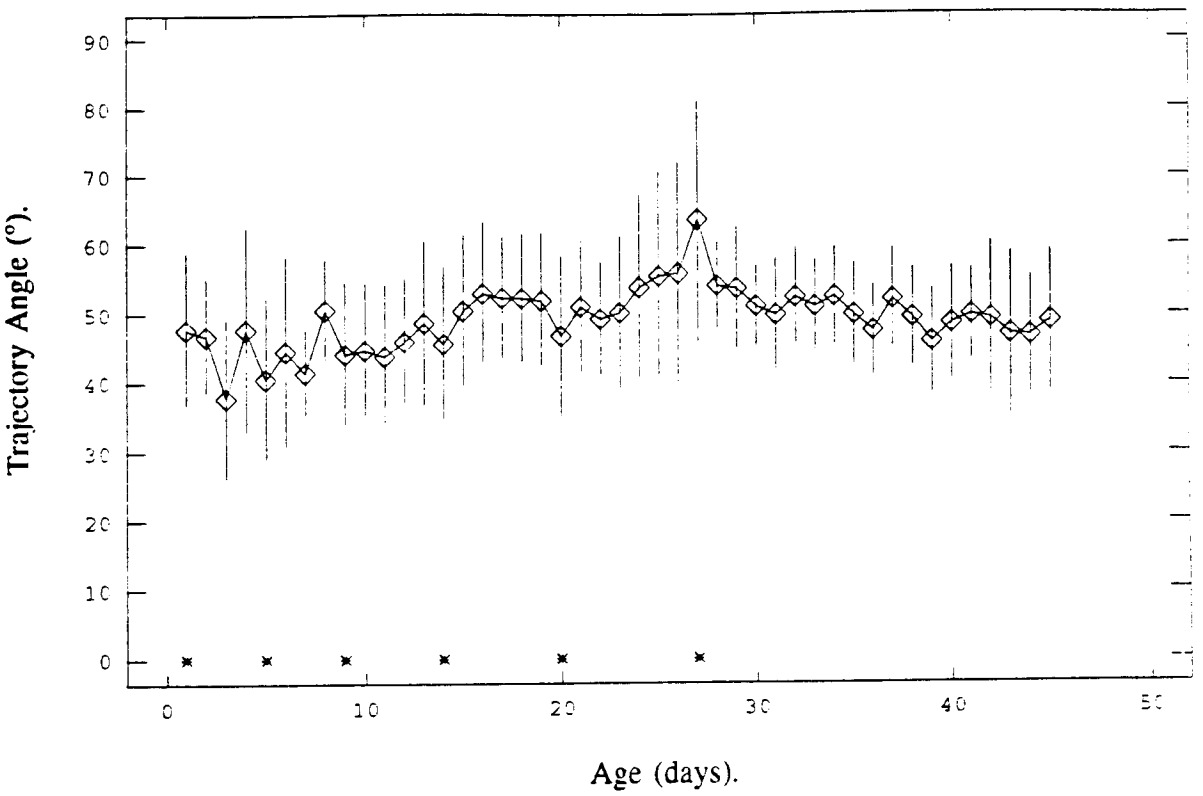

Figure 4.10.

The relationship of the trajectory angle of the jump and the age of the locust. Data are reported as means and standard errors of the mean. The first day of each instar is marked with an *.

constant take-off velocity, therefore, projectiles will cover the same distance over ground regardless of size. In general it is assumed that projectiles are launched at 45°, which maximizes distance covered for a given take-off velocity. Figure 4.10 is a plot of the mean trajectory angle of the jump as a function of age. These data indicate that locusts are capable of taking off at a wide variety of angles. On average, however, they leave the ground at angles between 45° and 55°, but individuals in this study were observed to adjust their trajectories between 15° and 90° to avoid obstacles in their paths. Given the capability to adjust their trajectory over a wide range, it is difficult to attach much significance to trajectory angles, but in general the trajectories were above 45°. Figure 4.11 uses the data on trajectory angle, take-off velocity and equation 4.1 to estimate the jump ranges of locusts on each day that they were tested. The sensitive dependence of distance on take-off velocity is reflected in the relatively constant distance travelled of 15 to 20 centimetres over the juvenile instars and the three fold increase in jump distance in adults. Bennet-Clark and Adler (1979) have suggested that as much as 10 to 20 % of the kinetic energy generated in the jump of the locust may be consumed in aerodynamic drag during the air-borne phase of the jump. Therefore, my estimates of jump distance should be viewed as overestimates, particularly in the case of the smaller sized locusts.

DISCUSSION

Scaling of Locomotor Performance. The large data set produced here for the jump of these functionally and morphologically similar animals that vary in body mass by more than two orders of magnitude allows us to address questions of how locomotor performance scales in hopping locusts. How might

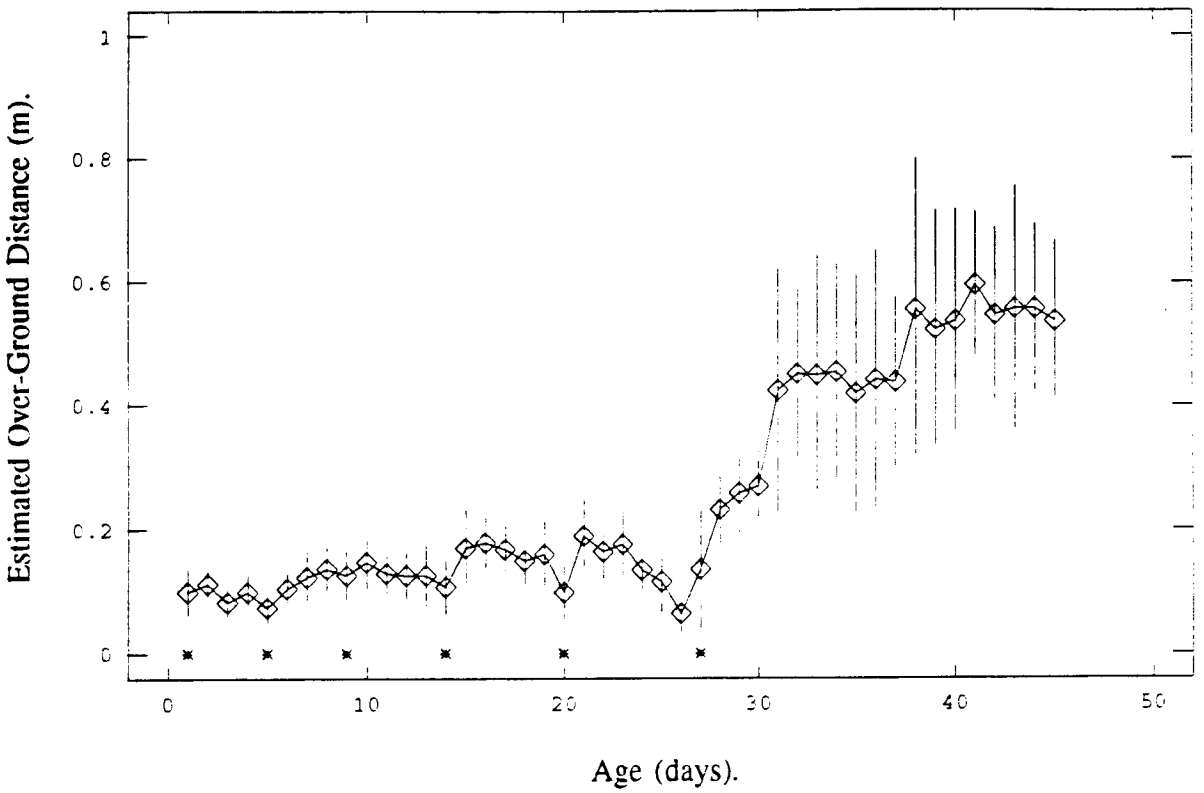

Figure 4.11.

The relationship of the estimates of the distance covered by the locusts as a ballistic object after they leave the ground and the age of the locust. A description of the calculation of estimated distance is in the test. Data are reported as means and standard errors of the mean. The first day of each instar is marked with an *.

performance parameters such as force, acceleration or velocity scale with body mass? Hill (1950) has provided a rationale for relating morphological dimensions to force, energy and power output by muscles and I have used this rationale to generate quantitative scaling predictions. All of the predicted scaling exponents that are generated, as well as the observed values for *Schistocerca gregaria* are summarized in table 4.I.

If muscle force is the ultimate power plant for the locust jump, accepting the energy storage role of the apodeme and other connective tissue structures (Bennet-Clark, 1975; Gabriel, 1985b), and the force produced by a muscle is a function of its cross sectional area (Hill, 1950), then we may be able to predict the scaling of force if we know how the muscles' dimensions scale. If we consider a generalized exoskeletal case where the cross-section of the muscle is proportional to the square of the diameter of the limb segment that houses the muscle, then we can make predictions about the scaling of force production. In the geometric similarity model (GSM) diameter scales to body mass raised to the 0.333 power (McMahon, 1984). Therefore, force would scale to mass raised to the 0.667 power (ie. $mass^{.333} \cdot mass^{.333} = mass^{.667}$), and acceleration would scale to mass raised to the -0.333 power (ie. $mass^{.667}/mass^{1.000} = mass^{-.333}$). The elastic similarity model (ESM), which predicts that diameter will scale to mass raised to the 0.375 power (McMahon, 1973), predicts that force production will scale to mass raised to the 0.750 power, while acceleration will scale to mass raised to the -0.250 power. Similarly, the constant stress similarity model (CSSM), which anticipates diameter scaling to mass to the 0.400 power (McMahon, 1984), predicts mass scaling exponents of 0.800 and -0.200 for force and acceleration respectively.

Interestingly, velocity is predicted to be mass independent in each model.

TABLE I.

Exponents for allometric equations describing both morphological and performance measures from models and those observed for *Schistocerca gregaria*. All relationships are modelled by the form $x \propto M^b$ where M is body mass in kilograms. The quantity x is the parameter that is scaled as listed below, and b is the scaling exponent.

	Model			Observed for
Scaled parameter	GSM	ESM	CSSM	*S. gregaria.*
Morphology				
Limb length	.333†	.250†	.200††	.377
Limb diameter	.333†	.375†	.400††	.311
Mechanics				
Flexural stiffness	1.333	1.500	1.600	1.532
$\mathbf{I}_{\text{entire cuticle}}$				1.195
$\mathbf{E}_{\text{entire cuticle}}$				0.311
Jump Performance				
Force	.667†††	.750	.800	.732
Acceleration	-.333	-.250	-.200	-.269
Velocity	.000†††	.000	.000	.053
Energy	1.000†††	1.000	1.000	1.114
Power	.667†††	.750	.800	.772
Specific Power	-.333	-.250	-.200	-.288
Movement of centre gravity	.333	.250	.200	.378

† McMahon, 1973
†† McMahon, 1984
††† Hill, 1950

Velocity in jumping animals is determined by the following relationship (Bennet-Clark, 1977, eq. 5):

$$v = \sqrt{2s \cdot a} \qquad \text{Eq. 4.2,}$$

where v is take off velocity, s is the acceleration distance (a function of leg length, Above and Fig. 4.9.), and a is the average acceleration produced in the jump. Therefore, we can relate the scaling of velocity to the scaling of leg length and acceleration. For each model, acceleration and leg length have scaling exponents that are equal in magnitude, but opposite in sign. Therefore, their product scales to body mass raised to the zero power and is scale independent.

Unlike the scaling of velocity, energy is predicted to scale directly with mass raised to the first power, but like the scaling of velocity it is model independent. Energy is the product of force, the product of two diameters, and distance, a length. So energy will scale directly with the volume of either the muscle producing the force, or the spring that stored the force.

The scaling of power output during the jump can be predicted from the scaling relationships between performance and body mass. Power is the product of force and velocity. As we described above, velocity is predicted to be scale independent by all models. Therefore, power output in the jump should scale to mass raised to the same power as does force for each model.

So how do the models anticipate the observed relations for *Schistocerca gregaria*? The observed scaling exponent for the dependence of peak force production on body mass (0.732, Fig. 4.4a.) most closely approximates elastic similarity; however, it proves to be statistically different from ESM's prediction of 0.750 (t_s = 2.393, df = 735, $0.1>p>0.05$). This scaling exponent for force

production in locusts is intermediate to that estimated for vertebrate hoppers from anatomical measures. Alexander et al. (1981) reported relationships between muscle masses, muscle fibre lengths and body mass for a variety of vertebrate hoppers. In all hind limb muscles reported, the mass of muscle scaled very close to body mass raised to the first power. By employing Alexander's (1977) method of estimating cross-sectional area of muscle I estimated that the fibre areas of deep hind limb flexor muscles of these vertebrate hoppers scaled to mass raised to the 0.65 power (similar to the prediction of geometric similarity), while in the quadriceps group it scaled to body mass raised to the 0.75 power (equivalent to elastic similarity), and in the ankle extensor group it scaled to body mass raised to the 0.80 power (equivalent to constant stress similarity). This suggests that within the morphological design program that produces geometrically similar amounts of muscle, these animals are increasing the muscles' force producing capacity per unit mass. They are presumably accomplishing this by changing the muscle fibre architecture, ie. increasing pinnation angle of the more distal limb muscles relative to those more proximal. It is tempting to suggest that these animals are adopting a distortive allometry (ie. ESM) that increases the cross-sectional area of muscle in larger animals relative to small ones in a way that biases the increase toward the distal end of the limb relative to the proximal end. It accomplishes this, however, without increasing the relative mass of muscle at the distal end of the limb, thus preventing an increase in the energetic costs of accelerating and decelerating the limbs during locomotion.

The scaling exponent of peak acceleration as a function of body mass (-0.269, Fig. 4.4b.) also is most consistent with elastic similarity, but again proves to be different statistically from ESM's prediction of -0.250 (t_s = 2.471, df. = 735,

0.1> p >0.05). The fact that the slope of acceleration on body mass differs from the model prediction to the same extent as does the slope of the relation between force and mass is not surprising as the acceleration data are normalized force values. Thus, it seems that the relationships between force production and body mass and acceleration and body mass are approximating the elastic similarity model. The statistical differences observed may reflect the influence of morphological scaling that produces longer, relatively more slender legs in larger locusts (chapter two). Nevertheless, as observed for the mechanical properties of the tibiae, the observed performance (ie. force production) approximates ESM in spite of a morphological program that deviates rather dramatically from elastic similarity.

All models predict mass independence for scaling of velocity in the jump, but we observed that the velocity scaled to mass raised to the 0.053 power. Where does this difference come from? The predictions are based on assumptions about morphology, but data in chapter two show that locust leg lengths scale to mass raised to the 0.377 power. Equation 4.2 allows us to eliminate assumptions about morphology and predict how velocity should scale given the scaling of leg length observed in *S. gregaria*. The square root of the product of acceleration and leg length (eq. 4.2.) should scale to body mass raised to the 0.054 power which is not significantly different from the observed value of 0.053. This explains <u>how</u> the scaling of velocity arises, but it does not seem to spotlight a design strategy per se that can explain <u>why</u> locusts produce relatively more elongate legs as they increase in size. That is, we have no *a priori* reason to anticipate a scaling exponent of 0.05.

The scaling slope of energy output that we observe in juvenile instars (1.114, Fig. 4.6b.) is higher than the models predicted. It may be that the

relatively larger output of energy seen in larger juveniles is a result of the increased quality of the material that stores the energy prior to the jump. Before the jump the energy is stored in the extensor apodeme and semilunar process (Bennet-Clark, 1975), and during the jump the energy is transmitted through the metathoracic tibiae to the ground (Brown, 1963). As such, the cuticular springs form an energy transmission system. Data in chapter two showed that the material resilience increases by approximately 20% from first to fifth instars. If we assume that this increase in resilience is reflected in all of the cuticular elements and adjust the amount of energy we measure in the jump by the energy loss characteristics of the transmission, then we can estimate how much energy was input to the system prior to the jump and how this quantity scales to body mass. The estimated energy input to the transmission system scales with body mass raised to the 1.08 power (F_s=10,129.02, df.=1, 735, r^2=0.932), which while closer is still statistically different from the prediction of 1.00 made by all the models (t_s=7.9997, df.=735, $p<0.05$).

Whereas each of the other measures of jump performance appear to scale close to the predictions of elastic similarity, peak power output scales to body mass in a manner most similar to the predictions of constant stress similarity (0.800). It does so in a sensible way, however, as it is the product of force, which scales approximately elastically (0.732), and velocity, which scales to higher exponent than anticipated (0.053). As a result, power outputs scale to body mass in a manner that is intermediate between the predictions of elastic and constant stress similarity (0.772). Because power is calculated within each impulse, the scaling exponent for power and body mass is numerically different from that which might be predicted simply from taking the product of the scaling relationships for force and velocity (ie. 0.732 + 0.053 = 0.785 vs. 0.772).

This difference indicates that the shape of the force and velocity envelopes contribute to the estimate of power produced in the jump. It also suggests that our examination of the slopes of the energetic relationships are independent; that we are not "boot-strapping" our data to compare the energy or power output and body mass relationships.

Overall these results have generated a data set for jump performance that is in the range of the predictions of models that are based on maintaining scale independance of mechanical parameters. However, the data do not absolutely match the predictions of any single model. Indeed, force produced in the jump, the parameter whose scaling prediction follows most directly from Hill's (1950) original assertion, scales in a manner closest to elastic similarity while power output scales more closely to the predictions of constant stress similarity. Has it been valid, or as suggested in chapter one, naive to doggedly compare the data on jump performance with the predictions of the various models? Do the violations of the models' theoretical underpinnings in the scaling of morphology fatally compromise their utility?

If each scaling exponent that we observe can be explained by the other measures of performance, then the data set will represent a single mechanical package--an internally consistent strategy. In the data for locusts there is a consistent strategy. A route to this conclusion is suggested by the scaling of movement of the centre of gravity (Fig 4.9), which, as discussed above, is directly reflecting the scaling of leg length. In discussing the scaling of each measure of performance we have seen that there is a rational basis for the statistical departures away from either similarity model in the context of force production scaling in a manner that is close to, but different from elastic similarity and the legs scaling in a manner that produces relatively longer and

more slender tibiae in larger locusts. Thus, it is fair to say that the scaling of jump performance seen in the locust is following a strategy that is separate from either elastic or constant stress similarity, but is itself an internally consistent package.

Clearly, the original assumptions of both ESM and CSSM are violated in that leg morphology does not follow either model. Does this violation make it inappropriate to compare the subsequent data on jump performance with those models? I believe that the comparison is still useful for two reasons. Clearly, we would not know whether the locust was demonstrating any particular model unless we actually asked the question. More importantly though, the results demonstrate that despite the unique morphological scaling, jump performance is scaling in a mechanically functional manner. The fact that the data are intermediate to the predictions of ESM and CSSM suggests that the mechanical consequences of those strategies (ie. constant strain or constant stress) represent real issues to which the design of the locusts' legs has responded. These design issues have had to be dealt with in the context of the observed morphological scaling, however, and this may have set constraints on the proximity to which the scaling of jump performance can approach a model such as elastic similarity.

I have asserted that elastic similarity is being approximated by the jump performance of the locust, but is that reasonable in that no measurement made so far is statistically elastically similar? My justification for referring to elastic similarity in this context is the scaling of ground reaction force output. Muscle force output is the most independent performance parameter that I measured, in that predicting the scaling of force relies on the fewest morphological parameters. It is also the parameter that scales most closely to

elastic similarity. Acknowledging that the locust is not adopting elastic similarity as developed by McMahon (1973) for vertebrate skeletal designs, it is **approximating** in performance a design that keeps the normalized deflections of a cantilever beam similar independent of size (ie. elastic similarity).

Acceleration and Design. Though we have not discussed the data for jump performance in terms of life history strategies, predator avoidance has been the context for previous analyses of jumping in locusts and anurans (Scott and Hepburn, 1976; Emerson, 1978; and Queathem, 1991). In each case the suggestion has been made that acceleration produced in the jump is the critical performance parameter. In discussing jumping in anurans, Emerson (1978) used scale independence of jump performance parameters to discriminate models that associated specific measures of performance with success in avoiding predation. She found that in *Rana pipiens* and *Pseudacris triseriata* average acceleration was relatively scale independent over a 30 fold range in body mass, while *Bufo americanus* showed a decrease in average acceleration with increasing size. By this criteria the ontogenetic data on locusts suggest that acceleration per se is not necessarily the key functional performance feature, but rather the velocity developed in the jump is perhaps more important. This suggestion is based on two observations. First, velocity, which is relatively scale independent over the first five instars, rather than acceleration, which varies four fold, is regulated by the developmental design programme. While there seems to be a functional relationship between falling accelerations and increasing body mass for juveniles, the duration of force development in the jump seems to be compensating quantitatively for the fall in acceleration to provide a relatively constant take off velocity. The scale

independence of take-off velocity suggests that if selection has operated on the jump performance of this locust, then velocity, or a consequence of velocity, is the key performance parameter. Secondly, there seems to be an unexploited potential to improve acceleration performance in flightless instars that is exploited to some extent in adults.

Figure 4.12 provides a comparison of the accelerations produced in jumping locusts with published values for the flea, *Spylopsyllus cuniculus* (Bennet-Clark and Lucey, 1967), click beetle (Evans, 1971), the mediterranean fruit fly larvae (Maitland, 1992), and the standing jump of the Kangaroo rat (Biewener et al., 1988). If we perform a two-point regression between a value for the average male adult locust and the flea (of all the animals reported in figure 4.12 these the flea and the locust are the ones that we know jump using similar cuticular spring mechanisms), the slope turns out to be -0.2499. The slope of the relationship between acceleration and mass predicted by ESM of -0.25 would seem to describe the adult fleas and locusts even better than the slope of -0.269 which describes the flightless locusts. The fruitfly maggot and kangaroo rat both produce accelerations that lie very close to the regression based on the performance of the flea and the locust. This suggests that the same functional design issues that determine scaling relationships in flightless, juvenile locusts act to determine the separate relationships for adult locusts and these other jumping animals of widely different designs. Apparently the robust predictions of ESM apply to these jumping animals generally, but the juvenile locusts are able to get by (in an evolutionary sense) with about one third lower accelerations per body mass than the heroic performance of the adults and these other animals.

A feature of these relationships is that if elastically similar jumping animals

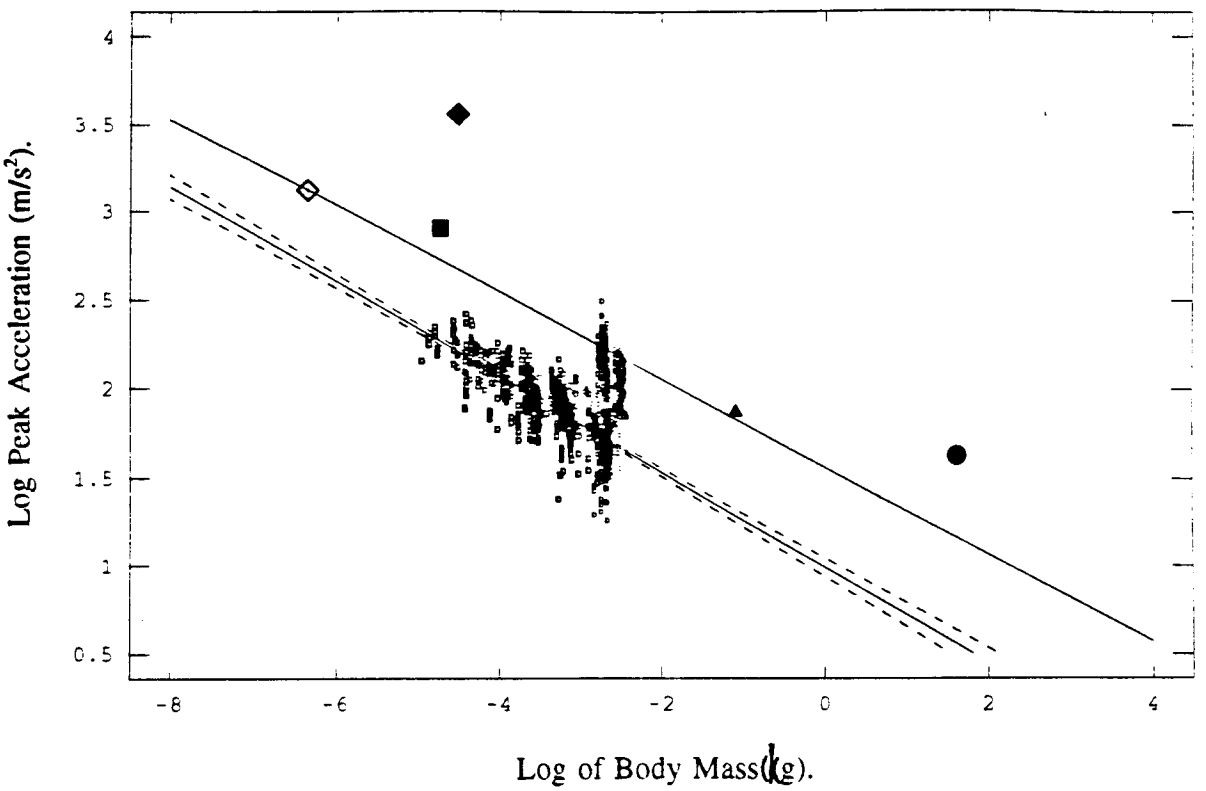

Figure 4.12.

The relationship between the log of peak acceleration produced in jumping and the log of body mass. This figure compares the data reported in figure 4c with published values from other jumping animals. Data is presented for the flea (◇), *Spylopsyllus cuniculus*, from Bennet-Clark & Lucey (1967), the click beetle (♦) from Evans (1971), the mediterranean fruit-fly larvae (■) from Maitland (1992), as well as the standing jump of the kangaroo rat (▲) from Biewener et al. (1988) and the continuous hopping of the kangaroo (●) from Alexander & Vernon (1975). The equation of the two-point regression made between the data from the flea and average calculated for all of the adult, male locusts had a slope of -0.2499, which seems indistinguishable from the prediction of elastic similarity (-0.250).

increase in size and travel down the line relating acceleration with body mass, there is a point where the accelerations fall to a level where the animal will beunable to leave the ground in a jump, and the body mass where this occurs will be an absolute limit to body size for a given jumping "design". Realistically, a functional limit will occur before this point, as decreasing accelerations produce slower and shorter jumps in the absence of spectacular compensatory specializations of leg length to increase the interval over which acceleration is developed. In any event, it seems that an animal that is elastically similar to juvenile locusts could not continue to get larger indefinitely, and for larger animals to jump they must move off the relationship between acceleration and body mass for juvenile locusts and produce higher accelerations at a given size.

There seems to be two design strategies that could allow an animal to move off of any of these relationships; either produce more force per unit body mass (ie. increase the proportion of body mass that is jumping muscle), or increase the efficiency of the energy transmission system in producing ground reaction force. Gabriel's (1985a) data on locusts suggest that adult locusts have increased the proportion of body mass that is jumping muscle to achieve the high accelerations seen in the adults. Gabriel (1984) made the point previously that in larger animals, where energy production capacity limits jumping performance, increasing the relative investment in jumping muscle is the most effective way of improving jumping performance. Clearly 40 kg. Kangaroos are not "elastically" similar to adult locusts (Fig. 4.12.), and it has been observed that as much as 8 to 10 % of the body mass is invested in hind leg muscle of a kangaroo (Alexander & Vernon, 1975) compared to 4.5 to 6 % in locusts (Gabriel, 1985a). Also, kangaroos are storing kinetic energy from one stride and using it in a following stride while locusts use only energy that is stored

during a single "stride".

It seems significant that the data for standing jumps in kangaroo rats and mediterranean fruit fly larvae lie so close to predictions based on adult locusts and fleas. In both cases the animals use quite different jumping mechanisms from the locust. Indeed, the fruit fly maggot is legless. In continuous locomotion the Kangaroo rat is known to use elastic energy stored from previous strides to increase the accelerations and energy output of a jump (Biewener et al., 1981), but in single jumps from standing starts they are not known to use stored spring energy. It is therefore interesting to see the data for a standing jump in the Kangaroo rat so close to the prediction made by adult locusts and fleas (Fig. 4.12.). This relation may reflect common design features in very different animals. It could be that for a given relative investment in jumping muscle each animal gets a similar acceleration output independent of morphological design. The limits to this suggestion are demonstrated by both the click beetle, which has a similar investment in muscle as the locust, but much higher relative accelerations (3800 m/s^2, Evans, 1971), and the fruit fly maggot, which has similar accelerations to the locust, but much larger investment in jumping muscle (16%, Maitland, 1992). It remains to be discovered if this relationship, which suggests that this variety of jumping designs are elastically similar, is other than a coincidence.

In going from the line for juvenile locusts in fig. 4.12 to the line for adults the relative muscle mass increases approximately 20%, but the kinetic energy output goes up by four fold (Fig. 4.6b.). Does the 20% increase in relative muscle mass between fourth instars and adults explain the increase in performance observed at the transition to adulthood? Where might additional energy come from? Gabriel (1985b) made the observation that the distance

covered as a ballistic projectile increased by 300% between fourth instar hoppers and adults. She explained that the increased energy produced in the jumps of adult locusts was the product of relatively stronger muscles applying more force to stiffer energy storage devices, and therefore storing more energy. She noted that adult extensor muscles' pinnation angle increased and relative muscle fibre length decreased relative to fourth instar locusts, indicating that the muscle was capable of producing more force per unit volume. She also showed that the adult apodeme increased in cross-sectional area by 440%, presumably increasing in stiffness relative to the fourth instar hoppers, and the semilunar process increased in measured stiffness by six fold (Gabriel, 1985b). She felt that the increased stiffness of the spring combined with the increased force output of the muscles could account for a large part of the increase in specific energy seen in the jumps of adults. This analysis, however, does not seem to describe the situation in locusts adequately. Gabriel reports functional cross section of the tibia extensor muscle as 5.7 mm^2 and 18.9 mm^2 for the fourth instar and adult respectively. When the area is normalized by the body mass being accelerated, the values are the same for the different age classes (20.40 $mm^2/g_{4th\ instar}$ vs. 20.58 mm^2/g_{Adults}). Similar forces applied to more easily deformed springs could also store relatively larger amounts of energy, but this also does not appear to be the case. Gabriel's data show that the force producing cross-sectional area of muscle is applied to a relatively larger cross-sectional area of apodeme in the adults compared to the fourth instars (1781 mm^2 muscle/mm^2 $apodeme_{4th\ instar}$ vs. 1092 mm^2 muscle/mm^2 $apodeme_{Adults}$). This results in the apodeme springs seeing 37% less force per unit spring area in adults. What we have, therefore, are similar forces applied to relatively stiffer springs resulting in smaller deformations of the springs and smaller amounts of

energy stored in adults relative to fourth instars. We are still left wondering where the additional energy comes from in the adults' jumps. It seems very likely that Gabriel's suggestion that the juvenile muscles are not working as hard as they are in adults is correct (Gabriel, 1985; Gabriel & Sainsbury, 1982).

The Ontogenetic role of Jump Performance. Bennet-Clark (1977) showed how body size plays an important role in jumping design. Chiefly, this results in the jumps of small animals being limited by their ability to generate power output, while the jumps of larger animals are limited by their ability to generate kinetic energy. Gabriel (1984) analyzed these ideas and predicted that small, power limited animals can achieve better performance by either getting larger or increasing their leg length. In the largest jumpers she felt that improvements in performance could optimally be achieved by increasing the fraction of the body mass that was committed to jumping muscle. Indeed, she reported that across the ontogenetic increase in body mass in locusts, jump performance improved by increasing body size up to the size of fifth instars. In adults, however, jump performance was improved by increasing the relative mass of jumping muscle by approximately 50% over that in fourth instars (Gabriel, 1985b).

These results indicate that the increase in jump performance seen in adults does not represent a change associated with body size, but rather a change in life style. It is no mere coincidence that the increase in jumping muscle occurs at a point where the mode of locomotion switches from hopping to flying. I suggest that one strategy may not appropriately describe the development of the jump performance. Rather it may be more reasonable to develop one framework to analyze the juveniles, and another to analyze the

adults; frameworks that are constructed to account for what may be entirely different ecological roles of the jump at different points in the life history. In small locusts we see an increase in leg length that is rapid relative to the increase in body size (chapter two) as a strategy for increasing jump performance. The increase in jumping performance in adults reflects a switch to flight, and the demand that flight makes for higher performance jumps. Indeed, this distinction has already been alluded to in discussing locust jump performance data (Scott & Hepburn, 1976; Gabriel, 1983; Queathem, 1991). This interpretation seems fundamentally separate from the switch to larger investment in jumping muscle mass in larger jumping animals that Gabriel (1983) anticipates. If I was keen to shoe-horn my observations into Gabriel's paradigm, then I might say that the locust exploits the increasing leg length strategy up to the point where the locomotor strategy changes and there is a demand for a fundamentally different, and stronger jump. If this represents a strategy, then I view it as a locomotion mode change issue, rather than a body size issue *per se.*

The ontogenetic increase in body mass and increase in peak force production are the result of a clear difference in developmental timing. The relatively early period of rapid mass increase would seem to indicate that for young, small locusts getting larger is a higher priority than increasing force production to maintain high accelerations in the juvenile instars. Once the locusts have achieved a large adult mass, the delayed period of rapid increase in force production results in relatively high forces that produce large accelerations quantitatively similar to those observed in first instar individuals.

Acceleration is dependant on the amount of force produced by the jumping muscles and the body mass being accelerated. So the adults are

producing 25 **g**'s of acceleration by producing more force per unit body mass than the flightless fifth instars of similar body mass (Fig. 4.12.). If survivorship required as high acceleration performance as possible, then why wait until adulthood to increase the force output of the jumping machinery? Acknowledging the teleological danger in asking "why" type evolutionary questions, it still seems that the high acceleration per body mass seen in adults could be achieved in juveniles with benefits to predator avoidance by advancing the developmental timing of jumping muscle growth. Certainly it has not been necessary to invoke predator avoidance as a "strategy" for the jump in the flea. Therefore, having high peak-acceleration as a strategy for predator avoidance seems questionable. If the jump of the locust produces one velocity, and therefore distance, in flightless individuals, and another velocity in winged ones, what then is significant about these two levels of performance? In flightless, juvenile instars the jump data predict a distance travelled of approximately 20 cm, a figure that is intermediate between the maximum performance of 30 cm and average of 11 to 14 cm for fourth and fifth instars observed by Gabriel (1985a). Regardless of the specific distance, the interpretation is the same: there appears to be a functional distance that is important to the hopping locust. To test this hypothesis it would be important to look for some characteristic dimension in the locust's environment that correlates with the jump distance. It may be that there is a pattern to the spacial organization of the vegetation that forms the food source for the hoppers that has a characteristic spacing of 20 to 30 centimetres.

In adults the important parameter may not be distance travelled, but rather take off velocity itself. It is significant that the two fold increase in take off velocity occurs at the point in the life history where the primary mode of

locomotion switches from hopping to flying. Weis-Fogh (1956) reported that locusts flying in wind tunnel experiments stop flying when the wind speed falls below two and a half meters per second. It seems unlikely that the minimum observed flight speed and the take off velocity in adults being the same is simply a coincidence (Fig. 4.5a). Because locusts use unsteady-state aerodynamics during take-off it is difficult to estimate what their minimum flight speed might be *a priori*. However, it seems reasonable to estimate what effect the increased take-off velocity might have on thrust production using actuator disc theory. With actuator disc theory we need not be specific about the anatomy or the mechanics of the thrust generating mechanism. For actuator-discs the thrust produced is proportional to the mass flux of fluid moving through the actuator times the velocity of the fluid. The quantitative relationship is

$$T = \rho S_d v (V + \tfrac{1}{2} v), \qquad \text{Eq. 4.3.}$$

where T is the thrust produced by the actuator-disc, ρ is the density of the fluid, S_d is the disc area--calculated as a circular disc swept out by wings of a known length, V is the forward velocity of the actuator relative to the fluid and v is the increment of velocity added to the fluid as it passes through the actuator disc (Blake, 1980). Figure 4.13 is a plot showing real solutions of equation 4.3 for v in terms of varying values of V. The data in figure 4.13 suggest that as the actuator disc moves through the fluid at higher velocities (V), the increment of additional velocity (v) falls rather quickly. For a 3.2 g female locust with 5.5 cm long wings to take off from a standing start, the wings must generate an air-flow of 2.62 m/s to generate sufficient thrust to balance body weight. By jumping off the ground at 2.5 m/s at an angle of 55° to horizontal, the additional velocity that the wings must generate falls to 1.12 m/s - a decrease of 57%. Were the adults to reach the same end-jump velocity as the fifth instars the wings would

Figure 4.13.

Increment of additional velocity required to produce thrust at 55° (ie. trajectory angle) large enough that its downwardly resolved component is sufficient to balance body weight for actuator discs moving at various velocities. The data are solutions for the following equation relating thrust produced by an actuator disc to the velocities of the fluid moving through the disc: Thrust = $\rho S_d v (V + \frac{1}{2} v)$, where ρ is the density of air, S_d is the area of the disc (the area swept out by wings of given length), V is the velocity of the disc (modelled here as the end jump velocity of the locust), and v is the increment of additional velocity to which the fluid must be accelerated as it passes through the disc in order to generate the required thrust. This formulation assumes that the actuator disc is oriented normal to the trajectory angle. A body mass of 3.2 g, a wing length of 5.5 cm and a density of air of 1.1746 Kg/mm^3 were used to calculate the data labelled 'Female' in the figure. A mass of 2.0 g and a wing length of 4.8 cm was used to calculate the data labelled 'Male' in the figure. The data indicate that producing 2.5 m/s in the jump of a 3.2 g female requires the production of 35.6% less additional velocity going through the disc, and 73.3% less power required, relative to an end-jump velocity of 1.1 m/s. The data also indicate that jumping at 2.5 m/s requires 57.2% less additional velocity than a standing start with a power requirement savings of 92%. The estimates for the smaller, male locusts suggest that the increase to adult take-off velocities lower the additional velocity required by 37.5%, and reduces the power required for take-off by 75.6% over the requirements imposed by the juvenile end-jump velocities.

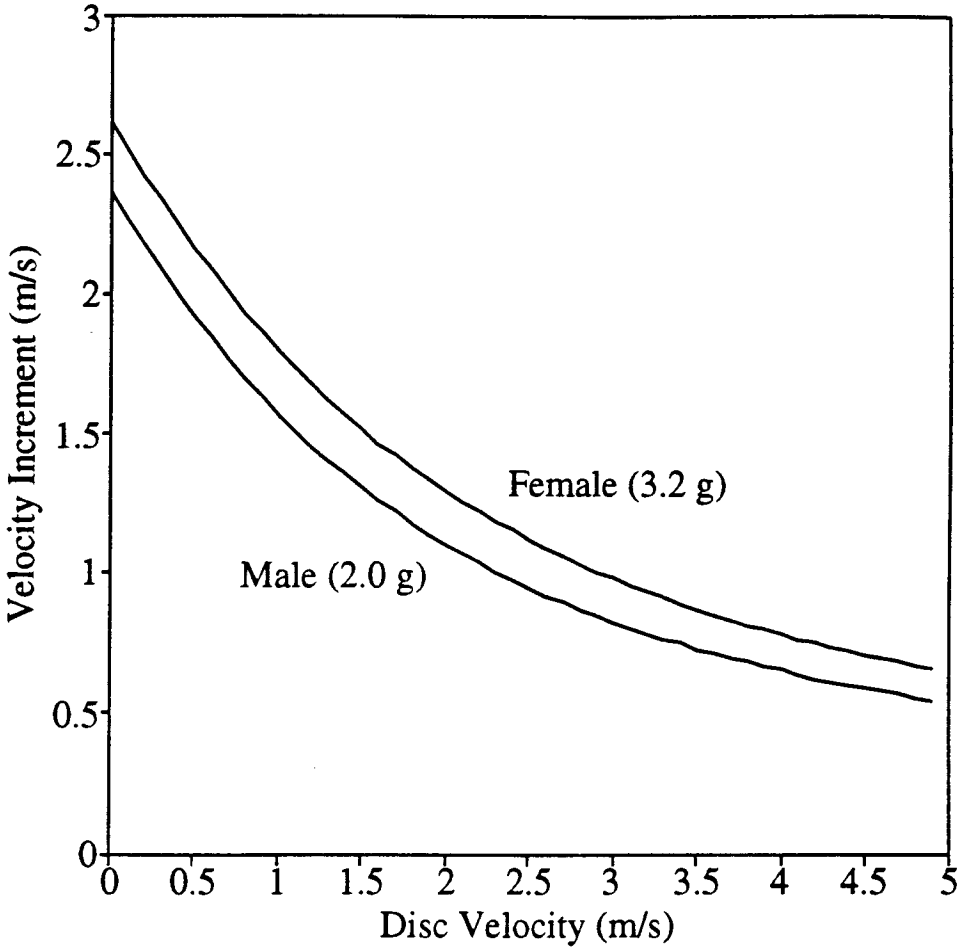
Velocity Increment (m/s)
3
2.5
2
1.5
1
0.5
0
Female (3.2 g)
Male (2.0 g)
0
0.5
1
1.5
2
2.5
3
3.5
4
4.5
5
Disc Velocity (m/s)

have to generate a flow through the disc of 1.74 m/s, a decrease of only 33% over a standing start, and 55% greater than the increment of velocity for a jump of 2.5 m/s. For a 2 gram male with 4.8 centimetre long wings the data in figure 4.13 suggest that jumping with a velocity of 2.5 m/s requires an additional increment of velocity of 0.95 m/s, a reduction of 60% from the standing-start disc velocity of 2.37 m/s. Since the power required by an actuator is proportional to the third power of the disc velocity (Von Mises, 1959), the difference in end-jump velocities between fifth instars and adults represents a 75.6% savings in power required to generate the thrust necessary to overcome the force of gravity. This power savings seems considerable, but without knowing explicitly what the power requirements are for flying at 1.1 m/s relative to the maximal power output capacity of the flight muscle it is impossible to say if the jumping velocity developed by juveniles represents an absolute limit to flight by locusts. Alternately, it may be that to jump much faster requires uneconomically high jumping muscle power output and the observed jumping velocity represents a balance between the falling demands for power from the flight muscle and the increasing demands for power from the jumping mechanism with increasing end-jump velocity.

These observations do suggest that achieving a high take-off velocity for the initiation of flight has demanded a higher performance jump than could be provided by the force production of the juveniles, and I believe that this increased demand for performance is the design issue that has driven the increase in power output in the jumps of adults over those of juveniles.

CHAPTER 5.

GENERAL DISCUSSION

In the case of each measure of mechanical performance that we can directly relate to morphological predictions (ie. flexural stiffness, force and acceleration) elastic similarity is approximated. In the case of power output and specific power output, which scale in a manner that is closer to constant stress similarity, the observed scaling for *S. gregaria* is quantitatively reasonable based on the dependence of power output on the other performance characteristics. However, the approximation of elastic similarity is achieved in spite of a morphological design program that produces increasingly spindly legs, and so deviates dramatically from elastic similarity.

If we were to adopt the adaptationist's paradigm, we might find the apparent approximation of elastic similarity a satisfying result. If function in a cantilever structure is dependant on controlling the deformation in bending, then as outlined in chapter one, if we want to adopt a similarity that results in devices to experience the same normalized deformation. This is the foundation of elastic similarity, and it provides a rationale for the locust's implementation of ESM in the mechanical design of its legs.

So locusts appear elastically similar in terms of mechanics, and we think that for bending structures this is a reasonable strategy. But if there is some value in adopting elastic similarity in the mechanical design of the legs, then why not be elastically similar in morphology as well? I can provide three somewhat speculative arguments to explain the morphological design that is

observed in the locust. Each is formulated in a separate context, but no single argument is exclusive of the others.

The manufacturing issue. It is possible that for a given adult morphology the constraints imposed by the process of moulting in exoskeletal animals determines the dimensions that the developing locust may adopt in proceeding toward the adult dimensions. Examination of the data in figure 2.5 & 2.6 suggests this possibility. Between each juvenile instar the external dimensions increase by a similar percentage. The lengths of the tibiae increase by approximately 50% while the diameters increase by approximately 40% after each moult. The process of moulting involves drawing the soft cuticle of the subsequent instar from within the hardened exuviae of the previous instar. Given the dimensions of the lumen of the old exoskeleton, it may be that the new cuticle's dimensions can only be increased up to a maximal amount through this drawing process. The scaling of the external dimensions is, therefore, indicative of the time spent within each instar and the amount that body mass increases within the same life history stage. Thus, it may or may not be demonstrating a specific design strategy that attempts to produce good jumpers throughout the life history of the insect.

The moult from the fifth instar to adult results in a smaller increase in dimension than any previous moult, suggesting that perhaps the moulting process does not limit the path that the external dimension may take in arriving at the adult condition. There are a number of distinctive changes that occur at this one moult, and it may not be fair to compare the process with the previous moults. For example, we have observed in chapter four that the mechanical events in the jump show sharp discontinuities at the moult to

adulthood. Therefore, the musculo-skeletal reorganization involved in this transition may place further constraints on the potential for change in the external dimensions occurring within a moulting event. Indeed, it is significant that there is a discontinuity in the scaling of each of the jump performance parameters at the moult to adulthood, but no discontinuity is observed in the scaling of dimensions or material and structural properties. A possible interpretation is that if the locust needs to be a competent hopper as an adult, and this requires a suite of parameters to have particular values, then growth in dimensions of the skeleton must follow a specific trajectory in time. Economy, however, does not likewise require performance parameters to follow a unique trajectory. So the juveniles can survive by producing lower forces per unit body mass than adults, resulting in the discontinuities seen in the moult to adulthood. However, the fact that the average body mass increases from fifth instars to adults in a way that maintains the scaling relationship between external dimensions observed across the juvenile instars suggests that there is a specific design program that is determining the scaling of the morphology. The following arguments discuss the nature of that specific strategy.

Force vs. body mass scaling. The morphological predictions that were laid out in chapter one were based on the loads experienced by the limbs being related directly to body mass. In chapter four we saw that the peak forces produced in jumping locust legs are five to twenty times body mass and scale to body mass raised to the 0.732 power. If the scaling programme is responding to peak ground reaction force rather than body mass, then it may be inappropriate to expect morphology to scale in an elastically similar manner. We could ask if force is not increasing as fast as the models predicted, then

what are the consequences of the observed scaling of external dimensions of the locust's legs?

If we re-examine equation 1.1

$$\sigma = \frac{(F\ell y)}{I} \qquad \text{Eq. 1.1.}$$

and use the observed scaling of peak ground reaction force, limb length, diameter, and second moment of area, we generate the following relationship for the scaling of peak stress:

$$\sigma \propto \frac{(Mass^{0.732})\,(Mass^{0.377})\,(Mass^{0.311})}{(Mass^{1.202})} = Mass^{0.218} \qquad \text{Eq. 5.1,}$$

and remembering that strain (ε) is $\sigma/\mathbf{E}$,

$$\varepsilon \propto \frac{(Mass^{0.732})\,(Mass^{0.377})\,(Mass^{0.311})}{(Mass^{1.532})} = Mass^{-0.112} \qquad \text{Eq. 5.2.}$$

Because the uncertainty of each scaling relation contributes to the uncertainty of the overall scaling of stress and strain it is impossible to distinguish the slope of the scaling of strain from a value of zero. Therefore, we cannot reject the idea that the leg's dimensions are actually adjusted to maintain a functional elastic similarity that is responding to the scaling of loading, rather than to the scaling of body mass *per se*.

Unfortunately, if we insert the predicted morphological scaling exponents into the above relationship where force scales to mass raised to the 0.75 power (the prediction from chapter four), we anticipate that strain will scale to body mass raised to the -0.125 power. This is also statistically indistinguishable from the exponent generated in equation 5.2. It seems that in order for the legs to actually follow a functional elastic similarity in the face of peak loads that are not increasing as fast is body mass, the locust would require even longer and

more spindly legs than it actually has. In fact, to maintain volume in such legs the length would have to scale to body mass raised to the 0.5 power while the diameter scale to the 0.25 power, producing legs that scaled length to the diameter raised to the 2.0 power.

It is important at this point to remember that this analysis is predicated on the assumption that muscle force scales to the 0.75 power of body mass. This assumption is based on Hill's (1950) suggestion that muscle force is proportional to a functional muscle cross-sectional area which in turn is the product of diameter squared. If we are going to suggest that the dimensional scaling of limbs loaded with forces that scale to mass$^{0.75}$ should produce even greater spindliness, then the prediction of 0.75 will change as well. In chapter four we assumed that the muscle in question is parallel fibred as a simplification, but in fact many muscles, the jumping muscle of the locust included, are highly pinnate. As such, our functional connection between the dimensions of the muscle and the functional cross-sectional area need to be adjusted. The fibres in a pinnate, jumping muscle will insert on the femoral wall and the apodeme tendon. The area of this insertion will be proportional to the cross-section of the muscle and will be proportional to the product of the length and the diameter of the insertion, rather than the square of the diameter of the muscle-housing limb segment.

If we once again reflect on equation 1.1, but this time resolve each mechanical parameter as a scaled function of dimensions and deal with pinnate muscle, the relationship between dimensions and strain becomes

$$\frac{(\ell \cdot d)(d)(\ell)}{(d)^4} = \text{Constant}$$

Remembering that a constraint of constant volume demands $M = \ell \cdot d^2$ leads

to both length and diameter scaling to body mass raised to the 0.333 power--geometric similarity. An important part of this prediction is that force will scale to body mass raised to the 0.67 power, not 0.75, and I will scale to mass raised to the 1.33 power, not 1.5. Therefore, in situations where the forces that the scaling strategy are responding to are produced by muscles I would anticipate the predictions of geometric similarity and elastic similarity to be indistinguishable. It is perhaps not surprising, therefore, that Alexander *et al.* (1979) found such a wide spread expression of geometric similarity in a wide variety of animals.

These calculations indicate that for animals where the peak loads are really functions of body mass, elastic similarity will produce limbs that become increasingly stout as McMahon anticipated (1973) and observed (1975). However, when the peak loads are functions of muscle forces, the limbs should produce geometric similarity. It is tempting to suggest that this difference represents a real difference in animal design. Indeed, any prediction that force will scale to body mass raised to a power less than one suggests that "spindly" elastic or geometric scaling will occur. In small animals, where the absolute value of the muscle forces are high relative to body weight, I anticipate this kind of strategy. In large animals, where the force of gravity will be large relative to the forces generated by the muscles, I would expect to see "stout" elastic similarity.

This discussion suggests that Prange's (1977) observations that cockroaches and spiders are apparently geometrically similar could also be interpreted as observations that these invertebrates are elastically similar. Locusts, however, have large pennate jumping muscles and are not geometrically similar. The scaling of force output does not follow from the

scaling of the product of a length and a diameter (0.732_{force} vs. 0.377_{length} + $0.311_{diameter}$ = 0.688). What does this mean? There are two parts to the answer: how and why. With respect to how, it is likely that the diameter of the femora scales to body mass in a manner different from the tibiae. I would predict that femoral diameters scale to mass raised to the 0.355 power, which would still produce spindly morphology, but would produce a predicted scaling of force to mass raised to the 0.732 power. The discussion of which force the design strategy is responding to has also ignored the effect of changing the material properties of the skeleton. Given a mutable material stiffness, an additional degree of freedom in adapting the structural design of the skeleton to the changing demands of increasing body size is supplied, and the limits to exotic morphologies are only limited by the scope of the material to stiffen. With respect to why, I would suggest that there is either a developmental constraint as outlined above as a manufacturing issue, or there is a functional role for the spindly morphology that the legs express that is associated with the jumping mode of locomotion.

Spindly levers as design strategies. If a design strategy could accomplish elastic similarity with a traditional model, where the limb skeletons become increasingly stout with increasing size, why then adopt a spindly strategy that produces fundamentally larger deformations, risking catastrophic rupture? Does the spindly strategy provide some benefit in performance? An answer is provided by turning the question around and asking what is the difference in performance if the tibia is relatively rigid or has some degree of compliance?

Figure 5.1a.

Diagramatic expression of how falling spring energy (SE) is balanced by increasing mechanical advantage (MA) to produce a parabolic ground reaction force (GF) envelope.

Figure 5.1b.

Diagramatic expression of the role of the energy "time machine" inherent in the locust legs design. In unloading stored spring energy into a rigid lever the force pays off against mechanical advantage to produce ground reaction force that follows the same parabolic trajectory as in figure 5.1a (dotted line). If some of the energy from the first spring is put into deforming a second spring, which pays back that energy in later when mechanical advantage is higher (heavy solid line), there is a delay in the point where peak ground reaction force is achieved. The consequences of this change are discussed in the text.

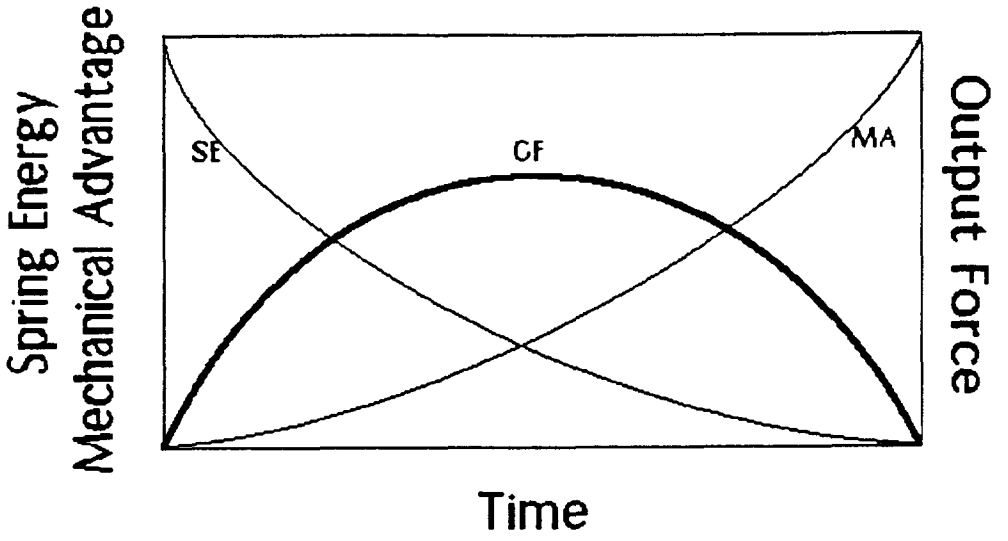
Spring Energy
Mechanical Advantage
SE
CF
MA
Output Force
Time

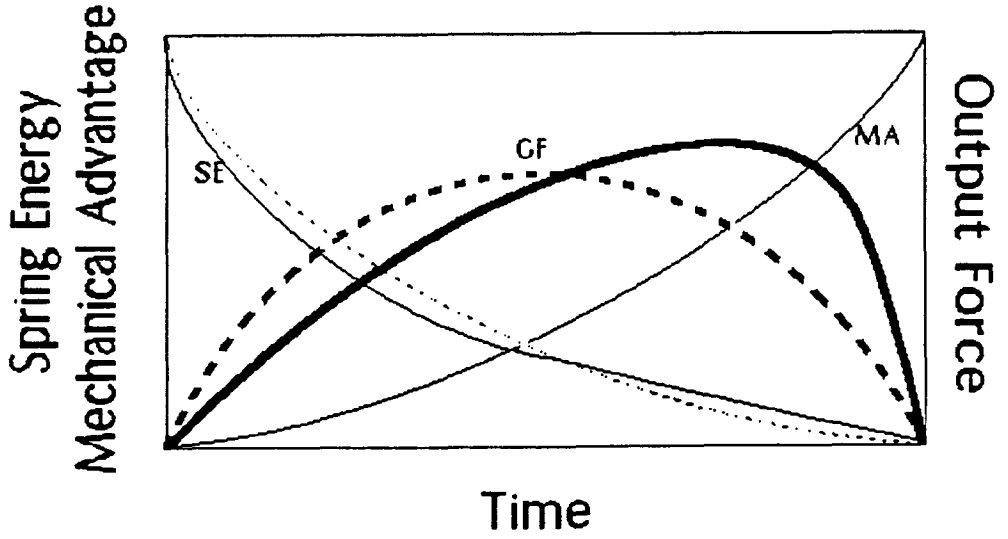
Spring Energy
Mechanical Advantage
SE
CF
MA
Output Force
Time

As mentioned in chapter four, Ker (1970) has pointed out that the production of ground reaction force during the jump of the locust is the product of the force stored in the spring, which decays gradually as the spring energy is converted to kinetic energy of the accelerated mass, and the mechanical advantage, which increases in an approximately inverse manner to the decay of spring force (Ker, 1970; Bennet-Clark, 1973 for locusts). Figure 5.1 is a diagram representing this trade off of spring energy and mechanical advantage for a theoretical spring system. If the lever arm whose mechanical advantage is changing is itself compliant (in the sense of being deformable rather than specifically 1/**E**), then it is possible that some of the spring force will go into deforming the lever which would then be returned later in the impulse at a time when mechanical advantage is high. Thus a spatially intermediate spring could provide a sort of "time machine", delaying the decay of spring energy until the mechanical advantage is able to make better use of the spring force. The dotted line in figure 5.1b represents the consequent trajectory of the spring energy decay of this design model. The heavy solid line is the resultant ground reaction force (ie. the product of the spring force and the mechanical advantage). If this model works, then the spindly legs of the locust may actually be designed to take advantage of the inherent deformability of long slender beams loaded in bending.

I have tested this design idea with a simple mechanical model shown in figure 5.2. A quarter inch steel rod was placed on a pivot and suspended with a Pesola spring scale. A 500 g mass was suspended from the rod and the rod was then depressed, preloading the spring scale to 1.40 kg and held in place by a piece of twine. The twine was set aflame and allowed to burn through, allowing the spring scale to unload and accelerate the mass. The entire

Figure 5.2.

Diagram of the mechanical model used to test the idea that compliant levers have a functional role in delaying the point of peak force. The device consisted of a rigid lever (a) mounted on a pivot with a teflon bushing (b). A Pesola spring scale was mounted on the lever (c) and was initially loaded to 1.4 Kg beyond the 0.5 kg mass being accelerated (d). The lever was held in the preloaded condition with a piece of string (e) attached to a concreate weight (below this view of the device). The experiment consisted of lighting the string on fire and observing the entire sequence of events on video. When the string broke and the mass was accelerated, its movement was noted on a piece of acetate film placed over the video monitor. For the experiment that modelled a compliant lever, a rubber band was placed between the mass and its attachment to the lever at point f.

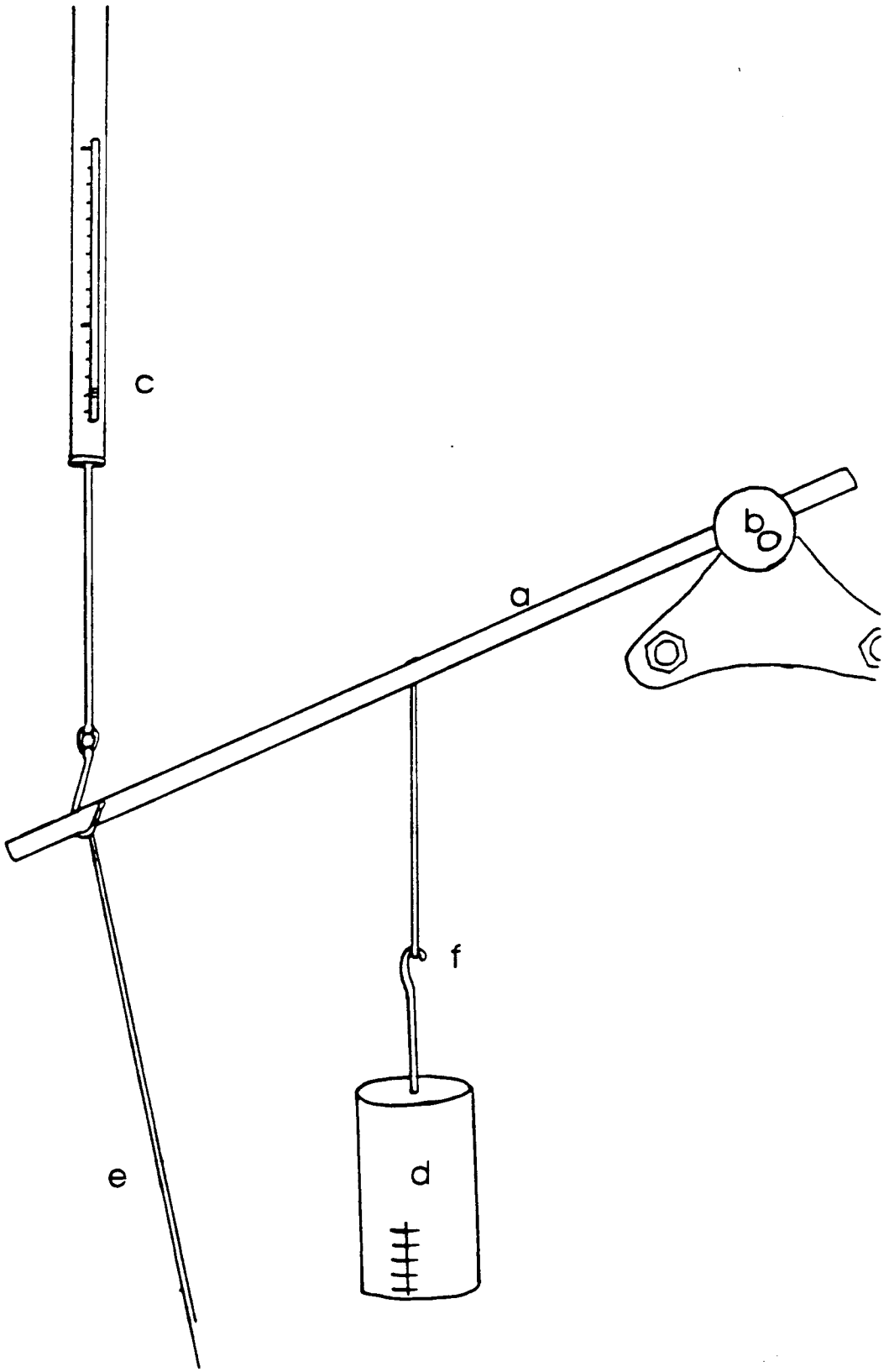
c
b
a
f
e
d

experiment was monitored on video, and the position of the mass was observed by advancing the video tape one field at a time, and noted on a piece of acetate film placed over the video monitor. The velocity and acceleration of the mass were estimated by differencing the position and velocity data respectively. The entire experiment was then repeated with a rubber band placed between the mass and the rod to model a degree of flexibility in the energy transmission system, similar to the tibial flexability of the locust leg.

In modelling the locust leg it seemed appropriate to define a reference point to evaluate the performance of the model. I have evaluated the model by comparing the velocity achieved by the mass at a point in time which represents the feet leaving the ground. What does that mean for a rotating rod and mass? I decided, perhaps arbitrarily, to define this "takeoff" point as the displacement where the mechanical advantage reaches a maximum, as seems to be the case in the locust. Therefore, the experiment was set up so that the spring scale gave 0 force, beyond the weight of the mass, when the rod was horizontal. The range of motion of the spring scale limited the prejump extension to 20 cm, and unfortunately, this really did not allow for a realistically large range of mechanical advantage as seen in the locust, but the pertinent features of the model are retained. For comparison purposes the velocity of the mass when it had travelled 20 cm were evaluated.

Figure 5.3 is a plot of the time course of the displacements of the mass connected rigidly to the rod and for the "compliant" rod. These data indicate that with the rigid connection the mass reaches 20 cm of displacement at approximately 180 ms; whereas with the compliant linkage, the mass reaches 20 cm at approximately 215 ms. Thus, the rigid lever has a higher average velocity over that interval. However, the position of the compliant lever was

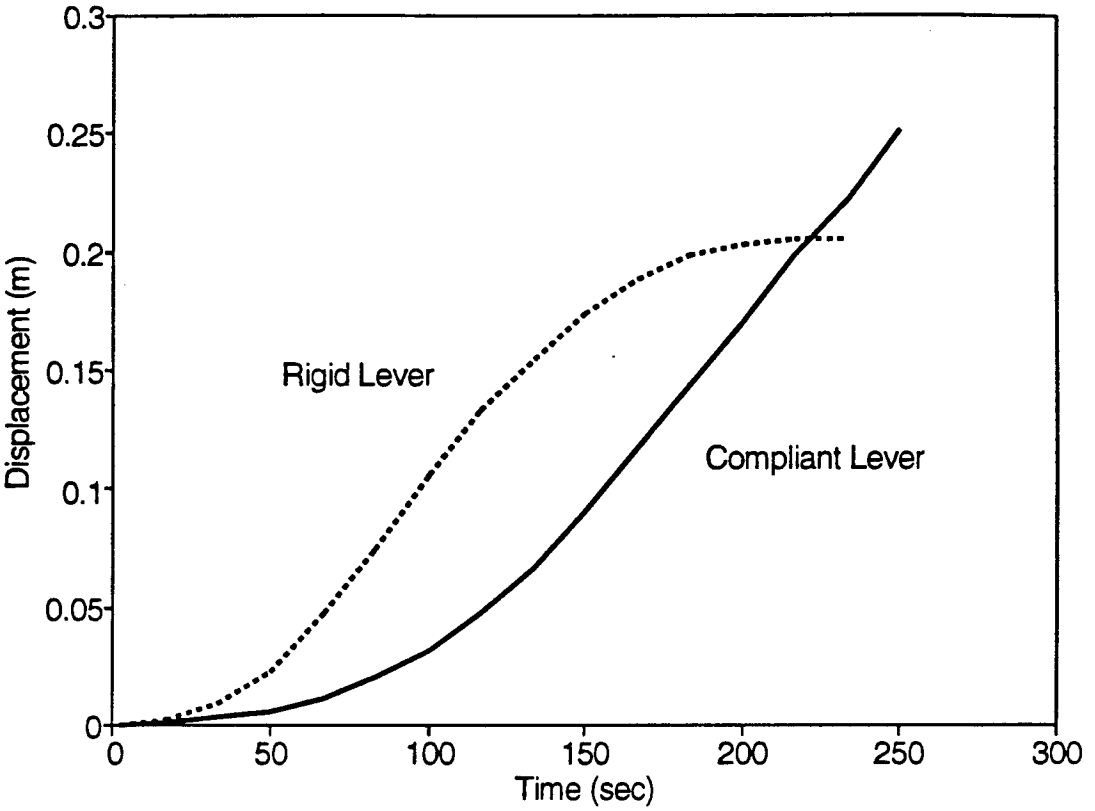

Figure 5.3.

Plot of the displacements of the mass in figure 5.2 through time for the rigid lever (dotted line) and the compliant lever (solid line).

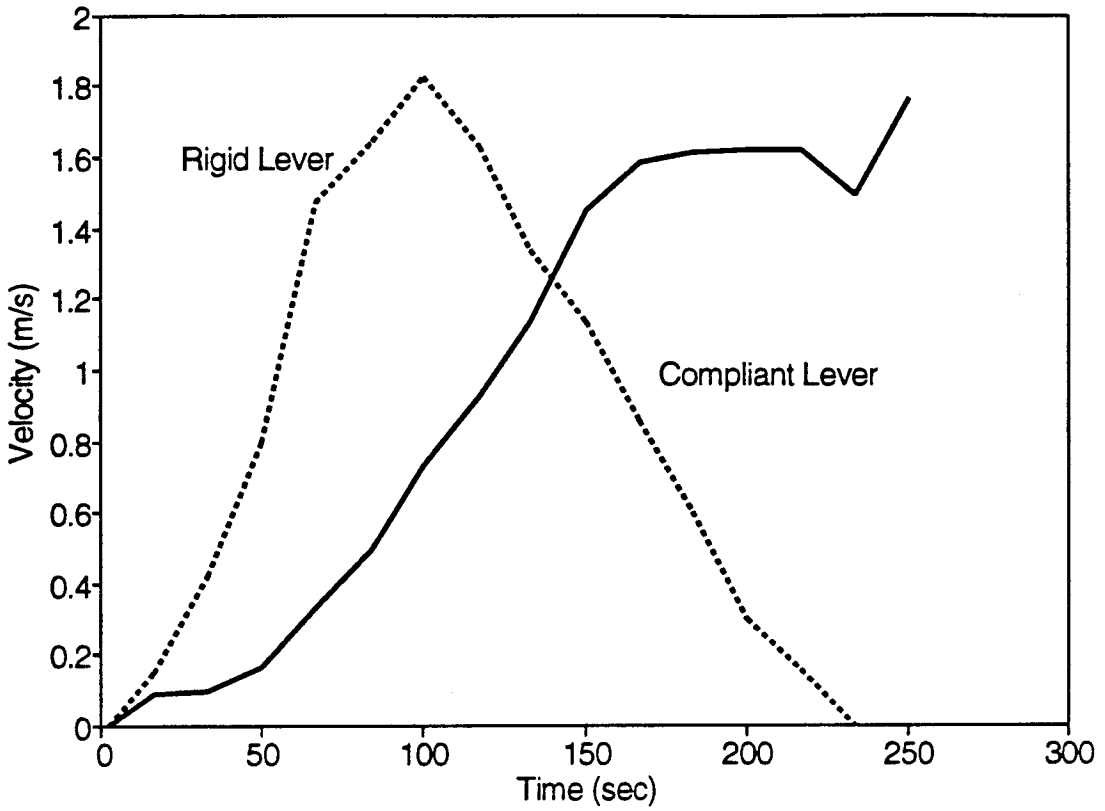

Figure 5.4.

Plot of the velocity of the mass in figure 5.2 through time for the rigid lever (dotted line) and the compliant lever (solid line).

continuing to rise when it reached 20 cm, while the rigid lever was slowing down. This impression is supported in figure 5.4 which plots the velocity of the mass during this modelled jump. At 180 ms the rigid lever had accelerated the mass up to approximately 0.6 m/s. At 215 ms, however, the compliant lever had accelerated the same mass to about 1.6 m/s - an improvement of 167%. Figure 5.4 does show how the peak velocity produced by the rigid lever was absolutely larger than that produced by the compliant lever (1.8 m/s vs. 1.6 m/s), indicating that the energetic hysteresis of the rubber band produced a larger take-off velocity at the cost of lower peak velocity.

Figure 5.5 is a plot of the acceleration of the mass during the modelled jump and provides an explanation of how this difference in performance is accomplished. The differencing procedure is inherently noise producing as small errors in measuring displacement are multiplied at each differencing step. Therefore, the data, represented by the dotted lines in figure 5.5, have been smoothed with a three point moving average, represented by the solid lines. The mass connected to the rigid lever reached a very high acceleration at approximately 60 ms and then proceeded to decline all the way to the take-off point of 180 ms. The mass connected to the compliant lever system did not reach peak acceleration until 150 ms and was positive all the way out to 215 ms when the feet "left the ground".

So the original hypothesis is supported. The built in compliance of the spindly tibiae may actually be acting as a time machine, delaying some of the transfer of spring energy to a point later in the jump impulse where the mechanical advantage is better able to use it. The mechanical advantage of the locust's tibiae has a larger range than my simple model, suggesting that they would get even greater benefit from this principle. However, for this model

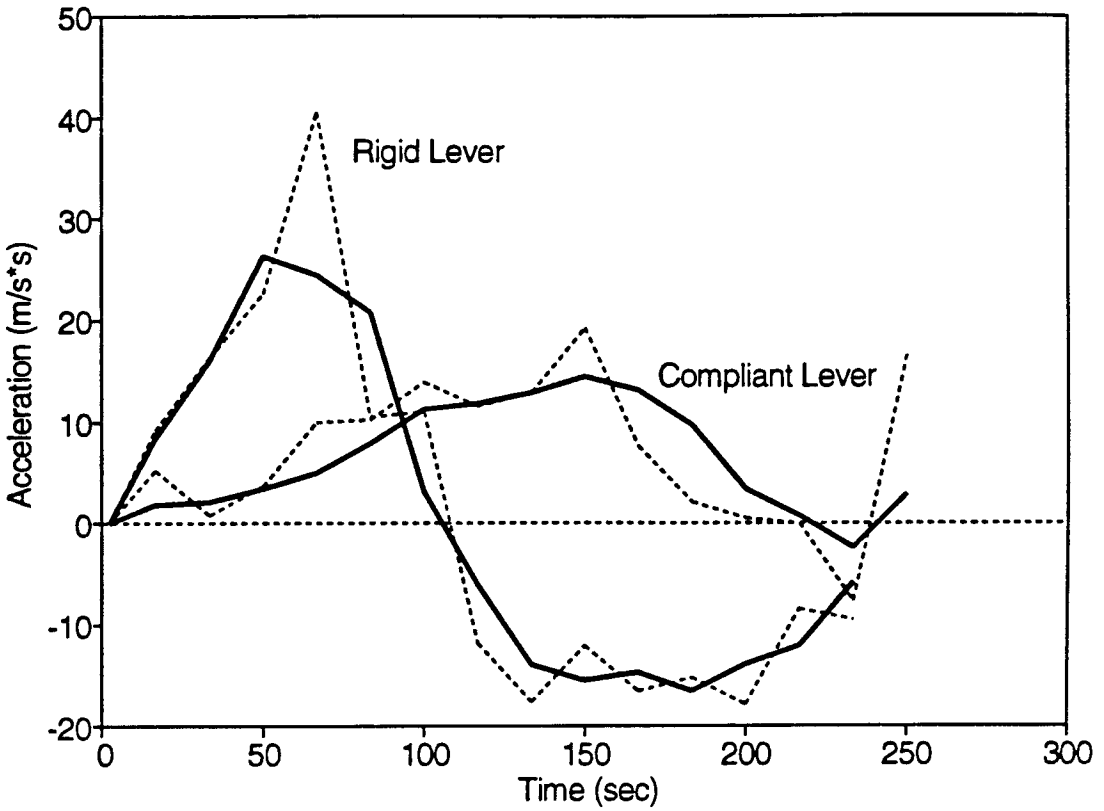

Figure 5.5.

Plot of the accelerations displayed by the mass in figure 5.2 through time for the rigid lever and the compliant lever. Because serially differencing the data in figures 5.3 & 5.4 produced a noisy signal, the original data (dotted lines) has been smoothed with a three-point moving average (solid lines).

to work the benefits gained from delaying the decay of spring force must outweigh the hysteretic losses in loading and unloading the second spring. We have seen in chapter two that the losses in the tibiae from hysteresis are indeed very low (ie. $\mathbf{R}\approx0.93$). Thus, the legs' mechanical properties are well suited to this strategy. Therefore, I believe that the scaling that I observed in the locust legs' external dimensions may represent a design strategy that takes advantage of the deformability of long slender beams.

Is there any evidence that this mechanism is actually used by the locust? Is there a characteristic signiture of the time machine that is demonstrated in the data on jump performance? If the time delay in ground reaction force is generated by deforming the tibiae as bending springs, then we might hypothesize that with increasing bending loads we would observe increasing time delays in peak acceleration (Fig. 5.6a). To test this suggestion, I have plotted the relative time within the period of the jump impulse where the peak in acceleration occurs as a function of the magnitude of the peak acceleration in figure 5.6b. The slope of the regression between the relative location of the peak acceleration and the magnitude of acceleration has a slope of 4.97×10^{-4} (SE = 4.53×10^{-5} , $r^2 = 0.482$) and is significantly different from zero ($t_s = 10.96$, df. = 129, $p < 0.05$). While the absolute value of the slope is low, it does mean that over the range of accelerations produced by the locusts (45 - 230 m/s^2) the position of the peak of acceleration moves from the 78% point in the impulse durration to the 90% point in the impulse. Therefore, there is at least indirect evidence that the locusts' legs are acting as energy time machines, and it is possible that they are obtaining the benefits in performance that are suggested by the model.

Figure 5.6a.

Diagramatic representation of the parameters reported in figure 5.6b. t_{total} is the total length of the impulse, and t_{peak} is the length of time from the begining of the impulse to the time of peak acceleration, and a_{max} is the magnitude of the peak acceleration.

Figure 5.6b.

The relationship between the normalized position in time of the peak of acceleration produced in the jump (t_{peak}/t_{total}) and the magnitude of the peak acceleration (a_{max}). The equation for the regression calculated for a sample of first instars, fifth instars and adults $Y = 0.784 + 4.967E\text{-}4 \times X$ ($F_s = 120.090$, df. = 1, 129, $r^2 = 0.4821$). This slope was significantly different from zero ($t_s = 10.959$, df. = 129, $p < 0.05$).

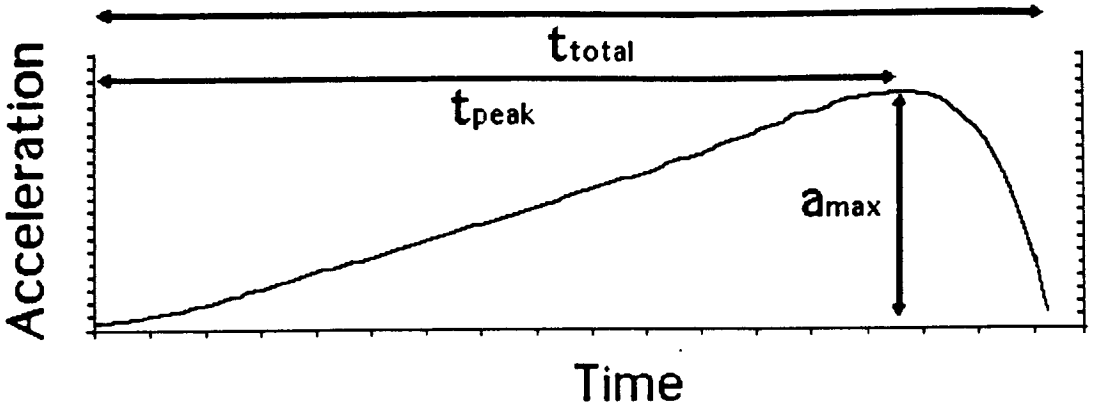
Acceleration
t_{total}
t_{peak}
a_{max}
Time

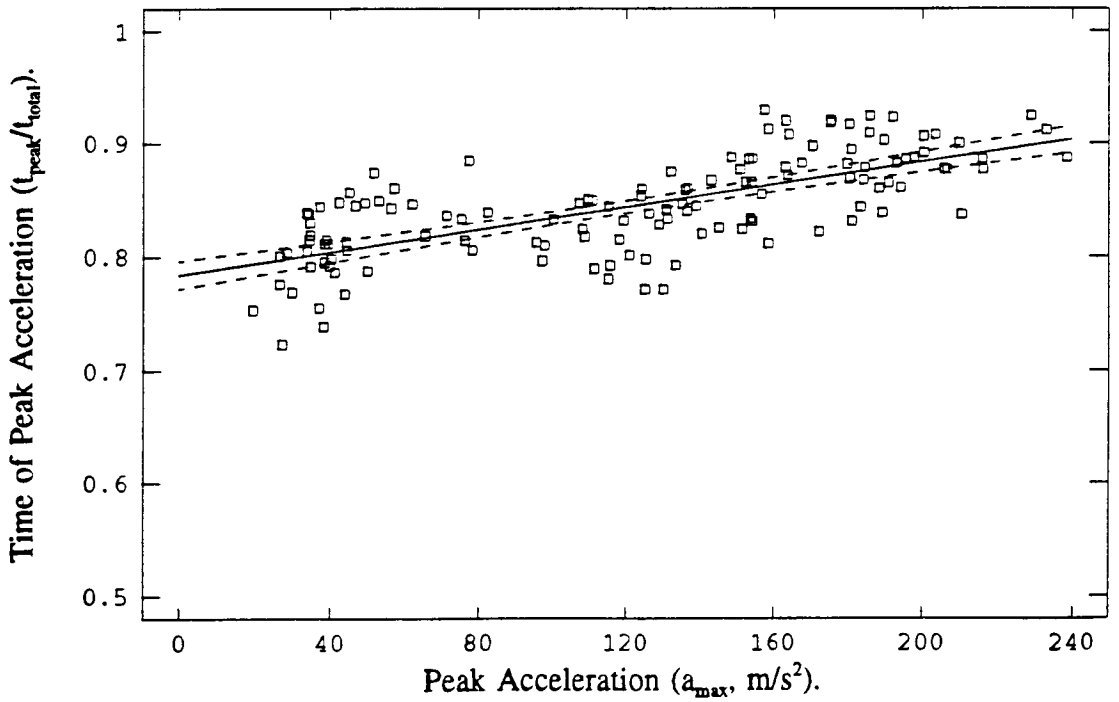
Time of Peak Acccleration (t_{peak}/t_{total}).
1
0.9
0.8
0.7
0.6
0.5
0
40
80
120
160
200
240
Peak Acceleration (a_{max}, m/s^2).

Degrees of freedom in design. Although this thesis has not concerned itself explicitly with the polymer physical chemistry or the composite material mechanics of the cuticle, I would like to suggest that it is the use of this protein exoskeleton that has allowed the distinctive scaling of skeletal morphology in the locust. I believe that by introducing an additional degree of freedom in the adaptive design of skeletal structures (ie. functional alteration of material properties) the locust provides a window on a new approach to scaling. When an engineer designs structures for human use, the design will to a large extent be determined by the building materials available: wood, steel, carbon fibre. The properties of these materials are relatively scale independent. The fact that vertebrate skeletons are all built of the same material (ie. bone) has suggested a set of models that allow only a discrete and finite set of design strategies. By using a building material whose properties can be modulated, the locust has shown that a continuous set of strategies exist to solve the problems for design imposed by scale effects. When human engineers alter the composition of composite materials to produce lighter and stronger structures than they could with steel, entirely new morphologies can be produced. To a certain extent this is an application of the principle that the locust has used in choosing the morphological design program for the scaling of its legs.

CHAPTER 6.

CONCLUSIONS

My final findings are that the African desert locust has adopted a scaling program that is consistent with the principles of the elastic similarity model proposed by McMahon (1973). However, this scaling is achieved without adopting a morphological scaling that is predicted by a traditional approach to elastic similarity. The scaling programme that the locust is expressing produces relatively longer, more slender limb segments in the metathoracic and mesothoracic tibiae.

I believe this scaling of external dimensions is accomplished by scaling the material stiffness of the cuticle material in addition to the dimensions themselves. This is a strategy allowed by the non-mineralized character of the cuticle and distinguishes the locust's scaling from vertebrate systems that other researchers have described. It has also been found that the exoskeletal condition itself determines a separate strategy for being thin walled that is also distinct from the vertebrate, thick walled design.

The reason for producing the relatively spindly scaling in the locust seems to be related to the jumping mode of locomotion. A simple mechanical model has demonstrated that introducing a long, and therefore deformable, lever into the jump mechanism can improve jump performance. I believe that this bending spring improves performance by delaying the decay of elastically stored spring force to a time when mechanical advantage produces higher take-off velocities.

In examining scaling of jump performance, it was revealed that there are

separate functional roles for the jump in the pre-adult and adult phases of the life history. Juvenile instars appear to be jumping to achieve a functional jump distance independent of size, while adults are jumping to produce a minimum end-jump velocity associated with take-off for flight.

LITERATURE CITED

Alexander, R. McN., (1977). Allometry of the limbs of antelopes (Bovidae). J. Zool., Lond. **183**:125-146.

Alexander, R. McN. (1983). Animal Mechanics. Oxford: Blackwell Scientific.

Alexander, R. McN. & Vernon, A. (1975). The mechanics of hopping by kangaroos (Macropodidae). J. Zool., Lond. **177**:265-303.

Alexander, R. McN., Jayes, A. S., Maloiy, G. M. O. & Wathuta, E. M., (1979). Allometry of the limb bones of mammals from shrews (*Sorex*) to elephant (*Loxodonta*). J. Zool., Lond. **183**:291-314.

Alexander, R. McN., Jayes, A. S., Maloiy, G. M. O. & Wathuta, E. M., (1981). Allometry of the leg muscles of mammals. J. Zool., Lond. **194**:539-552.

Anderson, S. O., (1976) Cuticular enzymes and sclerotization in insects. In *The Insect Integument* (Ed. H. R. Hepburn), pp. 299-321. Amsterdam: Elsevier Publishing Co..

Bennet-Clark, H. C. (1975). Energetics of the jump of the locust *Schistocerca gregaria*. J. Exp. Biol. **63**:53-83.

Bennet-Clark, H. C. (1977). Scale effects in jumping animals. In *Scale Effects in Animal Locomotion*. ed. T. J. Pedley. London: Academic Press.

Bennet-Clark, H. C. & Alder, G. M., (1979). The effect of air resistance on the jumping performance of insects. J. Exp. Biol. **82**:105-121.

Bennet-Clark, H. C. & Lucey, E. C. A. (1967). The jump of the flea: A study of the energetics and a model of the mechanism. J. Exp. Biol. **47**:59-76.

Bertram, J. E. A. & Biewener, A. A., (1988) Bone curvature: Sacrificing strength for load predictibility. J. Theor. Biol. **131**:75-92.

Bertram, J. E. A. & Biewener, A. A., (1990) Differential scaling of the long bones in the terrestrial carnivora and other mammals. J. Morph. **204**:157-169.

Biewener, A. A., (1982). Bone Strength in Small Mammals and Bipedal Birds: Do Safety Factors Change with Body Size? J. Exp. Biol. **98**:289-301.

Biewener, A. A., (1989). Scaling body support in mammals: limb posture and muscle mechanics. Science **245**:45-48.

Biewener, A. A., Alexander, R. McN. & Heglund, N. C., (1981). Elastic energy storage in the hopping of kangaroo rats (*Dipodomys spectabilis*). J. Zool., Lond. **195**:369-383.

Biewener, A. A., Blickhan, R., Perry, A. K., Heglund, N. C. & Taylor, C. R. (1988) Muscle forces during locomotion in kangaroo rats: Force platform and tendon buckle measurements compared. J. Exp. Biol. **137**:191-205.

Blake, R. W., (1983). Undulatory median fin propulsion of two teleosts with different modes of life. Can. J. Zool. **58**:2116-2119.

Bou, J., Casinos, A. & Ocana, J., (1987) Allometry of the Limb Bones of Insectivores and Rodents. J. Morph. **192**:113-123.

Brear, K., Currey, J. D. & Pond, C. M., (1990) Ontogenetic Changes in the Mechanical Properties of the Femur of the Polar Bear (*Ursus maritimus*). J. Zool., Lond. **222**:49-58.

Brown, R. H. J. (1963). Jumping arthropods. Times Sci. Rev. **Summer 1963**:6-7.

Carrier, D. R., (1983). Postnatal Ontogeny of the Musculo-Skeletal System in the Black-tailed Jack Rabbit (*Lepus californicus*). J. Zool., Lond. **201**:27-55.

Currey, J. D., (1980). Skeletal Factors in Locomotion. In *Aspects of Animal Movement* Society for Experimental Biology Seminar Series 5 (ed. H. Y. Elder & E. R. Trueman), pp. 27-48. Cambridge: Cambridge Univ. Press.

Currey, J. D., (1984). The Mechanical Adaptations of Bones. Princeton: Princeton University Press.

Currey, J. D., & Pond, C. M., (1989). Mechanical Properties of Very Young Bone in the Axis Deer (*Axis axis*) and Humans. J. Zool., Lond. **218**:59-67.

DeMont, M. E. & Gosline, J. M. (1988). Mechanics of Jet Propulsion in the Hydromedusan Jellyfish, *Polyorchis penicillatus* I. Mechanical Properties of the Locomotor Structure. J. Exp. Biol. **134**:313-332.

Denny, M. W., (1988). Biology and the mechanics of the wave-swept environment. Princeton: Princeton University Press.

Draper, N. R. & Smith, H., (1981). Applied regression analysis. 2nd. Ed. New York: John Wiley & Sons.

Economos, A. C. (1983). Elastic and/or Geometric Similarity in Mammalian Design? J. Theor. Biol. **103**:167-172.

Emerson, S. B., (1978). Allometry and jumping in frogs: Helping the twain to meet. Evolution. **32**(3):551-564.

Evans, M. E. G., (1971). The jump of the click beetle (Coleoptera, Elateridae) - a preliminary study. J. Zool., Lond. **167**:319-336.

Ferry, J. D., (1980) Viscoelastic Properties of Polymers. 3rd Ed. New York: John Wiley & Sons.

Full, R. J. & Tu, M. S., (1990). Mechanics of six-legged runners. J. Exp. Biol. **148**:129-146.

Gabriel, J. M., (1984). The effect of animal design on jumping performance. J. Zool., Lond. **204**:533-539.

Gabriel, J. M., (1985a). The development of the locust jumping mechanism. I. Allometric growth and its effect on performance. J. Exp. Biol. **118**:313-326.

Gabriel, J. M., (1985b). The development of the locust jumping mechanism. II. Energy storage and muscle mechanics. J. Exp. Biol. **118**:327-340.

Galileo, Galilei, (1638) Discourses and Mathematical Demonstrations Concerning Two New Sciences. (S. Drake, trans., 1974) pp. 169-170. Madison, Wisconsin: University of Wisconsin Press, Ltd.,

Gordon, J. E., (1978). Structures or Why Things Don't Fall Down. London: Penguin Books.

Gould, S. J., (1966). Allometry and size in ontogeny and phylogeny. Biol. Rev. 587-640.

Gould, S. J., (1975). On the scaling of tooth size in mammals. Amer. Zool. **15**:351-362.

Greenhill, G., (1881). Determining the greatest height to which a tree of given proportion can grow. Proc. Camb. Phil. Soc. **4**:65.

Harrison, J. F., Phillips, J. E. & Gleeson, T. T., (1991). Activity physiology of the two-striped grasshopper, *Melanoplus bivittatus*: gas exchange, hemolymph acid-base status, lactate production, and effect of temperature. Physiological Zool. **64**:451-472.

Heitler, W. J., (1974). The locust jump. Specialisations of the metathoracic femoral-tibial joint. J. Comp. Physiol. **89**:93-104.

Heglund, N. C. & Taylor, C. R., (1988). Speed, stride frequency and energy cost per stride: How do they change with body size and gait? J. Exp. Biol. **138**:301-318.

Hepburn, H. R. & Joffe, I., (1974). Locust solid cuticle-a time sequence of mechanical properties. J. Insect Physiol. **20**:497-506.

Hill, A. V., (1950). The Dimensions of Animals and Their Muscular Dynamics. Sci. Progs., Lond. **38**:209-230.

Huxley, J. S., (1932). Problems of relative growth. New York: The Dial Press.

Jensen, M. & Weis-Fogh, T., (1962). Biology and physics of locust flight. V. Strength and elasticity of locust cuticle. Phil. Trans. R. Soc. B **245**:137-169.

Ker, R. F., (1977). Some structural and mechanical properties of locust and beetle cuticle. Ph.D. Thesis, Oxford Univ..

Ker, R. F., (1981). Dynamic Tensile Properties of the Plantaris Tendon of Sheep (*Ovis aries*). J. Exp. Biol. **93**:283-302.

Lewis, E. B., (1978). A Gene Complex Controlling Segmentation in *Drosophila*. Nature **276**:565-570.

Lillie, M. A. & Gosline, J. M., (1990). The effects of Hydration on the Dynamic Mechanical Properties of Elastin. Biopolymers **29**:1147-1160.

Maitland, D. P., (1992). Locomotion by jumping in the mediterranean fruit fly larvae *Ceratitis capitata*. Nature 355:159-161.

Medawar, P. B., (1945). Size, Shape and Age. In *Essays on Growth and Form Presented* to D'Arcy Wentworth Thompson. (ed. W. E. Le Gros Clark and P. B. Medawar), pp. 157-187. Oxford: Clarendon Press.

McMahon, T. A. (1973). Size and shape in biology. Science **179**:1201-1204.

McMahon, T. A. (1975). Allometry and biomechanics: limb bones in adult ungulates. Am. Nat. **109**:547-563.

McMahon, T. A. (1984). Muscles, reflexes and locomotion. Princeton, N.J.: Princeton University Press.

McMahon, T. A. & Bonner, J. T., (1983). On size and life. New York: Scientific American Library.

Neville, A. C. (1975). Biology of the Arthropod Cuticle. Berlin: Springer-Verlag.

Pennycuick, C. J. & Lock, A., (1976). Elastic Energy Storage in Primary Feather Shafts. J. Exp. Biol. **64**:677-689.

Pitcher, T. J. & Hart, P. J. B. (1982). Fisheries ecology. Westport: AVI Publishing Co..

Prange, H. D. (1977). The Scaling and Mechanics of Arthropod Exoskeletons. In *Scale Effects in Animal Locomotion.* (ed. T. J. Pedley), pp. 169-181. London: Academic Press.

Prange, H. D., Anderson, J. F. & Rahn, H., (1979). Scaling of skeletal mass to body mass in birds and mammals. Am. Nat. **113**:103-122.

Queathem, E., (1991). The ontogeny of grasshopper jumping performance. J. Insect Physiol. **37**:129-138.

Schmidt-Nielsen, K. (1984). Scaling Why is animal size so important. Cambridge: Cambridge University Press.

Scott, P. D. & Hepburn, H. R., (1976). Femoral stiffness and jumping in grasshoppers and locusts. J. Insect Physiol. **22**:913-916.

Smith, R. J., (1980) Rethinking allometry. J. Theor. Biol. **87**:97-111.

Sokal, R. R. & Rohlf, F. J. (1981) Biometry. San Fransisco: W. H. Freeman and Co..

Steeves, J. D. & Pearson, K. G., (1982). Proprioceptive gating of inhibitory pathways to hindleg flexor motorneurons in the locust. J. Comp. Physiol. **146**:507-515.

Thompson, D'A. W., (1961). On growth and form. (Abridged edition, ed. J. T. Bonner) Cambridge: Cambridge University Press.

Vincent, J. F. V., (1975). Locust Oviposition: Stress-Softening of the Extensible Intersegmental Membranes. Proc. R. Soc. B **188**:189-201.

Vincent, J. F. V., (1980). Insect Cuticle: A Paradigm for Natural Composites. In *The Mechanical Properties of Biological Materials* 34th Symposium for the Society for Experimental Biology. (ed. J. F. V. Vincent & J. D. Currey), pp. 183-210. Cambridge: Cambridge University Press.

Vincent, J. F. V. & Hillerton, J. E. (1979). The Tanning of Insect Cuticle - A Critical Review and a Revised Mechanism. J. of Insect Physiol. **25**:653-658.

Von Mises, R. (1959). Theory of flight. New York: Dover Publications Ltd..

Wainwright, S. A., Biggs, W. D., Currey, J. D. & Gosline, J. M. (1976). Mechanical Design in Organisms. London: Edward Arnold.

Weis-Fogh, T. (1956). Biology and physics of locust flight. II. Flight performance of the desert locust (*Schistocerca gregaria*). Phil. Trans. R. Soc. Ser. B **239**:459-510.

Zacharuk, R. Y., (1976). Structural Changes of the Cuticle Associated with Moulting. In *The Insect Integument* (Ed. H. R. Hepburn), pp. 299-321. Amsterdam: Elsevier Publishing Co..

Zar, J. H., (1968). Calculation and miscalculation of the allometric equation as a model in biological data. Bioscience **18**:1118-1120.